University of Padova
Department of Information Engineering

Università
degli Studi
di Padova

Ph.D course in: Information Engineering
Curriculum: Information Science and Technology
Cycle: XXXIIII

Thermal comfort control in public and residential buildings via Fourier-based feed-forward disturbance compensation

Coordinator: Ch.mo Prof. Andrea Neviani
Supervisor: Ch.mo Prof. Luca Schenato

Ph.D. student: Marco Barbiero

Year 2021

Università degli Studi di Padova

Dipartimento di Ingegneria dell'Informazione

Thermal comfort control in public and residential buildings via Fourier-based feed-forward disturbance compensation

Ph.D. student
Marco Barbiero

Supervisor
Ch.mo Prof. Luca Schenato

Director & Coordinator
Ch.mo Prof. Andrea Neviani

Ph.D. School in
Information Engineering

Department of
Information Engineering
University of Padova
2021

"Those who dream by day are cognizant of many things which escape those who dream only by night."

Edgar Allan Poe, Eleonora

Abstract

Optimizing energy consumption for buildings heating and cooling has always been a goal for energy engineers, but, in recent years, this branch is gaining momentum. The most important motivation is obviously economic savings, but politics has also made its contribution. A building, especially if built during the new millennium, has a lot to offer to reduce energy utilization. In this thesis, an approach for modelling and control of a building is presented. Even if the focus is on residential buildings, the work can be easily adapted to large public buildings as well. We developed a methodology based on the Lumped-Parameter method to obtain a virtual environment of the building, carefully modelling external disturbances too. The equivalent electrical model was then developed and, using a graph-based algorithm, it was possible to solve the electrical network in closed form and obtain the representation of the linear system in state space. Using real blueprints and data, we built a virtual environment and simulate its behaviour using MATLAB/Simulink. Subsequently, a controller based on LQR and feed forward was proposed and developed to control the system, using a noisy version of the model built from blueprints. The innovative part of the work is the use of a frequency feed forward based on historical profiles. Exploiting the fact that external disturbances, temperature, and Sun irradiance, are quasi-periodic signals, an average profile can be defined. Then, the profile is decomposed into all its frequencies to weight the impact of each one according to their contribution to the system output. The profile is transformed into the frequency domain using Discrete Fourier Transform and the corresponding rejection signal is created for each frequency. Each contribution is then summarized, thus calculating the control signal to be applied in each period. The same operation can be done for the reference signal, which is usually in the form of a square wave. It is therefore possible to obtain a offline nominal control for periodic signals by matching input and output harmonics, since these signals are constant in frequency domain. To improve performance, the profiles can be adapted using the weather forecast of the next day, i.e., minimum and maximum outdoor temperature and maximum Sun irradiance, which can be easily obtained from local weather service thanks to the Internet. Due to the CoViD outbreak, the validation of the control system has been carried out in simulation, using the virtual environment created

previously. The results show how the new technique allows to reduce the temperature tracking error by a factor 2.6 (from standard deviation error 0.50 °C to 0.19 °C) compared to the PID solution, using a lower amount of energy. Furthermore, the feed forward part shows to be reliable and allows to reduce up to 12% the tracking error. The feed forward system also proved to be an excellent starting point for access to energy trading, as it provides a sufficiently detailed overview of the expected consumption for the next day, divided into time slots.

Sommario

Ottimizzare il consumo di energia per il riscaldamento e il raffreddamento degli edifici è sempre stato un obiettivo per gli ingegneri energetici ma, negli ultimi anni, questo ramo sta guadagnando sempre più peso. La motivazione più importante è ovviamente il risparmio economico ma anche la politica ha dato il suo contributo.

Un edificio, specialmente se costruito nel nuovo millennio, ha molto da offrire per ridurre l'utilizzo di energia. In questa tesi, viene presentato un approccio per la modellazione e il controllo di un edificio. Sebbene il focus sia sugli edifici residenziali, il lavoro può essere facilmente adattato anche a grandi edifici pubblici. Abbiamo sviluppato una metodologia basata sul Lumped-Parameter-Method per ottenere un virtual environment dell'edificio, modellando attentamente anche i disturbi esterni. Il modello elettrico equivalente è stato poi sviluppato e, utilizzando un algoritmo basato su grafi, è stato possibile risolvere la rete elettrica in forma chiusa e ottenere la rappresentazione del sistema lineare in spazio di stato. Utilizzando planimetrie e dati reale di progetto, abbiamo costruito un virtual environment e simulato il suo comportamento utilizzando MATLAB/Simulink.

Successivamente, è stato proposto e sviluppato un controller basato su LQR e feed forward per controllare il sistema. La parte innovativa del lavoro è l'utilizzo di un feed forward in frequenza basato su profili storici. Sfruttando il fatto che i disturbi esterni, la temperatura e l'irraggiamento solare, sono segnali quasi-periodici, un profilo medio può essere definito e poi trasformato nel dominio della frequenza usando la Trasformata Discreta di Fourier. Decomponendolo in tutte le sue frequenze, è possibile pesare l'impatto di ciascuna di esse secondo il loro contributo all'uscita del sistema e definire il corrispondente segnale di feed forward che cancelli il disturbo. Tutti i contributi vengono poi sommati, calcolando così il segnale di controllo da applicare in ogni periodo. La stessa operazione può essere fatta per il segnale di riferimento, dal momento che solitamente ha la forma di un'onda quadra. È quindi possibile ottenere un controllo nominale per i segnali periodici facendo corrispondere le armoniche di ingresso e di uscita, poiché questi segnali sono costanti nel dominio della frequenza. Per migliorare le prestazioni, i profili possono essere adattati utilizzando le previsioni meteorologiche del giorno successivo, cioè la temperatura esterna

minima e massima e l'irraggiamento solare massimo, che possono essere facilmente ottenuti dal servizio meteo locale grazie a Internet.

A causa della pandemia da SARS-Cov-2, la convalida del sistema di controllo è stata effettuata in simulazione, utilizzando il virtual environment creato in precedenza. I risultati mostrano come la nuova tecnica porti un miglioramento fino al 275% nell'inseguimento della temperatura rispetto alla soluzione PID, utilizzando una minore quantità di energia. Inoltre, la parte feed forward si dimostra affidabile e permette di ridurre fino al 12% l'errore di inseguimento. Il sistema feed forward ha anche dimostrato di essere un eccellente punto di partenza per l'accesso al commercio di energia, in quanto fornisce una panoramica sufficientemente dettagliata del consumo previsto per il giorno successivo, suddiviso in fasce orarie.

Acknowledgements

The work presented in this thesis was carried out with the support of my supervisor, Prof. Luca Schenato, and my company, EDILVI S.p.A. I am profoundly grateful to Luca for his help and concern before and during the Ph.D. programme: his (virtual) office has always been open for ideas and advices and, even in the most discouraging moments, he was able to give the best cues not to get discouraged and to strengthen me.

I would like to thank EDILVI S.p.A. and Geom. Diego Pavan for the opportunity given to me: I hope that the number of enlightened entrepreneurs who believe in the value of research and training to remain competitive will grow more and more in near future. Indeed, the possibility to combine theoretical research and practical implementation allowed me to gather the best from the two approaches, especially thanks to the contribution of my colleagues Alessandro, Denis and Federico.

I must express my profound gratitude to my family: without your support, these Acknowledgements would have not been possible. It has been a long journey, full of difficulties, but I hope it has been worth it.

I am thankful to all my friends too, that took care of me and supported me through all these years, from kindergarten to today. You are too many to list but you have all left a sign on me. In particular, heartfelt thanks go to Ilaria and Alessandro, friends before colleagues, and Matteo, with whom I have shared the journey to here.

This journey would not have come to an end without the support of my girlfriend Maricarmen. You supported me day after day and helped me overcome the obstacles encountered along the way. I thank you profoundly for all the days shared before and during this journey: this work is dedicated to you.

Contents

1 Introduction

1.1 Motivation

Optimizing energy consumption for buildings heating and cooling has always been a goal for energy engineers, but, in recent years, for several reasons this branch is gaining momentum. The most important motivation is obviously economic savings: for example, in USA, in 2017 the residential and commercial buildings weight for about 40% of total US primary energy used [1] and the majority of this energy is consumed by the HVAC (Heating, Ventilation and Air Conditioning) system to maintain thermal comfort for occupants. This means about 6000 TW h: reducing consumption in this sector by a small amount would have a major impact on overall primary energy consumption [2]. Politics has also made its contribution: the requirement that allows to build nZEBs (near Zero Energy Buildings) only in force in Italy starting from January 1, 2021, thanks to European Union's Directive 2010/31/EU, forced construction and HVAC systems companies to rethink construction schemes and products [3, 4]. Savings policies such as Energy Performance Contracting (EPC) introduced by the European Union Directive 2012/27/EU, have forced manufacturers and designers to maximize production efficiency and minimize dispersions [5]. The aim of these contracts is to improve the energy efficiency of building without putting too much strain on the owners' pockets. In these types of contracts, indeed, an Energy Service Company (ESCo) offers to renovate, requalify and manage a building asking in exchange the payment of a

recurrent fee for several years. The fee is calculated from the energy saved and it should cover the refurbishment costs and the recurrent expenses of utilities to be a gain for the ESCo. Therefore, it is essential that the day-to-day management of the facility is as efficient as possible, without compromising comfort.

A building, especially if built during the new millennium, has a lot to offer to reduce energy utilization: even older ones, with small, targeted interventions, can become very efficient if conducted in the best possible way. The first area in which we have concentrated our main efforts is the data collection and exploitation. It is critical to know the status of what we want to improve, its behaviour and what the scope for improvement may be. A building produces an immense amount of data and this could easily be used to improve comfort or reduce energy consumption. The most immediate example is the use of tenants' habits: if the supervisor knows that no one will enter the room for an interval of time, it can decide to reduce the level of heating or cooling and save energy. Also, if it knows that the room is south-facing, it can turn down the heating because the sun will help during the middle of the day to heat the room, allowing the heat pumps to work at a lower rate and, therefore, to have a better COP: in other words, to save money and energy providing the same (or a better) service. These types of plant supervisors are called Building Energy Management System (BEMS) [6]. BEMS normally deals with performing scheduled operations, and controlling and managing energy demand by giving inputs to power supplies or heat pumps. In addition, it should be able to perform optimization functions: in particular, having a night cycle for pre-set or dynamic temperature, an economizer cycle for optimizing the fraction of recirculation air, a cycle for optimizing air conditioning valve openings based on outdoor and indoor temperature. The complete mechanical management is also entrusted to this system, such as the switching on and off of refrigeration and heating systems and the secondary water loop. Usually, it is also entrusted with operational functions, such as collecting information to define heat pumps energy profiles, fault diagnosis and safety alarm management, as well as consumption measurement. All these operations require large amounts of data, so the various systems are usually integrated and connected as much as possible.

The most important data for the thermal building control is the air temperature of each room: if this is available along with the ability to directly drive the actuator, it allows to provide very precise control and to optimise loads. Differently from what happened towards the end of the last century, when the building was divided into zones of several adjoining rooms and only one thermostat per zone was used, such precise temperature monitoring is becoming more and more popular, thanks also to the low cost of wireless temperature sensors and the spread of home automation and remote control. A more

detailed information about temperature also makes it possible to provide better comfort: different people have different temperature preferences and providing a different temperature for each room makes it possible to provide better overall comfort. This can be especially true in working environments, where the dress code can be different for different offices even in the same area and, especially in summer, can make a big difference to both consumption and comfort. Obviously, as mentioned above, it is necessary to have precise control for each room to get the most out of it. With the spread of fan coils and all-air systems into the domestic environment, room air temperature management has become much simpler and more effective and can also be adopted outside offices, where this methodology is state of the art. Sunshine data is also very important since the Sun contributes a lot to the heating and lighting of a building [7]: knowing its impact allows better distribution of loads and to reduce the load peaks. Thanks to the widespread use of photovoltaic panels, this information is easy to obtain as it is possible to calculate the sun's irradiation on the roof in real time and, with appropriate formulas, derive the impact for each external surface of the building. This information, however, can be easily obtained by using online weather services, which are more and more widespread and very often available free of charge. An internet connection allows to obtain all the real-time information about the building surrounding environment, including the outside temperature and, above all, the weather forecasts for the next days. These are very useful because they permit to distribute the thermal loads taking into account what will happen in the near future: knowing the external temperature that will be there the next morning allows the controller to better calculate the optimum time to turn on the HVAC systems after the night shutdown or, otherwise, to assess whether it is more appropriate to maintain a minimum (or maximum) temperature during the night so as not to overload the thermal plants.

Knowledge of the environment is not so useful if it is not paired with a perfect knowledge of the characteristics of the building. Information about the behaviour of main components within a building as external disturbances or applied inputs change is of fundamental importance. For this reason, a work on improving consumption and comfort must also focus on thermal modelling. In past years, this was a major stumbling block as the design and the real building could differ greatly, especially from the thermal behaviour point of view. The introduction of more effective design methods, such as BIM, and the need to verify the state of the buildings by means of APEs, has made it possible to obtain, in a faster a more practical way, more accurately design data. Building information modelling (BIM) is a design process that, taking advantages of various tools and software, optimize the planning, realization, and management of buildings. The basic philosophy is to gather all relevant data of a construction and collect, combine, and link them digitally. This methodology, if

shared between all stakeholder, allows to obtain an all-in-one project that includes all the information needed during the life of the building, from the design to the management. This makes everything simpler since what is present in each volume of space and its characteristics are available digitally at any time. Furthermore, Italian law has made it compulsory for the sale of real estate to draw up an energy performance certificate in order to inform buyers of the energy performance of the building. This certificate, called APE in Italy, contains the description of the energy demand. To be draw up, an Energy Engineer needs to make an inspection of the building, take measurements, and create a reduced model of the building's behaviour by means of some software that simulate it and calculate the energy demand during the year. If the project was done following the BIM methodology, the work to be done is greatly simplified. Moreover, since this work is mandatory, this information can then be reused for improved building control with quasi-zero effort.

1.2 EDILVI S.p.A. - ESCo

EDILVI S.p.A. [8] is a company founded in 1984 in Treviso as a complete construction company: it offers both the design and construction for new buildings and sales services for finished or unfinished housing units. Since 2011, it also carries on the activity of Energy Service Company (ESCo) through an ad-hoc division, leading to maximum integration by including refurbishments and after-sales services too. Indeed, ESCos mainly carry out interventions aimed at improving energy efficiency, both from the point of view of upgrading and energy management.

The main products of the company are the construction of new houses through the patented process called "Casa Smart Plus", and the renovation of buildings and their upgrading, both in terms of anti-seismic and energy saving. For condominiums and public buildings, through the ESCo division, it also offers monitoring and management services for air conditioning systems as well as consumption accounting. For the latter, it is also possible to combine the upgrading with the post-renovation management by means of an Energy Performance Contracting (EPC). Citing Energy Efficiency Directive 2012/27/EU, an Energy Performance Contracting (EPC) is a *a contractual arrangement between the beneficiary and the provider of an energy efficiency improvement measure, verified and monitored during the whole term of the contract, where investments (work, supply, or service) in that measure are paid for in relation to a contractually agreed level of energy efficiency improvement or other agreed energy performance criterion, such as financial savings.* In other words [9], an ESCo designs and implements the energy upgrade at a reduced or zero price to the beneficiary in exchange for part of the profits obtained during the years of the contract from

the increased energy efficiency of the building, i.e., the savings of energy not purchased. Very often, post-intervention management of the building is also offered as part of the contract, to increase the savings even more thanks to the ESCo's knowledge of the building's thermal behaviour. Depending on the building, savings of up to 80 percent can be achieved. This type of contract is very well considered by politicians as it allows to improve the quality of buildings and reduce pollution in cities at zero cost to the community since all risks and costs are absorbed by the ESCo. Furthermore, if the contracted minimum efficiency requirements are not met, the ESCo will not be able to recoup completely the costs of the intervention: therefore, the design and the post-intervention management must be as accurate as possible so that the company does not incur in losses, that could be very significant.

Currently, the ESCo division has several facilities under management, both in the form of EPC and standard conduction. Since they have good energy efficiency, all facilities are equipped with heat pumps and chillers, air conditioning can be managed for each tenant, and monitoring and management can be done remotely. Several new "Casa Smart Plus" homes are also managed by the ESCo: they are equipped with heat pumps and all-air systems, allowing effective management to improve energy efficiency. Considering this scenario, improving facility management allows ESCo to increase margins or be more competitive in the market. For this reason, EDILVI S.p.A. decided to collaborate with the university to finance a Ph.D. programme about these issues.

1.3 Challenges

The company commissioned us to develop an after-sales building management and control methodology to maximise profits and reduce energy and money waste. As the company plans to focus on the residential housing business in the short term, we have decided to concentrate on this sector, but without neglecting the large public buildings that are still the core business.

Several challenges presented themselves in front of us, in both modelling and control. The main challenge is not to require additional purchases and, therefore, to use what is already there by default. As a target model, we used a newly built Casa Smart Plus house, in order to achieve a future-proof result. These houses have been designed following the BIM methodology and are equipped with all-air HVAC systems: this system has one air temperature and flux sensor per room in addition to the outdoor air temperature and the sensors built in its air handler. This allowed us to easily obtain data, both for modelling and control, but at the same time forced us to extract 100% from it since no other data is available. For this reason, we cannot use historical data for modelling but have to rely

solely on design data. As far as control is concerned, data from nearby weather stations can also be used to obtain forecasts since the houses are equipped with an internet connection. In addition, they are equipped with solar panels and their instant production can also be exploited to calculate the solar insolation in real time.

The company needs to improve control and management of large public buildings, too: therefore, the methodology must be flexible enough to adapt to both situations. These two scenarios are not so far apart and, with some adjustments especially regarding the control part, can be traced back to a common methodology. Indeed, the thermal control of a gymnasium is easier because there are fewer rooms and area to be controlled, but on the other hand, large volumes put more strain on measurement and construction errors and their inertia is larger. Making everything scalable proved to be quite a challenge but, at the same time, allowed us not to fall into the trap of overfitting. In fact, there is always the risk of creating something that in simulation is quite perfect but in reality adapts badly because of the different characteristics that were not foreseen or known during the model phase.

1.4 State of Art

This work touches on two different areas: building modelling and thermal control. These two areas are very closely linked and, usually, in the state of the art they have been treated together since, to achieve good control, a good model is necessary. To simplify the discussion, we have decided to separate the two topics except in cases where this is not physically possible, as in the case of new artificial intelligence algorithms.

The most common methodologies for thermal modelling of buildings are the statistical models (black box), the physical principle modelling (white box) and hybrid method (grey box) [10, 11]. The colours do not indicate how good the method is, but only the degree of adherence to the physical laws of the obtained model: using a white box approach, the model is created exploiting the physical laws that describe the phenomenon while the black box model uses tools completely unrelated to the physics of the phenomenon to be described. The colour can also represent how the obtained model is available for inspection: the gears of a white model are very clear and easy to understand, while the inside part of a black one is much more difficult to analyse and modify for trial. The latter is often due to the overlapping of the modelling and control part, which makes operation using the black box methodology obscure. Indeed, the choice of the modelling approach depends mainly on the goal to be achieved: analysis and energy assessment require very precise modelling methodologies but have no limit to their complexity; on the other hand, control models must sacrifice some precision in order to be lighter but above all provide a physical interpretation,

so as to facilitate controller development.

The current research trend is mainly concentrated in *black box* modelling as clearly reported in [12]. Over ten thousands of paper are published showing different problems that can be solved exploiting these data-driven techniques. These methods use historical data as inputs and states of a building to derive a quite-fully automatic model of its actual or future behaviour, and to control its behaviour. This methodology can be used in a lot of situations: the main ones are energy consumption prediction, load prediction, fault detection and diagnosis, energy baseline estimate, prediction of the impact of human activities in buildings, and, obviously, for control: several different type of control can be performed, like HVAC control, lighting control, and Thermal Energy Storage control. Black box methodology found widely adoption in demand response too, as reviewed in [13], thanks to the Reinforcement Learning (RL). Reinforcement learning and reinforcement learning-based control are the current trend in this area as reported in [14], a review of the most important works about applying machine learning in a building life cycle. The section concerning modelling and control is one of the richest, thus emphasizing the great contribution of novelties in this area.

Most of these methods rely on machine learning or artificial intelligence techniques, like neural networks, genetic algorithms, and fuzzy techniques: the growing computational capacity of computing systems has made feasible them even for large buildings, increasing the efforts in this area. In [15], a review tailored on energy consumption is provided, demonstrating that the data-driven approaches have well addressed a large variety of problems in buildings modelling and control. Although it is an important area of research, industrial applications are not widespread [12]. The main cause is the lack of model transferability, which limits a model trained with one data-rich building to be used in another building with limited data or to test the impact of modification in the same buildings. Indeed, since physical law are not exploited in this type of model and there are not physical parameters to be set, they cannot be adapted to trial different approach. Despite these premises, it is equally useful to investigate the state of the art of these techniques as researchers are making progress in eliminating this drawback from neural network, like [16] and [17]. In [18], authors predict the day-ahead building cooling demand using a clustering-enhanced adaptive artificial neural network (C-ANN): the network was trained using synthetic data provided by *TRNSYS 18*, a widespread energy simulation software, and uses weather forecast to make the day-ahead prediction. This avoids the need for real historical data with sufficient input variety to derive all building behaviours under different climatic conditions but at the same time requires a simulation model of the building, thus moving the problem downstream. In [19], authors model energy used

by a building during the year and show the potential of this research path, especially for modelling human contribution, comparing a custom Artificial Neural Network to EnergyPlus, a state-of-the-art white box software. The results are very precise, better than the ones produced by the white box software, but they show the limit of this methodology: their model cannot allow to test different behaviours and cannot be used to trial new strategies since they can only be evaluated after the on-site implementation. For this reason and for the fact they need a large amount of sufficient varied historical data that usually is not available, we decide to not adopt these techniques since they do not suite well with our situation.

System identification techniques are also utilized as reported in [20]. This branch of research is very active since there is a need for models in state space that can be used for control. The most important techniques are the Subspace methods (4SID) [21] and the Prediction Error Methods (PEM). The subspace methods are a set of system identification algorithms that fit historical data to a MIMO state space model exploiting the factorization of controllability and observability Grammians. In prediction error methods, instead, the structure is assumed to be known and the parameters shall be identified from experimental data: based on the chosen model structure, a system predictor is built and used to estimates the parameters by minimising prediction errors. However, PEM methods are designed mainly for SISO systems and should be used with caution if adopted to work in MIMO scenarios. SISO systems are not useful in our scenario, as reported in [22]: authors clearly show how a MIMO model shall be used to model conditioning process in buildings in order to obtain good performance. Using these system identification techniques, however, does not solve the problem of sufficiently varied historical data to be obtained; furthermore, it is also necessary to determine a priori the type and characteristics of the model to be obtained, finding the most suitable to avoid overfitting or oversimplification phenomena. Consequently, these techniques are much more suitable for a grey box approach in which a physical model is already defined.

The *white box* methodology, unlike the black box methods, completely ignores historical building behaviour and uses only measured physical parameters to define the model [11]. In fact, the system relies entirely on physical laws to describe the plant behaviour and does not require prolonged data collection over time. This concurs to have minor disadvantages in the collection data but at the same time it demands much more time to develop the model. However, the complexity of building the model is repaid in being able to clearly determine the relationships between the different components of the building and test possible changes easily. Several commercial and open-source applications that exploit this methodology are available: the most important are *TRNSYS* [23], *EnergyPlus* [24], *Modelica* [25], and

IDA Indoor Climate and Energy [26]. The two main areas of research of the white box methodology are the Finite Element Method (FEM) and the Lumped-Parameter Method (LPM).

The idea behind the finite element method is to divide a complex problem into small elements or volumes that can be solved in relation to each other using simple mathematical techniques, such as algebraic equations. This methodology exploits Galërkin's methods, which allow to obtain an approximate solution by transforming a problem defined in a continuous space into a problem defined in a discrete space [27]. This idea is used in many areas that need to solve continuous problems, such as to describe electromagnetism [28]. However, this class of methods is very difficult to apply manually when the dimensions become important and, for this reason often support software is used: usually, this software allows the user to start from a 3D drawing of the building to formulate the problem and obtain a simulation of its behaviour. A whole branch of software research was born for this: Computational Fluid Dynamics (CFD). A CFD software is an engine for solving Navier-Stokes equations for each several discrete volume in which the total volume is divided. These equations model the behaviour of a viscous fluid, such as air, as thermal and momentum conditions change. By means of a CFD, fluid behaviour in an environment can be described with an arbitrary precision: these techniques can also be applied outside buildings energy modelling, such as in aerospace, hydraulic engineering, etc. This method is very precise but computational heavy, as reported in [29]: in this paper, a work to reduce the computational load by exploiting a multi-zone model program is presented. In [30], instead, this method was adopted for simulating the envelopes characteristics. Furthermore, more data-driven approaches have also emerged in recent years that use this method only to simulate part of the entire behaviour, as in [31]. Anyway, since our goal is to develop a model that is useful for control, we cannot use methods that take hours to resolve a system state. Consequently, our gaze has turned to the LPM.

The principle of the nodal approach [32] or multi-zone technique, assumes that each zone of a building is a homogeneous volume in which all variables are uniform within it. In other words, each zone of the building, whether it is a room, a wall, or another type of volume, is described by a single state value for the whole volume: for example, the temperature is taken constant throughout the volume considered, ignoring possible gradients. The heat transfer equations are then solved only as a one-dimensional heat transfer between the two surfaces of adjacent volumes in contact, ignoring all possible gradients, both on the contact surface and within the volume itself. This is a very important simplification, but it allows the complexity of the model to be cut down by several orders of magnitude, while maintaining a sufficient degree of accuracy. In the literature, two different approaches within this methodology are

present but the most popular is the finite difference or lumped-parameter method. This method uses the electro-thermal analogy to describe the heat flows between different zones. This technique was introduced by Rumaniovski in [33] and is very widespread because it greatly simplifies model development. Since the equations governing the model are linearized, the computation time is negligible for modern systems. The basic idea is to associate a thermal volume with a capacitance whilst a thermal resistance with a resistor. Applying the law of electromagnetism and solving the equivalent circuit, the behaviour of the building can be retrieved taking into account that the voltage at the ends of the capacitor represents the temperature of the corresponding thermal volume. A compendium of buildings modelling using LPM can be found in [34]: this work is the basis on which many new works draw inspiration. Indeed, many papers based on this methodology have been presented in recent years, showing that this branch of research is still alive: in [35], a multi-layered building is accurately modelled and simulated. In [36], authors show how to model a building by means of LPM to obtain the equivalent electrical circuit. In [37] is reported an example of this method coupled with a non-linear model of the HVAC system in order to obtain a full thermal model of a building. In [38], this methodology was adopted to obtain a RC model that is then used in a series of parametric analyses to investigate the impact of the Urban Heat Island effect. In [39], two types of lumped parameter techniques are tested against TRNSYS software to prove its reliability. In fact, a building component can be modelled by means of an arbitrary number of resistors and capacitors. For example, in [40], a 3R2C model has been proposed and tested against experimental data, showing respectable performance in predicting the thermal energy consumed. The most common trade-off between complexity and reliability is to use two resistors and one capacitor for describe a component: this methodology is called 2R1C.

All these works state that the main benefits of using RC model are its simplicity and computational efficiency. Furthermore, its simplicity allows for better understanding the physics of the problem whilst the evaluation of modelling hypotheses and the sensitivity of different parameters are made easier. Indeed, the lumped parameter methodology is also used in the ISO 13790 standard. Using this methodology, it can happen to obtain a linear model with a dimension that is excessive compared to the computational capacities available. Several authors have focused on this issue, proposing methods to reduce the size of the states without loss of performance. There are two philosophies regarding this type of model reduction: with loss or without loss of meaning of the states. In the first case, the state of the new system has no physical meaning while in the second case it retains it, although transformation matrices are often required to access to the state. An example of the second technique, mandatory to be used in the case of thermal control of the rooms of a

building, is reported in [41] where, by means of Markov chains, it was possible to reduce the size of the state without losing any information. In [42], the authors use the balanced truncation method to reduce the states in a non-fully linear concentrated parameter model that also accounts for relative humidity. The reduction takes place on the linear part of the system, since the non-linear one is sparse: in fact, they use a decomposition on the reachability graphs to obtain a base transformation matrix that groups the most important dynamics of the system in the first states. This allows authors to truncate the final states without appreciable loss of information. The root mean square error in the predictions is 0.5 K, of the same order as the spatial error of the temperature within a zone.

One of the limitations of this methodology is the on-the-field collection of model parameters: tools are not always available to determine them rigorously. For this reason, mixed techniques were born in which the model is built exploiting white box techniques, but the parameters are estimated using temporal data: these techniques are called *grey box*, since they try to mediate the two extreme techniques. Several grey-box methods are available: in [43], a system identification technique to reckon the value of the lumped parameters is presented. The work was completed using only the time series of outdoor and indoor temperatures and heat input measured in the building, due to both the action of the Sun and internal loads, such as electrical consumption. The results are not very reliable since the error made is not completely negligible for a simulation. In [44], Dynamic Semi-Physical Modelling (DSPM) is presented and utilized, in this case, to model a drying process: although the area is slightly different, the methodology can easily be adapted to the case of buildings modelling as well. This method consists in developing a model using physical laws, in this case the laws of conservation of mass and thermodynamics, and then use them to develop a neural network: the neural network is then trained using temporal data. In this way they can combine the two philosophies, the black box and, the white box, within a single model. In [45], the authors compare four grey-box models to determine the best method for their needs. They set out to find a parameter estimation method based solely on historical data. They used indoor and outdoor temperature, building energy consumption, and total solar radiation as data. As for the model, they used different RC models with different complexity while, to fit model parameters they used a PEM method optimizing the root mean square error of indoor temperature with respect to the predictions. In [46], authors use a optimization function based on temperature and consumption, reaching good performance in prediction future energy usage. In case of grey-box models, it is also very important to be able to compare the different models obtained, especially to determine the correct model complexity in order to avoid possible overfitting. For example, in [47], authors present a method based on likelihood ratio test for choosing among different models.

1.4.1 Control

The choice of modelling method depends greatly on the desired type of control to be performed. Indeed, although a model is necessary to obtain satisfactory performance from a control, not all controls can be applied to all type of models. Controls based on feedback from the state, in fact, need a state space model. Controls based on numerical optimization, on the other hand, can be adopted even on models with a not well-defined structure, such as neural networks. In recent years, researcher developed statistical methods that allow modelling and control to be integrated into a single tool too. Choosing which control technique to use is always difficult: matching available inputs, execution speed, learning phase, and, of course, available hardware capabilities is not trivial at all. In [48], a review on state of the art about systems for thermal control in buildings is presented. The review shows that there are many technologies for thermal control of buildings and many more are being developed, especially in the on-line learning MPC and reinforcement learning areas. To make it easier to analyse, it is necessary to divide the discussion into three different groups: those based entirely on a model in state space, those based on numerical optimization, and those created using machine learning techniques that integrates a model. For the sake of brevity, we do not report non-model-based controls even though they are actually the most common in buildings, especially domestic ones. An example are thermostats, ON-OFF controllers with hysteresis, still used today to regulate the temperature of domestic rooms. Their low cost and ease of installation and setup still make them unbeatable in domestic buildings, although from an energy-saving standpoint they are not the best solution. Another type of control that we will not cover because it is not based on any plant modelling are fuzzy control techniques. These control techniques implement responsive rules that overcome Boolean logic, allowing expressions to be evaluated based on their truth percentage. An example can be found in [49], where a housing comfort controller is designed, tested, and presented using fuzzy logic.

Methodologies for designing controllers for state-space models are diverse although most illustrate a method for effectively defining the system's feedback matrix or propose adding new states. The simplest of these is Proportional–Integral–Derivative controller (PID), which through the action of three different parts, it improves closed-chain control. A PID controller receives as input the difference between the reference and the output of the system to be controlled and returns a value to be applied to the plant proportional to the instantaneous error and the historical sum of the errors: to increase responsiveness, there is also a part proportional to the instantaneous derivative of the error. This controller was introduced in the second decade of 1900 but is still used today, both as a controller for heat pumps and as a controller for a whole building, as presented in [50]. To properly tune a PID controller,

empirical methods like ones described in [51] can be used: however, methods based on analysing the plant transfer function can be adopted. This type of controller is available in both an analog version, built by means of resistors and capacitors, and a digital version, i.e., implemented in a microcontroller. This technology is very cheap and provides good performance, although the controller performance is limited by knowing only the output of the system and not its state or the environment in which the system acts.

Linear-Quadratic Regulator (LQR) is an optimal control methodology via feedback from the state [52]. Thanks to the information on the system state, it is possible to define a cost function to be minimized: usually, a penalty is applied for the non-zero state and for the cost of applying inputs to the plant. To reduce computation complexity, the cost function is minimized in an infinite temporal horizon. Indeed, by using a cost function that is quadratic in states and outputs, by means of Riccati equations it can be minimized to obtain a closed form feedback matrix that can be applied to the system closed-loop. Usually, it is not possible to obtain measurements of the state of a system, so it is necessary to estimate it. The optimal method is the one described by Kalman in [53], where he introduces the famous Kalman filter. Given a model of the plant, this filter allows to estimate the state of the system through its outputs and applied inputs after properly defining a cost function on the measurement and process error to be minimized. This procedure is the dual of the Linear-Quadratic Regulator and, when applied in pairs, the resulting controller is called Linear Quadratic Gaussian controller (LQG). An implementation of this methodology applied to thermal control of buildings can be found in [54]. Often, to achieve better performance, an integral part is added, as reported in [55].

Another technique that is based on the optimum control is Model Predictive Control (MPC). An overview of the latest works can be found in [56]. This technique, developed starting from the 80s of last century, extends the concept of LQR optimal control by adding the concept of constraints to the cost function. Also this method derives the input to be applied through the minimization of a cost function but, in this case, the minimization must be performed taking care of the constraints that are set. An example of applied constraints can be the maximum input that the system can accept: the LQR control cannot impose or exploit instantaneous limits on the input but can only minimize its value in the long run, thus failing to avoid saturation phenomena that introduce non-linearity and ruin future estimates. The addition of the constraint concept brings more optimization of the input but, at the same time, a greater computational complexity, forcing in most cases to use numerical optimization techniques given the lack of a closed form. For this reason, the optimization is no longer performed on an infinite horizon as in the case of the LQR methodology but on a finite horizon. This makes the system readier and more optimizable, since even external

forecasts and data can be integrated into the cost function without substantial changes to the control system: the system still has to recalculate the inputs at regular intervals due to the finite horizon. Furthermore, a custom cost function based on comfort can be used, for example exploiting Fanger's equation to implement Predictive Mean Vote (PMV) [57]. At the same time, however, the stability easily guaranteed using the LQR methodology is no longer valid and shall be integrated in the cost function: for example, this can be guaranteed if the cost function forms a Lyapunov function for the closed loop system [58]. An implementation of an MPC control for a building can be found in [59]. In this work, the authors rely on an RC model to predict the behaviour of their plant. In [58], authors provide a detailed description of an MPC implementation on a real building and report the results from two months of operation: also in this case, the model on which the control is based has been developed using the lumped parameters method (LPM). In [60], this method is used to modulate heat pump system by exploiting the maximum coefficient of performance (COP), in order to optimize the production of heat per watt. In [61], authors present a predictive control scheme with reduced order models for building components and for thermal storage. In [62], the authors present their implementation of an MPC control in a real office building. After validating their controller using EnergyPlus, they interfaced it with the building's BMS and achieved up to 20% better results than the existing solution. For this work, they exploited the MATLAB building modelling toolbox presented in [63]: this toolbox allows a fast generation of models for MPC from basic building geometry, construction and systems data. As reported in [64], there is a lot of activity around MPC. With the advent of increasingly powerful microprocessors, computational complexity is no longer an issue, and indeed, it allows the use of increasingly accurate models to improve performance. This has made increasingly complicated to squeeze everything out of MPC control, as more and more accurate and detail-rich models are needed. Indeed, as reported in [65], the identification of the system dynamics in robust manner even in the presence of noise is perceived as a major challenge for a successful implementation of this method.

For this reason, hybrid approaches are emerging: in these approaches, models are developed using data-driven techniques and integrates model and controller development into a single process. In [66], a neural network is developed and trained to predict the building's comfort specifications, environmental conditions, and power consumption. Using these predictions, a MPC controller provides control inputs for the thermal and lighting systems to achieve the desired performance: from their results, this hybrid method performs significantly better than the conventional MPC based on a white model. Another example can be found in [67], where the authors propose a framework aiming to achieve optimal control over air handling units by implementing a Long-Short-Term-Memory (LSTM) network

trained using deep reinforcement learning (DRL) techniques to approximate real-world HVAC operations. In [68], propose a DRL-based framework for thermal comfort control in buildings: it is composed by a deep neural network for predicting the occupants' thermal comfort along with a deep deterministic policy gradients (DDPGs)-based approach for learning the optimal thermal comfort control policy. In both works, the results are very encouraging even if the complexity is very high and not compatible with a residential building budget.

1.5 Contribution

This work aims to provide a complete solution for modelling and control of a building. The focus is on residential buildings, but the work shall be easily adapted to large public buildings as well. Taking into account the state of the art, we decided to develop a methodology based on the Lumped-Parameter method to obtain a virtual environment of the building, carefully modelling external disturbances too. The equivalent electrical model was then developed and, using a graph-based algorithm, it was possible to solve the electrical network in closed form and obtain the representation of the linear system in state space. After deriving the equations and matrices describing the model, we implemented them using MATLAB/Simulink in order to obtain an efficient simulation system. This system contains also a custom model of main disturbances in a building, i.e., external temperature, ground temperature and solar radiation. Then, the company provided to us project data and blueprints to extract the physical parameters we needed, such as the layout of the walls and their composition. At this point, the building's virtual environment was ready. The initial idea was to validate the model using its real counterpart, which was being built in the meantime. For this purpose, a data collection and storage platform were created, based on MySQL DBMS and PHP, to provide a user-friendly environment for model analysis and validation, as well as providing a secure space to store data collected in the plant. In fact, we contacted the vendor to help us automate data collection via FTP protocol. This platform was named EPCA and is also used for accounting and documentation management of the facilities.

Due to the pandemic caused by the spread of SARS-CoV-2 virus, the validation program cannot be completed. As a result, we decided to postpone this part to future work and focus primarily on thermal control of that building. The company, in fact, mainly needs methods to optimize energy consumption. Therefore, we developed a controller based on LQG technology and optimized the comfort and the energy usage by using weather forecasts, thanks to a newly developed feed forward method based on Discrete Fourier Transform.

The LQG control is very powerful, but it is a reactive control: it acts proportionally to disturbances, after they have started. As a result, the controller chases them with a bit of delay. A way to reduce this phenomenon and help the controller is to bring the knowledge of the disturbance to the control system. By adding a system that compensates for disturbances based on historical knowledge, i.e., a feed forward compensator, the LQG part of the controller shall compensate only the part that was not predicted, reducing its load, and improving its performance. In fact, the novelty of the work is the new frequency-based feed forward system: by analysing the meteorological data, we realised that the external disturbances have a certain periodicity, and they repeat themselves day after day. Usually, nominal feed forward is implemented using constant values obtained as average of a profile but, in this case, the periodicity of disturbances is very pronounced and losing all this information leads to very low feed forward yields. The disturbances periodicity is very clear for solar radiation, which peaks at noon and has a bell-shaped pattern every day. The external temperature follows this behaviour with an almost sinusoidal pattern, with the minimum reached shortly after sunrise and the maximum shortly after midday. Since the inputs are periodic with a day-long period and the system is linear, the effects of this disturbances on the output shall also be periodic. For this reason, instead of optimizing the control on time domain, we work in the frequency domain, by decomposing the profile into all its frequencies and weighting the impact of each one according to their contribution to the system output. The profile is transformed into the frequency domain using the Fourier transform and the corresponding rejection signal is created for each frequency. All contributes are then summarized, thus calculating the control signal to be applied in each period. The same operation can be done for the reference signal, which is usually in the form of a square wave. However, we noticed that disturbances could have very different extension from one day to the next, although respecting the same form and periodicity. Consequently, we create normalised profiles and adapt them by modifying daily excursion using the next day weather forecasts that online weather stations provide. This permits to improve control and know in advance the expected consumption for the next day. To make things easier for defining offline profiles, the EPCA application was enhanced to allow logging of historical temperature data from online weather stations.

The decision to use these technologies to develop the controller instead of using more complex techniques such as MPC is due to several factors. The most important is the cost of the hardware: a controller developed with LQR/LQE technology can be implemented in a microcontroller costing a few euros, whereas an MPC control requires much more sophisticated software and, therefore, much more powerful hardware. Since our idea is to apply this control to the residential case, we cannot afford to spend big amounts of money

and we shall mainly use what is already available in the houses. One possibility to mitigate this problem would be to rely on an online service to calculate the reference signal using MPC, so that a less powerful machine can be used in the plant without sacrificing control quality. The use of remote computing, however, is a bit risky, especially in more mountainous regions where the internet signal is not very stable. For this reason, a mitigation and control system would need to be developed in order to control the plant in a sub-optimal working state without internet connection since a heating plant shall be working in all conditions. This mitigation would impact a lot in the development time and for this reason we decide to not use MPC technologies; indeed, the solution we present already has this mitigation by design since, in case no new data is present, the system automatically uses the standard historical profile.

The validation of the control system has been carried out in simulation, using the virtual environment created previously. In order to provide more plausible results, this test was carried out assuming a variability of up to 20% of the nominal value of the constitutive parameters in the model. The results show how the new technique brings an up to 275% improvement in temperature tracking compared to the PID solution, using a lower amount of energy. Furthermore, the feed forward part shows to be reliable and allows to reduce up to 12% the tracking error. The feed forward system also proved to be an excellent starting point for energy trading, as it provides a sufficiently detailed overview of the expected consumption for the next day, divided into time slots.

1.6 Outline

The dissertation consists of 6 chapters that can be summarized as follows.

After the introduction, Chapter 2 describes the hardware and software that are normally available in a building, paying attention to the differences between residential and public buildings. This chapter reports also on the developed and used data collection system.

Chapter 3 provides an in-depth description of the modelling technique used to create the virtual environment, with the focus moving from the building description to the environment modelling.

Chapter 4 outlines the problem formulation and the techniques adopted for control: a meticulous description of the control systems used is given along with the reasons for the choice of design parameters.

Chapter 5 focuses on the case study and the performed tests. The potential of the model and the controller is evaluated against widespread technologies.

Chapter 6 summarizes the conclusions and gives suggestions for future research.

2

Hardware and Software within Buildings

In recent years, buildings are becoming increasingly connected, intelligent and independent of humans. This chapter will describe these new smart buildings, the devices used to make them smart and the contribution of internet to this revolution. Finally, some ideas will be given to make smart older buildings and how an ESCo can exploit this revolution.

2.1 Building Energy Management System (BEMS)

A smart building is a building that exploits *information and communication technologies (ICT) to enable automated building operations and control* [69]. By means of these tools, it is possible to control in an automated way HVAC systems, electrical systems, lighting, shading, and, in the case of more advanced systems, even accesses and security. These systems are usually integrated in a single structure called Building Management System (BMS) or Building Automation System (BAS) that may vary in complexity between buildings. Mostly of the time, they can be accessed by the manager from remote thanks to internet. Usually, they are equipped with microprocessors to analyse immense amounts of data needed to perform their operations in real time. Although, initially, these systems were aimed only at large public buildings, in recent years they have also spread to the residential sector and, to date, even medium budget houses are equipped with these systems.

Several operations are required for a building to be called smart. The most important

is centralized and optimized control of HVAC systems. The management software, by analysing data from temperature, carbon dioxide ratio, position, or lighting sensors placed inside the building, calculates the power to be sent to each room, the ventilation needed, the amount of recirculation, and optimizes the operation of the centralized system improving the comfort for the occupants. The system is often integrated with lighting and shading management, allowing the trade-off to be found between the need to comfortably illuminate a building with natural light to save lighting cost and the need to reduce the impact of the sun's heat to reduce air conditioning power in the summer or heating power in the winter. Also the control of access and occupation of rooms are also connected to this: if the system is aware that in a room people are not present, it can reduce the power to be sent and, if it is equipped with the analysis of behavioural patterns, it can completely block the supply of air conditioning in that room if it is aware that the person is absent from that moment on, saving a lot in energy consumption. In [70], authors review some of the most interesting researches about this, showing outstanding result in reducing energy usage without sacrificing comfort.

In recent years, these systems are also dealing with energy peak load: electricity suppliers, in order to reduce the probability of blackouts and allow a more optimized use of sources, charge a different rate to electricity depending on the period and apply a penalty if a certain power threshold is exceeded in certain periods. Furthermore, since all new buildings are equipped with photovoltaic panels, shifting loads at the time of maximum production allows them to reduce energy waste and at the same time, request less energy from the grid. For these reasons, a building supervisor must also be able to manage electrical loads in a smart manner, both on the HVAC side and for electrical power loads. In [71], the last trends on peak optimization and management are extensively reviewed.

The activities described above cannot be accomplished without the necessary information, such as temperature, lighting, and occupancy. To obtain this data, it is necessary to set up sensors throughout the building and interconnect the HVAC systems to the supervisor.

2.2 Sensors and Data

A building, in order to comply with the demands of an intelligent supervisor, needs different types of sensors. Similar to a human being who needs senses to determine his state and that of his surroundings, a building also needs very specific senses, depending on the functions required. The most common and widespread sensor is the temperature one: it is used to measure the air temperature inside a room or of an environment. Indirect methods based on the effects of heating or cooling processes are generally used to obtain these measurements:

the most commonly used method is to measure the thermal expansion undergone by bodies and its effect on electric resistance. A historic method is resistance thermometer: it exploits the change in resistivity of a metal as its temperature changes to return a temperature value. The resistivity of a metal, in fact, can be approximated well as function of its temperature: for example, the Callendar–Van Dusen equation describes the behaviour of a platinum resistance [72] in the interval $[-200, 600]$ °C by means of a forth-degree polynomial:

$$R(T) = R_0[1 + \alpha T + \beta T^2 + (T - 100)\gamma T^3]$$

where R_0, α, β, γ are experimentally determined coefficients and $R(T)$ the measured resistance. Consequently, after calibrating the system, by measuring the resistance it is possible to obtain the temperature value. This quartic function can be rewritten implicitly. Using one of the various root finding methods, which also exist in closed form for polynomials of this degree, it is possible to trace the temperature. Anyway, for more common uses, it is possible to reduce the equation to the first degree without major loss of accuracy, making it possible to use analog electrical circuits without microcontrollers, thus greatly reducing costs. The same approach is used in thermistors where a semiconductor resistance is measured. In this case, however, the materials can be classified by two different types of behaviours, called Positive Temperature Coefficient (PTC) and Negative Temperature Coefficient (NTC) depending on whether the resistance increases or decreases with increasing temperature. Normally NTC materials are used since Steinhart-Hart's law can be exploited [73]:

$$\frac{1}{T} = \alpha + \beta \ln R(T) + \gamma \ln^3 R(T)$$

where R_0, α, β, γ are experimentally determined coefficients and $R(T)$ the measured resistance a temperature T. To use these materials, it is necessary to use a microcontroller for the transformation, since the complexity of the function is important. Nowadays, however, this is no longer an issue, especially with IoT sensors that already have electronic logic to connect to the internet. The integrated circuit revolution has also brought improvements to temperature measurement: silicon manufactures introduced transducers that exploit the properties of semiconductor junctions, such as those of diodes and transistors. For example, in the case of p-n diodes, the current-voltage relationship depends on temperature in this way:

$$I = I_S \left(e^{\frac{q_e V}{kT}} - 1 \right)$$

where I_S is the reverse saturation current, k is the Boltzmann constant and q_e is elementary charge. In this case, T is expressed in K. Again, using a simple microcontroller, it is possible to obtain the temperature measurement given the measured voltage and current. This methodology and the transistor-based methodology are the most popular for air temperature sensors, since they are very cheap and sufficiently accurate in the usual measurement range of air temperature. The fact that we don't need such a precise measurement of air temperature can also be seen in light of the appreciable vertical gradient in rooms air temperature: indeed, it is recommended to install these sensors at a height of 1.50 m, the average height of a person's face, to increase a little the reliability and usefulness of measure since the face is the mainly human temperature sensor.

Humidity and, more precisely, relative humidity are also a very important quantities for comfort [74] and, for this reason, shall be monitored. Relative humidity (RH) represent the ratio between the mass of water contained in the volume to be tested at temperature T and the maximum amount of water that can be evaporated in that volume to saturation at the same temperature. This quantity is very sensitive to temperature variation, and therefore the same evaporated water mass per volume can have different relative humidity values, since the higher the temperature, the higher the saturation point. This value is very important for comfort as it represents how effective the sweating system is: the higher the relative humidity, the less powerful this mechanism is. A lot of technologies are available to measure it [75]: the most popular are Capacitive Humidity Sensors, Resistive Humidity Sensors and Thermal Conductivity Humidity Sensors. A capacitive humidify sensor consist of a substrate of glass, ceramic or silicon on which a thin film of polymer or metal oxide is deposited between two conductive electrodes. The relative humidity of the environment influences the dielectric constant of the sensor and, for suitable materials, this behaviour can be described by a quasi-proportional function of relative humidity. These systems are very accurate, with an error under 2% in an interval between 5% and 95% relative humidity. A resistive humidity sensor instead exploits the variation of resistance at the ends of certain types of substrates as the relative humidity changes. They are faster than capacitance-based ones but their behaviours is less proportional to HR and they are more delicate. The most complicated are the thermal conductivity humidity sensors: this technology uses two diaphragms in which one are present a resistor and a sensor. One of diaphragms contains a protected and predetermined atmosphere while the other is free to be in contact with the air to be measured. The two resistors are heated and once the set temperature is reached, they start to cool down. By comparing the cooling times, it is possible to calculate the relative humidity of the environment to be measured, comparing it with the known one [76].

In addition to temperature and humidity, air quality depends on the concentration of

carbon dioxide. An atmosphere containing more than 7% carbon dioxide is deadly to humans, but the effects begin to be seen even at lower concentrations. In fact, the standard limit is 30,000 ppm while ACGIH (American Conference of Governmental Industrial Hygienists) suggests a maximum concentration of 5,000 ppm in workplaces. For this reason, it is essential to measure its concentration so that action can be taken if these thresholds are exceeded, such as by reducing air recirculation [77]. The main methods to build a CO_2 concentration sensor are using semiconductors, solid electrolytes, optic fibres, laser diodes, or by means of non-dispersive infrared (NDIR) technologies [78, 79]. The latter technology is the most widespread nowadays and is based on the characteristic absorption of light radiation at 4.26 µm caused by carbon dioxide. This radiation was chosen because it is strictly characteristic of this gas and others, such as water vapour, do not interfere with light at this wavelength. A sensor of this type consists of an infrared emitter and a pyroelectric detector: the radiation is emitted in the direction of the detector and, depending on the concentration, more or less power reaches it. From the knowledge of the distance between emitter and detector and their areas, it is possible to estimate with very good accuracy the concentration of carbon dioxide. The same principle, subject to wavelength change, can be used to measure other gases as well, such as carbon monoxide [80].

2.2.1 Communication Architecture

At regular intervals, all these sensors provide information about the state of the environment at the location where the sensor has been placed. It is essential to place it in the best location for measurement: in past years, this was not entirely possible because the sensors had to be connected by wires and, therefore, the positioning depended largely on the availability of the connection. Thanks to the Internet of Things (IoT) revolution, various wireless technologies have been introduced to communicate with the sensors, thus allowing sensors to be placed in the most correct and best places. In [81] and [82] can be found some example of monitoring and control solutions for buildings based on IoT devices. Depending on the area to be covered, different extensions to the IEEE 802.15 protocol have been developed: for example, Zig-Bee (IEEE 802.15.4) [83] and 6LoWPAN [84]. Both protocols are designed to be low-power, so that sensor batteries will last a long time, but, at the same time, to be reliable. Obviously, some concessions were necessary to meet these criteria: these protocols were designed for low transfer rates. Actually, this is not a problem for building sensors data, since the data volume is very low, the dynamics are very slow and sampling times above one minute are the practice. Experts consider a sampling time of fifteen minutes more than sufficient. In light of this, even low transfer rates around 20 kbps are more than sufficient for thermal control of a building. Much more important for our work is the maximum distance:

ZigBee has an approximate range of 30 m indoors. Consequently, for industrial buildings, it is usual to install wired or wireless gateways to increase the range. In the case of private homes, a single gateway is sufficient for the whole house.

After connecting the sensors to the network, it is critical to have a logging system in place. Although many supervisors only use real-time data, it is critical for an energy engineer or facility manager to have historical data available at all times. From these it is possible to calculate the COP of the heat pumps, the energy signature of the building, the historical consumption, very important information to evaluate the state of the building and the possible maintenance it needs. Different logging methods are possible, from local to cloud-based, as reported in [85]. Leading cloud service vendors already provide off-the-shelf systems to upload their sensor data to the cloud, where thanks to pre-developed libraries, it can be analysed. However, some companies prefer to keep their data inside their servers: EDILVI is one of them and in Section 2.5 our implementation for a data collector is described.

2.3 Actuation in Commercial and Residential Buildings

Although they have a lot in common in terms of construction techniques, residential and commercial buildings differ significantly in terms of management and equipment. Since commercial buildings are used by a large number of different people and all of them shall be satisfied, these buildings have got automatic air-conditioning management systems that allow few changes to set points, thus trying to maintain the same temperature inside the building. In Italy, temperatures in these buildings are defined by the Presidential Decree number 74/2013: for winter, the decree stipulates 20 °C with a two degrees tolerance in offices whereas 18 °C in buildings used for industrial or craft activities; in the summer, the temperature must be no lower than 26 °C. These values have been provided as a guide to reduce consumption without sacrificing too much comfort. Based on the Predictive Mean Vote (PMV), ISO 7730 [86] defines different temperature values to achieve comfort in offices: it suggests (24.5 ± 1.0) °C in summer whereas (22 ± 1) °C in winter. In residential buildings, temperature management needs to be much more flexible. Not all rooms have the same function and thus require different temperatures: the bathroom will need a higher temperature than the living area whereas the bedrooms need a lower temperature to facilitate comfortable sleep. For this reason, domestic buildings are often equipped with thermostats that can be adjusted in each zone to set the best temperature for the room and the activities to be carried out there.

Temperature management is not the only thing that differentiates the two types of buildings: the management of the heating and cooling units are normally different and,

consequently, the available control modes are also different.

In large buildings, the most commonly used air-conditioning methods are all-air systems and air/water systems with fan coils. The first type of system aspires air from outside and, after treating it by passing through an Air Handling Unit (AHU), injects it into the room by means of air vents. The air handling unit filters, heats or cools the supplied air by means of filters and exchangers fed by a thermal fluid. Usually, the fluid is heated or cooled by heat pumps to improve energy efficiency. At the same time, part of the air in the room is taken and sent through an air recirculation unit: this unit divides this flow into two parts, one to be sent to the air handling unit for a treatment before reintroduction into the room, and the other part for expulsion to the outside: to improve the efficiency of the system, the exhausted air is sent to a heat recovery unit before being released outside. The control of all the microclimatic quantities is carried out by means of the air: they can be regulated by varying the temperature at which air is introduced into the room (constant flow systems) or by varying the quantity of air introduced in the unit of time (variable flow systems). In both cases, a description of the heat flow is the following:

$$\dot{Q} = \dot{V} C_v (T_a - T_i) \tag{2.1}$$

where $\dot{V}$ is the volume flow rate in $\mathrm{m^3\,s^{-1}}$, C_p is the air volumetric heat capacity at constant volume in $\mathrm{J\,K^{-1}\,m^{-3}}$, T_a is the injected air temperature whereas T_i is the room air temperature, both in °C. Usually, in buildings modelling, $C_p = 1210\,\mathrm{J\,K^{-1}\,m^{-3}}$ is used: the physic conditions are temperature equal to 23 °C and a dew-point of 9 °C (40.85% HR) at standard pressure (1 atm). An example of this air-conditioning methods is reported in Figure 2.1. In constant flow systems, control system can change the T_a set-point to modify room air temperature whereas in variable flow systems, it can modify on the volume flow rate. This type of system is well suited to large environments where the required conditions are uniform and defined by design, such as theatres, cinemas, gymnasiums, and shopping centres.

In the air/water systems with fan coils, the water, heated or cooled by a central heating unit, flows through a coil contained in the so-called fan-coil units (FCU): the air in the room, extracted from room by means of a fan, passes through the coil where gives or acquires heat, varying its temperature. In this case, the temperature is controlled only by varying the speed of the fan, which varies the air flow rate, thus the volume of air at constant temperature supplied. The description of the heat transfer is the same of an all-air system and is reported in (2.1): remember that T_a can be approximated by the average of water temperature input and output. Theoretically, it is also possible to modify the temperature of the fluid, but this is not recommended, since it is better to use the fluid at the temperature

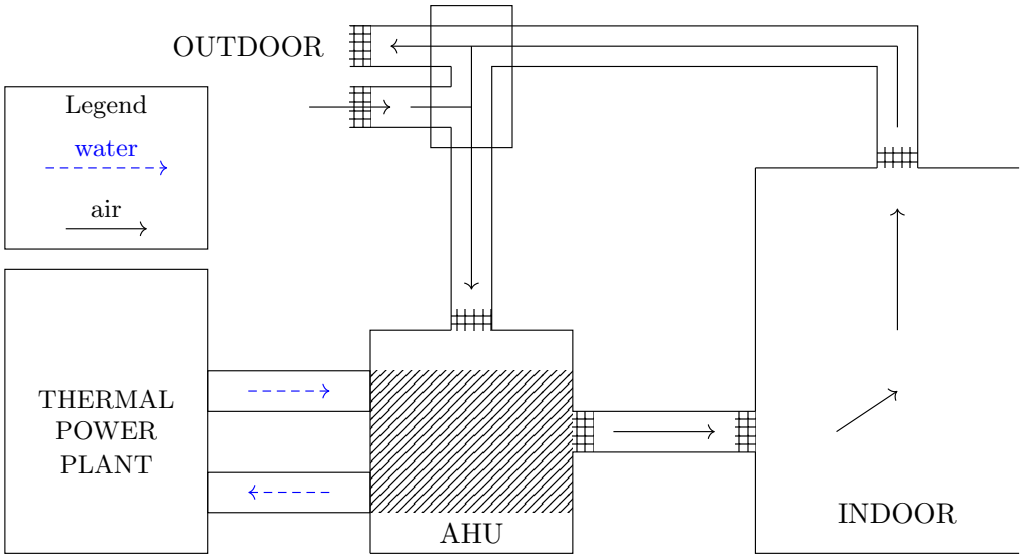

Figure 2.1: Graphical representation of an all air conditioning system.

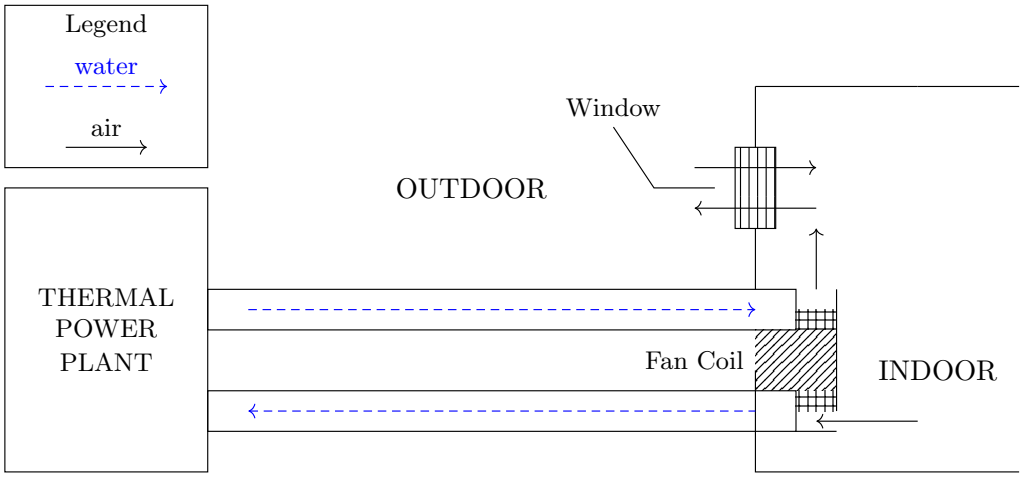

Figure 2.2: Graphical representation of an air/water conditioning system.

of maximum efficiency of the heat pump or chiller, varying the flow rate if necessary. This type of system, reported in Figure 2.2, is well suited to buildings with a split volume in several rooms, such as offices and schools.

These two heating methods, although they allow quick heating and cooling of even large rooms, are not very comfortable. The air movement induced by ventilation is not very pleasant, especially in the proximity of the vents or fan-coils, and produces annoying noises. For this reason, although adopted in large buildings, it is not installed in houses and apartments. In the residential case, the most common type of HVAC system is the air/water

system, although radiators or underfloor heating are used instead of fan-coil units, especially for heating. In a house with radiators, the air in the room is naturally in contact with the radiant elements and due to the phenomenon of convection, it exchanges heat and changes its temperature, introducing natural ventilation. Natural ventilation is better tolerated by the human body, allowing adequate comfort to be maintained. The equation (2.1) describe the heat transfer, although it is more difficult to determine the volume flow rate: indeed, the air flow is not forced but is natural, since it depends on the motions caused by heat transfer by convention. Underfloor heating, on the other hand, uses radiation to transfer heat to the elements, animals, and humans in the room. In this way, natural ventilation is practically absent, achieving greater comfort: the temperature is almost horizontally uniform throughout the overall volume. The heat transfer description is more difficult to obtain, as reported in [87]. In both cases, to modify the room temperature it is possible to change the switch-on time of the water circuit or to vary the fluid flow by means of special valves.

Depending on the heating system used, different sensors are available by default from the manufacturer. In the case of an all-air system, it is available the measure of the temperature of the technical water at the inlet and outlet of the coil, the speed of the air passing through it and the flow rate of the vents. From this data, it is possible to calculate the mass of air entering the room and its temperature, thus being able to calculate the amount of heat released into the room. In the case of a air/water system, it is more difficult to access to precise data per room since, normally, only the values of flow and return temperature and the flow rate of the technical water at the pump are available: the division by rooms is not always present, except in new buildings equipped with remotely controlled valves. However, since 2017, to be compliant with law, energy counters have been installed in the radiators in all Italian apartment buildings. These devices provide a real-time reading of the calories fed into the room by the radiators, i.e., the energy given to the room. For this reason, even with this type of system, it is relatively easy to measure the energy input into a room.

2.4 The Internet Contribute: Weather Status and Forecast

Optimised building control cannot be achieved without knowledge of the status of the external environment. This information allows the temperature in the rooms to be regulated more efficiently and, at the same time, to optimise the operation of the heating plant. Although it is possible to measure the state of the outdoor environment directly on-site using weather stations, it is usually preferred to rely on data from local authority weather stations. This saves costs as this data is freely available on the internet. In Italy, this service is

provided by the regional ARPAs, with hundreds of weather stations located throughout the country. The most important data collected for control and management are air temperature and solar radiation, but they also provide other data, such as air quality data and wind speed, which are useful for analysing the healthiness of the air near the site. In addition to real-time environmental data, the portals of these authorities provide local weather forecasts based on the data collected. As reported in Chapter 5, the use of weather forecasts can reduce consumption and increase comfort. The most useful forecasts are the next day maximum and minimum air temperature, as they allow precise adaptation of temperature profiles. However, the contribution of the internet revolution in building management is not limited to access easily to weather forecasts. The most important feature is connecting the plants and being able to access them remotely, without having to be physically present. Although most control systems are autonomous, regular checks by a professional are essential, both to verify performance and to note maintenance needs. Analyses of system behaviour are very important and require appropriate tools, such as logging software and databases.

2.5 Integrating Heterogeneous Resources into a Single Platform: EPCA

The purpose of an ESCo, as stated in the Italian decree law 115/08, is to provide energy services and other energy efficiency improvements to buildings and plants, and it is paid for these services based on the energy efficiency and performance improvement achieved. To obtain optimal results, an ESCo shall use and exploit all the available data to optimise both the processes during the restructuring and the management phase. The main tasks that an energy manager has to carry out for each plant are numerous and can be divided into day-to-day operations and long-term optimisation operations. The most frequent activities are monitoring and fault detection: the energy manager, through an alarm system, controls the behaviour of the plant and, if there is an alarm, it analyses if it is impacting or not the continuation of the plant activity. If there is a risk of a plant stoppage, it will immediately do his best to define the perimeter of the problem, check whether it can be resolved remotely and, if not, contact the appropriate maintainer. The most important activities for performance are analyses of historical data on plant behaviour. On a regular basis, normally weekly or monthly depending on the volume, the energy manager collects energy consumption data and evaluates it in the light of daily electrical and thermal load curves. In this way, it can determine the performance of the thermal power plant and take action to improve it, depending on the data obtained. An energy manager shall also take into account the variability of weather and occupancy conditions, which can vary

considerably even within the same week. In case the plant is equipped with a power plant for the production of electricity from renewable sources, such as solar panels, in addition to the daily monitoring of alarms, the energy manager has to evaluate very often the daily production: verifying the performance of the production plant is very important since the amount of energy harvested are often linked to state incentives, fundamental for profitability. The main problem for the analysis is the extreme variability of production between different days and even within contiguous time slots. Energy production from photovoltaic panels is highly dependent on the availability and amount of sunlight, and even a passage of clouds can significantly alter instantaneous production. For this reason, it is essential to carry out the analysis by comparing production with meteorological data, in order to determine whether the drop in production is due to less sunlight or to wear and tear on the photovoltaic panels. The impact of dust and soot on the performance of a solar panel should not be overlooked: it is an energy manager's task to determine the best trade-off between the drop in production and the cost of frequent cleaning of the solar panels.

The activities described above are closely linked to the data: the unavailability or difficulty of accessing the data makes the efficient work of the energy manager impossible. All recent BEMS provide rich interfaces for visualisation and quantitative analysis, as well as a database to store all the data collected by the sensors. The problem about relying completely on these products is the lack of interoperability between different brands. Usually, an ESCo uses different BEMS suppliers in different plants, basing the decision on convenience and system adaptability to the plant. However, each supplier is very jealous of its technology and does not allow management of its plant by competing brands software. This leads to fragmentation and makes the energy manager's job difficult, forcing him to look at many different dashboards and not having the situation of all his plants under control at a single glance. In light of this scenario, for the long-term monitoring part, it may be convenient to create a company IT platform that connects to all plants and collects the data provided into a single database. BEMS brands usually provide methods and functions to export the data collected by their sensors on a daily or weekly basis. Using data parsers, it is possible to read this data and load it into an ad-hoc database shared among all plants, thus creating a common analysis for all of them. This is what has been driven to the development of the *EPCA* platform, a web-based platform for monitoring, analysing and accounting for plant consumption developed for EDILVI S.p.A.

The platform is based on HTML/JS technology and Bootstrap framework for the interface whereas we used Chart.js framework for the creation of charts and the display of Key Performance Indicators. The back-end, however, relies on PHP technology for the creation of dynamic web pages whilst the database is managed by a MySQL/MariaDB

Figure 2.3: EPCA software screenshot showing the energy signature of a system.

DMBS. By means of CronJob software, it was possible to execute ad-hoc scripts developed in PHP to analyse and load data from the plants into the database. Some BEMS, in fact, allow to set up a scheduled export of a *.CSV* file to a remote destination via FTP protocol or e-mail. Through the script, started every night, the parser, developed ad-hoc for each plant, reads the data, cleans them and loads them into a dedicated table in the database. The same script is also responsible for downloading the previous day's weather data and loading it into the database. All this data is then analysed and presented in a useful form to the energy engineers: one of the most important KPI is the *energy signature* [88]. An example of it is shown in the Figure 2.3. The image, taken from our software, shows the energy signature of a plant based on weekly date, i.e., the average energy use of the system per week depending on the outside temperature normalised for the hours of use. The energy signature groups the performance of the building and control into a single indicator: the aim is to make it as low as possible to achieve the best savings. The idea is to calculate the energy signature both experimentally and using design data in order to determine similarities and differences between the design and the real counterpart. Obviously, to be able to calculate this indicator and all others, it is essential to have a data logging system from which to extract the necessary data like EPCA.

2.6 Features Required and Exploited in this Work

In this work, we try to use most of the features presented in this chapter in such a way as to provide a result that is in step with the times but, at the same time, implementable today.

Therefore, we avoid using technologies that are immature or very complicated to operate effectively. For these reasons, let us assume that we have to model and control a modern house with an all air system with heat pump controlled by a modern BMS. The controller is connected directly to the BMS and communicates to it the setpoints to be applied to the heating system. The BMS and controller interface with the EPCA platform for logging and exchange of acquired data. Therefore, the design data of the house, the blueprints, and the thermal system are available as well as an internet connection to access the EPCA platform, which we assume is in the cloud. The platform has access to historical weather data and forecasts provided by local or regional weather stations. The EPCA platform has the dual role of storage for the collected historical data and acquisition for the forecast data. We collect various data on a daily basis from the weather station: the maximum and minimum outside temperatures of the location where the house is built and the maximum solar radiation. In the design phase, we also use daily profiles of these data, with a sampling time of a quarter of an hour. From the building, on the other hand, we collect, every minute, the temperatures measured in each room by the thermostats, the percentage of opening of the vents, the supply and return temperature of the technical water to the coil, as well as the fan speed, which gives us the air flow rate. With these measurements, we can estimate the amount of thermal energy supplied to each room: the controller controls the energy supplied to each room and then the BMS takes care of transforming this value into a percentage of opening of the vents. In fact, in order to improve energy efficiency, the supply temperature of the technical water shall be set at the best working point of the heat pump, i.e. the one that gives the best COP.

3

Building Model

This chapter introduces the modelling techniques that were exploited to create the building model. We used white box methodology based on the Lumped-Parameter Method (LPM): the approach we choose is often identified as 2R1C. We also use this approach because of the wide availability of data on buildings: Italian legislation, with Law 10 of 1991 and Ministerial Decree 37 of 22 January 2008, requires planners to draw up a technical report for each new or renovated building, also known as *ex Legge 10*, listing all the materials used in the construction of the building and their characteristics such as resistance, thermal capacity, and reflectance. The report must also describe how these materials make up the various elements of the building, such as walls, floors and windows, with their surface area and position. This makes it very easy to obtain the data to construct a physical model of a building.

3.1 A Primer to Heat Transfer

In order to model a building from a thermal point of view, it is necessary to start by describing heat behaviour in fluids and solids. The first step to be performed are to provide a definition of heat and to define the perimeter within which we will move by means of some assumptions.

Heat is defined as the amount of energy transferred between two systems or between two

parts of the same system, not attributable to thermodynamic work, to a conversion between two different types of energy or to transfer of matter. The transfer takes place from the hotter to the colder body until the two bodies reach an equal temperature, as described in the second principle of thermodynamics.

The transfer of heat between systems can take place in three different ways [89]. The first is by conduction and happens when the two bodies are in contact: the heat flows from the hotter to the coldest through the common contact area. The second is by convection and it takes place when a fluid, between two bodies, is in contact with the walls of both and subjected to the force of gravity: the different temperatures within the different parts of the fluid (due to conduction transfer with the surfaces) create a gradient and, with the help of gravity, the fluid sets itself in cycle motion carrying heat from one body surface to another, until equilibrium is reached. The third is by radiation: bodies that are not in contact exchange energy via electromagnetic waves, from the hottest to the coldest.

One of the earliest descriptions of the transfer of energy between two bodies by conduction is the famous postulate of Fourier on thermal conduction. Let us take a material in which the phenomenon takes place, an infinitesimal plane of area dA and a line normal to the plane. Inside the material, let P_1 and P_2 be two points lying on that line, dn apart, one above the plane and one below. If the two points are at temperature T_1 K and $T_2 = T_1 + dT$ K (a Dirichlet boundary condition), then there will be a heat exchange between the two points P_1 e P_2 described as follows:

$$dQ = -\lambda_n dA \frac{dT}{dn} d\tau$$

where λ_n represents the thermal conductivity of the material and $d\tau$ the infinitesimal time. In the simplest and most common case, heat transfer occurs between two outer surfaces of a conducting material. Let the material be in the form of a parallelepiped of thickness s and area A and let the heat propagate along the direction of the thickness. Integrating by space and time, the equation describing the heat flux $\dot{Q}$, measured in W, can be rewritten as follows:

$$\dot{Q} = -\lambda_n A \frac{T_2 - T_1}{s} = \frac{\Delta T}{R} \tag{3.1}$$

where $\Delta T = T_1 - T_2$ represents the difference of the two surfaces temperatures and $R = \dfrac{s}{\lambda_n A}$ the thermal resistance of the body. Thermal resistance is measured in $\mathrm{K\,W^{-1}}$ and allows to connect mathematically heat propagation and electrons behaviour. Indeed, the fall of potential ΔV at the ends of a resistor R due to the current I flow is well described by the

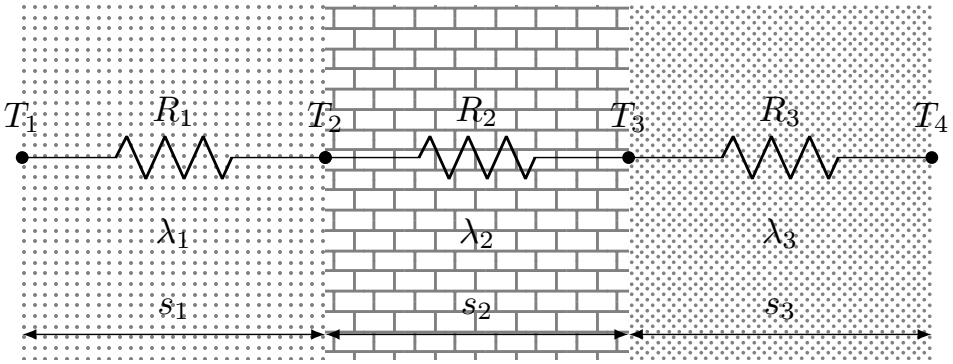

Figure 3.1: Heat flow through different surfaces using the electrothermal analogy.

famous Ohm's law:

$$\Delta V = RI$$

making the two descriptions analogous by associating the heat flow $\dot{Q}$ with the electric current I and the temperature difference ΔT with the potential difference ΔV. Obviously, the law also applies in the case of several parallelepipeds in contact with each other along the direction of thickness, since the Fourier postulate shows the linearity of the gradient temperature, after taking into account λ. In this case, using the analogy just described, the resolution is immediate and much easier than integrating the Fourier postulate for the different materials. Let $\lambda_1, \ldots, \lambda_n$ be the thermal conductivity of the n materials, all linked to the following through a surface of area A. The thickness of each material is instead defined by s_i, $i \in [1, n]$. Therefore, the thermal resistance for each section is $R_i = \dfrac{s_i}{\lambda_i A}$. As reported in Figure 3.1, by means of the analogy, the heat flow between the point at temperature T_1 and the point at temperature T_4 in that situation is equal to the flow through a material with thermal resistance equal to the sum of the three individual resistances, i.e, $\dot{Q} = \dfrac{T_1 - T_4}{\sum_i R_i}$. This is very useful for describing bodies composed of different elements, as in the case of the walls of buildings, which are composed of several vertical layers to optimise insulation and tightness. According to heat transfer theory, this approximation works only if the Biot number is smaller than 0.1. This guarantees the temperature difference between the middle and surface of the material is less than 5%, thus it can be assumed the internal temperature distribution to be uniform [90]. As reported in [91], all building elements are well below this threshold, allowing us to take advantage of this simplification

Exchange by convention can also be traced back to an equivalent Ohm law, as reported by Newton in 1701. According to his law, let T_s K be the temperature of the surface of the body in contact with the fluid at temperature T_f K. Then, the modulus of heat flow is defined as follows:

$$|\dot{Q}| = \alpha_c A |T_s - T_f| \tag{3.2}$$

where A is the area of the surface in contact with the fluid and α_c is *convective heat transfer coefficient* in $\mathrm{W\,m^{-2}\,K^{-1}}$. As in the previous case, the electrothermal analogy can also be emphasised here by defining $R = \dfrac{1}{\alpha_c A}$. Unlike the law of conduction, this is an approximation of reality and its applicability must be assessed on a case-by-case basis. In the case of low-speed motions, such as air in buildings, the law is sufficiently precise. For example, in [92, Table 14.2], some convective heat transfer coefficients are reported: for free air, the coefficient can be picked between 2.5 and $25\,\mathrm{W\,m^{-2}\,K^{-1}}$, depending on fluid velocity and temperature difference. In [93], a review of the main methods for calculating this value in buildings are presented. It can be seen that almost all works agree that, for unforced air, it is correct to choose a value around $3\,\mathrm{W\,m^{-2}\,K^{-1}}$ since the temperature difference is normally below 10 K.

The third way of exchanging heat between different bodies is by radiation. The description of this behaviour is provided by Plank's law for black bodies, an extension of Stefan-Boltzmann's law. The simplest version defines the heat flow $\dot{Q}$ between two bodies, not necessarily in contact, one at temperature T_1 K, the other at temperature T_2 K, as:

$$\dot{Q} = \epsilon \sigma F_{1\to 2}(T_1^4 - T_2^4)$$

where $\epsilon \in [0, 1]$ is the emissivity, $F_{1\to 2}$ is the view factor, and $\sigma \simeq 5.67 \times 10^{-8}\,\mathrm{W\,m^{-2}\,K^{-4}}$, the Stefan-Boltzmann constant. The view factor represents how much radiation from the first body is intercepted by the second and depends only on the distance and surface geometry of the two bodies. If the surfaces are Lambertian, it is possible to switch to the double integral and calculate the value in closed form precisely, since the individual infinitesimal contributions are weighed only by the cosines of the angles between the normals of the two infinitesimal areas and the line joining the centres, (θ_1, θ_2) i.e.,

$$F_{1\to 2} = \frac{1}{\pi A_1} \int_{A_1} \int_{A_2} \frac{\cos\theta_1 \cos\theta_2}{\mathrm{dist}(dA_1, dA_2)}\, dA_1 dA_2$$

In the case of buildings, the contribution of this type of transmission is negligible except for solar radiation. In this case, however, it is possible to provide a more precise description

using a different treatment, as reported in Section 3.3.

So far, the discussion has focused on defining the amount of heat transmitted from one body to another. From the principles of thermodynamics, the heat flow goes from the hotter body to the colder one and stops when the two bodies have reached equilibrium. To determine and describe this heat behaviour in bodies, it is necessary to introduce the notion of internal thermal energy of the body:

$$U_T(T) = \rho V c_v T$$

where ρ is the density, V the body volume, c_v is the specific heat at constant volume and T the temperature. From the principle of conservation of energy, excluding all work contributions ($\Delta L = 0$) and phase change of the material, the energy balance for a full heat transfer to a body with temperature T to a body with temperature $T_2 > T$ in $\mathcal{T}$ s thanks by conduction can be written in this way:

$$\int_{t=0}^{\mathcal{T}} \dot{Q}\, dt = U_T(\Delta T) + \int_{t=0}^{\mathcal{T}} I \Delta V dt$$

where $\Delta T = T_2 - T$ is the difference of temperature and $I\Delta V$ represents the Joule effect for the passage of a current I through the material with a potential difference ΔV. Assuming zero the latter, which we only need later for thermal control, and moving to an infinitesimal time from the (3.1):

$$\dot{Q} = \frac{\Delta T}{R} = \frac{U_T(dT)}{dt} = \rho V c_v \frac{dT}{dt}$$

where dT is the change in temperature of the body during infinitesimal time dt. Rearranging the formula gives

$$\dot{Q} = \frac{T_2 - T}{R} = C\frac{dT}{dt} \tag{3.3}$$

where $C = \rho V c_v$ is the heat capacity in $\mathrm{J\,K^{-1}}$. The formula is analogous to a first-order differential equation of charge of the electric capacitor:

$$RC\frac{dT}{dt} + T = T_2 \rightarrow RC\frac{dV}{dt} + V = V_0$$

and a solution for $T = T(t)$ is:

$$T(t) = (T(0) - T_2)\, e^{-\frac{t}{RC}} + T_2$$

where $T(0)$ is the temperature of the body at the start of the heat transfer.

This concept, described here for body-to-body exchanges, can also be extended to body-to-bodies exchanges, again using the electrothermal analogy. As shown in the following section, it is possible to combine all these exchanges and create a complete electrical network. A summary about analogy between thermal and electrical quantities is reported in Table 3.1.

Table 3.1: Analogy between thermal and electrical quantities

Thermal			Electric		
Quantity		m.u.	Quantity		m.u.
Temperature	T	K	Potential	V	V
Temperature Diff.	ΔT	K	Voltage	ΔV	V
Thermal Flux	$\dot{Q}$	J/s = W	Electric current	I	A
Resistance	R	K/W	Resistance	R	Ω
Capacitance	C	J/K	Capacitance	C	F

3.2 2R1C Modelling Technique

As reported in previous section, the description of heat behaviour in fluids and solids can be simplified without great loss of information by using first order differential equations. This makes it possible to obtain models that are accurate but at the same time not too complex and applicable to control. The approach we have followed is the lumped parameter method (LPM): in this case, each element of the building is described by means of a differential equation. It is essential to define what the elements of a building are and what their characteristics are in order to choose the right description for each one.

3.2.1 Elements of a Building

Several architectural elements constitute a building. Each element has a particular description of the heat exchange with the surrounding environment, but it is possible to simplify the treatment by dividing the elements into two groups according to their thermal inertia. The first group is composed by elements with high thermal inertia, such as external walls, foundations, floors, and roofs. These elements are very voluminous and massive, and they retain heat for a long time. The other group consists of elements with low thermal inertia, such as windows, doors, and internal walls. Room air is excluded from this subdivision: due to its particular behaviour, a individual analysis is performed.

The elements of the first group, since they have an appreciable thermal inertia due to their high heat capacity, can be described using the equation (3.3). Using this equation,

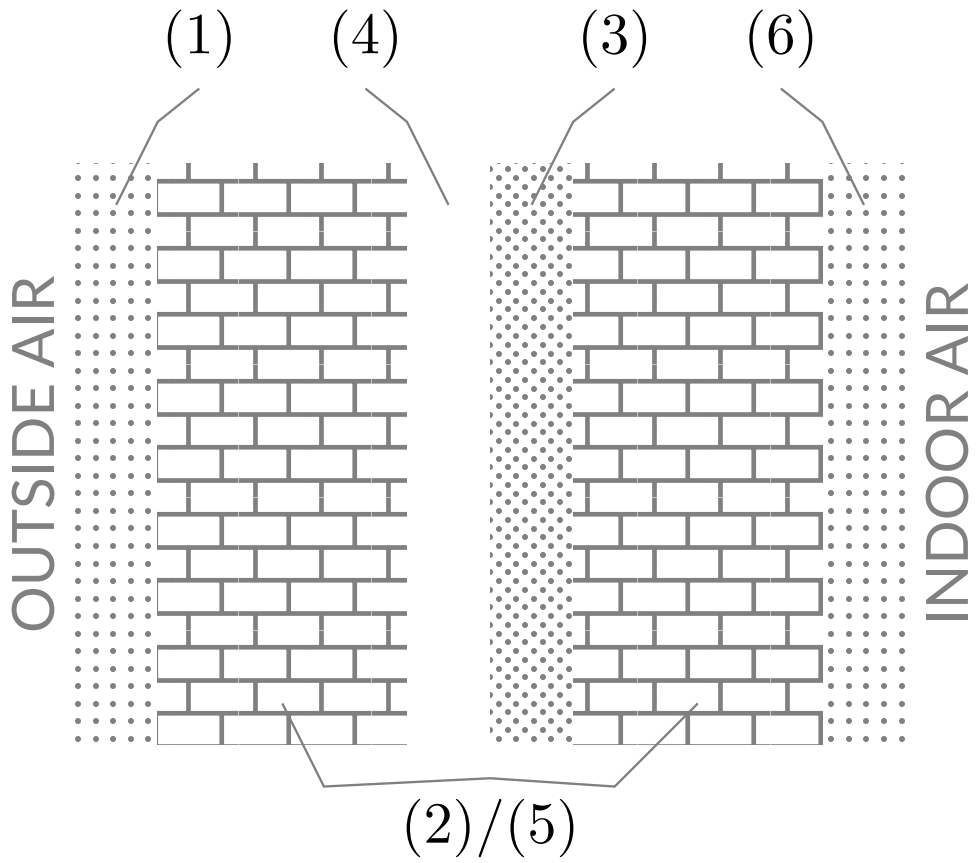

Figure 3.2: Statigraphy of a external wall: gypsum plaster (1), bricks (2), air (3), insulation (4), bricks (5), interior layer (gypsum plaster and paint - 6)

let us assume, as it is usually the case to improve thermal performance [94], that we are modelling an external wall composed of several layers. In fact, an external wall is usually composed, starting from the outside, of a layer of pure gypsum plaster, a layer of perforated bricks before an air gap. Then, there is a layer of insulation before meeting another layer of perforated bricks. The final layer is composed by interior gypsum plaster and paint. An example is shown in Figure 3.2. Each of these layers exchanges heat horizontally with both the previous and the next layers: to take that into account, it is necessary to modify the equation (3.3). Let us consider a layer l which is in contact with layer l_{-1} and l_{+1}. We assume that the temperature is uniform throughout the layer: the considered layer is at temperature T whereas the other two contacting surfaces are at T_{-1} and T_{+1}. Since the heat transfer occurs by conduction, we can exploit (3.1). Therefore, each layer transmits to

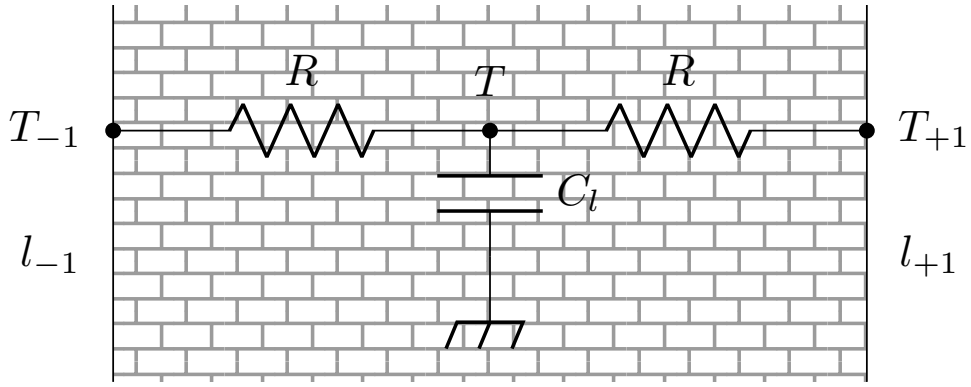

Figure 3.3: Electical model of heat transfer from layer l_{-1} to layer l_{+1}.

layer l the following heat flow:

$$\dot{Q}_{-1} = \frac{T_{-1} - T}{R} \quad \text{and} \quad \dot{Q}_{+1} = \frac{T_{+1} - T}{R}$$

where $R = \frac{R_l}{2}$ by assuming to measure the temperature in the middle of the layer, as suggested by [95]. Combining everything with (3.3), we obtain that the layer has the following behaviour [96]:

$$C_l \frac{dT}{dt} = \dot{Q}_{-1} + \dot{Q}_{+1} = \frac{T_{-1} - T}{R} + \frac{T_{+1} - T}{R}$$

where C_l is the thermal capacity of the layer l. The following equation is equivalent to the electrical circuit reported in Figure 3.3.

By reproducing this description for all layers, a complete model of the element's behaviour can be obtained. The circuit consists of a series of resistors interspersed with capacitors. However, the model is too detailed for our target: therefore, it is usual to group the resistors and capacitors together in order to reduce their number. Depending on the reduction, several modes are obtained: the most widely used is 2R1C, which describes the entire element by grouping the behaviour of the individual layers into a total of two resistors and one capacitor. The heat capacity of each layer is summed up into one while the total resistance is normally divided into the two resistances equally, although it is possible to make the parameter free to be fit by a system identification technology. Also widely used is the 3R2C mode, in which three resistors and two capacitors are used, arranged as in Figure 3.4. Even in this case, the physical quantities are split equally among all elements, for example as reported in [97]. The description carried out for the external wall is equal also for roofs, foundations, and

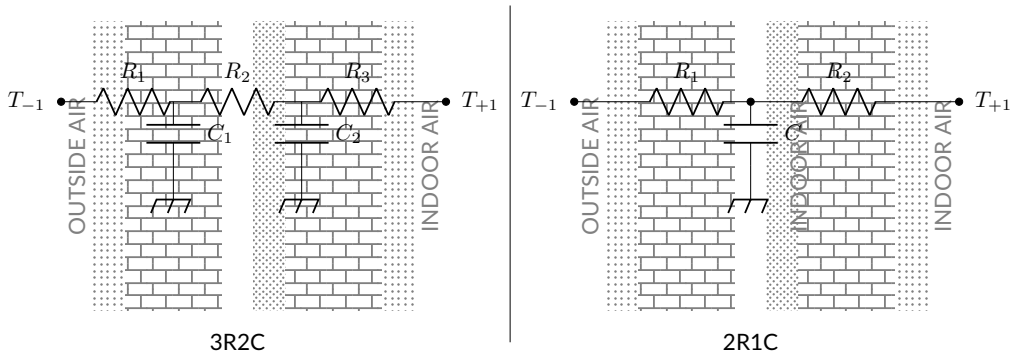

Figure 3.4: Differences between the 3R2C and 2R1C approaches to modelling an external wall.

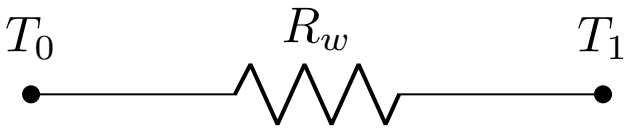

Figure 3.5: Electric equivalent model of a heat exchange through an internal wall.

floors since they all share the same construction model and features.

Unlike the previous elements, elements with negligible thermal inertia can be modelled by directly exploiting the equation (3.1), since the heat transfer is made by conduction. These elements, such as windows [98, 99], doors and internal walls, can be fully describe by a single thermal resistance. Therefore, given two rooms at temperatures T_0 and T_1 divided by an internal wall, the heat flux exchanged through the wall is:

$$\dot{Q} = \frac{T_0 - T_1}{R_w}$$

where R_w is thermal resistance of the internal wall. The equivalent RC model can be obtained, as shown in Figure 3.5, by means of a single resistor linking the two states.

By means of the elements described in this section, we are able to describe the thermal behaviour of the main solid components of a building. The only element left uncovered, but at the same time the most important one, is the air that permeates the rooms. We are interested in knowing the air temperature of the rooms in order to be able to control it. In most of the literature, it is preferred to describe the behaviour of the air mass only from the point of view of the heat capacity, thus using only a condenser, and assuming that the thermal resistance is negligible. This choice, made for example in [41] and in [100], depends

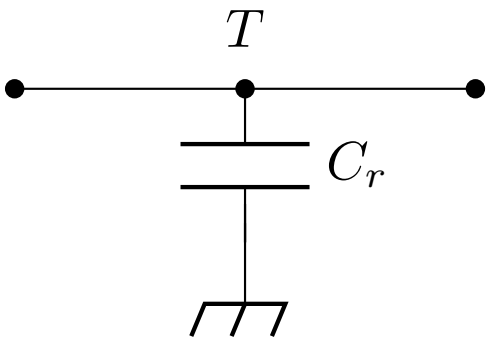

Figure 3.6: RC model for heat behaviour of air.

on the low weight of air in the dynamics of a building. In some works, like [101], only furniture is considered. In other works, indeed, the description is completely omitted and the node is left without thermal capacity, as in [34]. For this reason, even if heat exchange by convention happens, thus requiring using equation (3.2), this part is omitted and it is assumed that only conduction exchanges take place. The explanation can be found in the values of the quantities involved: air has a heat capacity of about $1\,\mathrm{kJ\,m^{-3}\,K^{-1}}$ whereas for building elements, in this case bricks, this value is about $1.6 \times 10^6\,\mathrm{kJ\,m^{-3}\,K^{-1}}$. Although the volumes may be very different, a difference of more than six orders of magnitude demonstrates the lack of relevance of modelling the impact of indoor air on the total building dynamics.

For the sake of completeness, we nevertheless decided to model the air in the room using a single condenser but omitting resistors. This approach was also chosen to simplify the resolution of the network: as reported in section 3.5, the model allows us to know the voltage, and therefore the temperature, only at the ends of the capacitors. Consequently, we would have been forced to define a dummy capacitor to obtain the temperature value of the rooms: given this constraint, instead of using dummy values, we decided to use the standard air heat capacity for the volume of the individual rooms plus a contribution for furniture, taking inspiration from [102]. The contribution we have added is $c_f = 30\,\mathrm{kJ\,K^{-1}}$ per square metre of floor space in the room. Consequently, the interior of a room has been modelled as follows:

$$C_r = \rho_a c_{p_a} V_r + c_f S_r \tag{3.4}$$

where C_r is the modelled thermal capacity of the room, V_r its volume whereas S_r the floor surface. Note that $\rho_a = 1.204\,\mathrm{kg/m^3}$ is the air density at $20\,^\circ\mathrm{C}$ and $1\,\mathrm{atm}$ pressure and

$c_{p_a} = 1007\,\mathrm{J/kg/K}$ is the air specific heat at 20 °C and 1 atm pressure. We decided to use these conditions because they are the most representative of a real scenario in which this work could be applied. The electric components used to model air in room are shown in Figure 3.6.

3.3 Disturbances modelling

To predict the behaviour of the real building in a useful way, it is also mandatory to model the surrounding environment and connect it to the description obtained in the previous section. Indeed, a full functional virtual environment shall take into account external causes that modify its internal temperature. There exist three main causes of a temperature variation within a building: external temperature, sunshine, and internal loads. A graphic representation is reported in Figure 3.7.

The first effect tries to impose a temperature on the building until when the external temperature is the same as the internal one: when an equilibrium temperature is reached, heat exchange stops. This is derived from the modelling of heat transfer by conduction, as reported in (3.1). The other two, instead, try to change the temperature of the building by directly supplying heat to it, regardless of its actual temperature. In fact, these types of loads do not have an equilibrium temperature and are ideally equally effective across the temperature range of the individual elements. In the case of sunshine, the heat exchange takes place by radiation but the temperature difference between the Sun and the building elements is so great that the energy exchange can be approximated as depending only on the temperature of the sun and therefore independent of the state of the elements. For internal loads, on the other hand, this description is a simplification of heat transfer: since internal loads, whether living or inanimate, dissipate a power that is easily measurable, it is simpler to assume a contribution of that amount of heat power without modelling the whole heat transfer model. Take, for example, a television set: since it does not produce mechanical work, all the used electrical energy must necessarily be transformed into heat and released instantaneously into the surrounding environment.

These two behaviours can be described, by means of the electrothermal analogy, by an ideal voltage or current sources. A voltage source, in fact, imposes a voltage (a temperature) to load terminals, regardless of the current required to maintain this potential difference. A current source, on the other hand, imposes a current, i.e., provides a flow of heat, between the load terminals, regardless of the voltage applied. These two behaviours perfectly describe respectively the contribution of external and ground temperatures and the internal loads or solar heat. Usually, ground temperature is set constant at T_g °C since its influence on

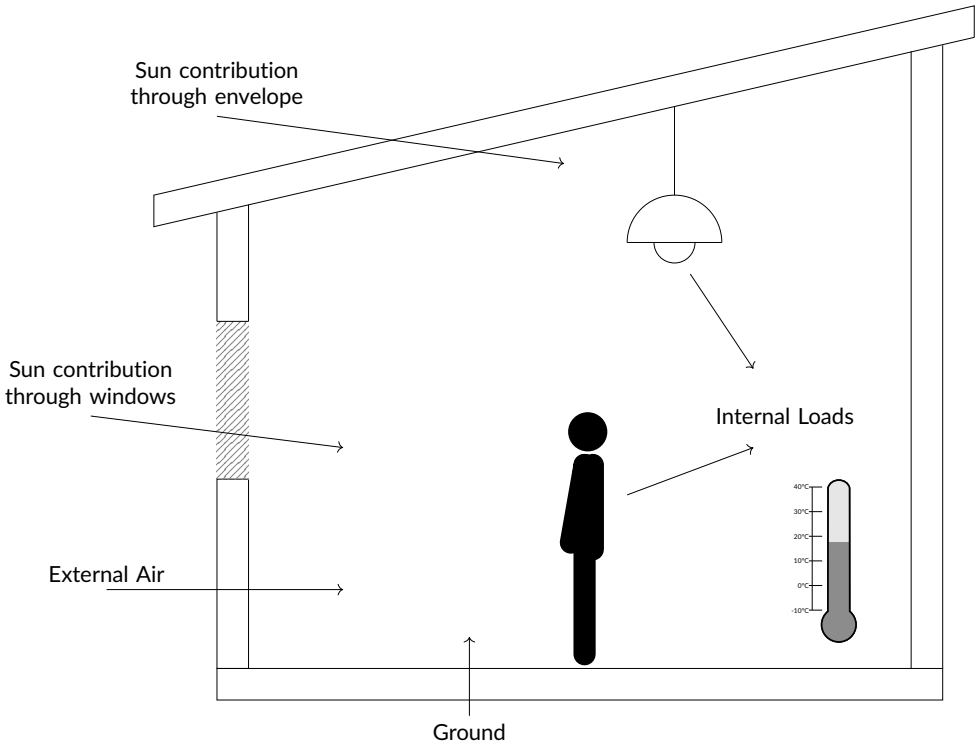

Figure 3.7: Building Energy Balance

model dynamics is very small [103]. A RC representation of these two types is reported in Figure 3.8. Voltage sources, one representing external air and one representing the ground, shall be connected to all the blocks in contact with them respectively. The generator voltage must be equal to the instantaneous disturbance temperature. Current sources, instead, shall be connected only to the capacitor inside the node. The supply current must be equal to the power fed into the environment: in the case of internal loads, the electrical power dissipated. This is not strange because the units of heat flow are in fact nominally equal to the heat output since they represent the same physical phenomenon. In the case of the Sun, an ad-hoc analysis, reported in the subsection 3.3.1, should be carried out, since the effect of the sun is both on external surfaces and on internal rooms through the contribution of windows.

3.3.1 Sun Radiation

The Sun contribution to the heating of a building is not negligible and, especially in summer, it is very appreciable, also from the point of view of energy saving. The Sun's rays strike

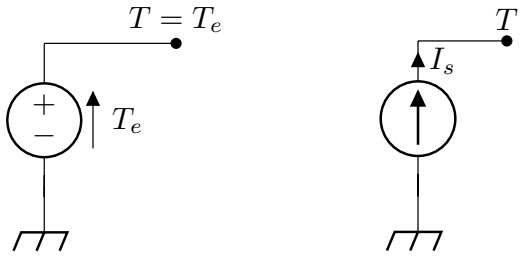

(a) External Temperature **(b)** Internal Load/Sunshine

Figure 3.8: An External Temperature and Internal Load/Sunshine 2R1C blocks.

and heat all the external surfaces of the building, each at a different angle. Even more precise methodologies can be used, such as the one reported in [104] that use historical data, we describe its impact exploiting Lambert's cosine law and the position of the Sun in the sky. This law states that the amount of radiation E on a surface caused by a light source of intensity I is:

$$E = \frac{I}{r^2} \cos\gamma = p_s \cos\gamma$$

where γ is the angle of incidence and r the distance from the light source. Since, in our case, r is the distance of our surface from the Sun, we can approximate it as a constant and substitute $p_s = \frac{I}{r^2}$: this is the power that the Sun radiates on the ground per unit area. A graphic representation of the idea is shown in Figure 3.9. To describe the Sun impact with respect to the envelope and to calculate the amount of heat that actually reaches the envelope surfaces, there are two different problems to face: estimate the intensity at the ground p_s and the angle γ of incidence of Sun rays with the surface, i.e., the position of the Sun in the sky.

Nowadays, the first problem can be solved by relying on online services, even free of charge, that provide direct sunlight in real time given a location. It is also possible to install a light sensor, which nowadays are very cheap. If the building is equipped with solar panels, as required by the latest building regulations, it will be sufficient to check the output of the solar panels to obtain a good estimate, for control purpose, of the solar radiation in real time. With one of these three methods it is possible to obtain accurately and real-time the power radiated by the sun at the surface $p_s(t)$.

To solve the second issue, the faster and cheaper way is to model the Earth motion of rotation and revolution. During the day, indeed, the apparent position of the Sun changes and walls that at one time of the day are directly lit, at others are shaded. Furthermore,

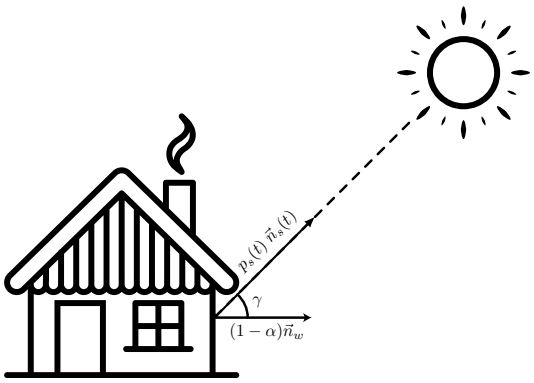

Figure 3.9: Model of the incidence of sunlight on the external surfaces of a building.

during the year, the apparent direction of the Sun rays changes and this influences the amount of heat absorbed by the envelope. Practically, to determine the angle γ, we calculate the dot product between the vector representing Sun ray direction and the normal of the surface. We assign to each surface of the envelope a 3D vector representing the outer normal $\vec{n}_w \in \mathbb{R}^3$ and model, by means of algorithms such as [105], the vector representing the Sun's rays direction $\vec{n}_s(t) \in \mathbb{R}^3$ given the day and the time t, and the latitude.

It should not be forgotten, however, that every surface has an albedo, i.e. it reflects part of the incident radiation. Therefore, we weigh each input using $1 - \alpha$, where $\alpha \in [0, 1]$ represent the surface albedo. For example, concrete has $\alpha \in [0.2, 0.4]$ whereas the roof area has an albedo around 0.20. This particular is very important, as reported in [106]. Therefore, the formula we use to estimate the Sun's contribution for each envelope surface is:

$$p_w(t) = A_w \ (1 - \alpha) \ p_s(t) \ \vec{n}_w \cdot \vec{n}_s(t)$$

where A_w is the surface area and $p_w(t)$ is the instantaneous current flow in the ideal supply connect to element w. If the surface is transparent, as in the case of windows, the current flow is applied directly to the internal node representing the room. In this case, instead of the albedo, the solar heat factor $g \in [0, 1]$ is used, which represents the amount of solar energy that the glass (or other material) lets through. A $g = 1$ represents full transmittance while 0 represents no solar energy transmittance: usually, $g \in [0.2, 0.7]$. Consequently, the formula in the case of windows becomes:

$$p_w(t) = A_w \ g \ p_s(t) \ \vec{n}_w \cdot \vec{n}_s(t)$$

where A_w is the window area and $p_w(t)$ is the instantaneous current flow in the ideal supply connect to the respectively room.

3.3.2 People Impact

A human being in a building is not only the target for comfort, but also a potential disturbance for control. A person, on average, introduces about 120 W of heat [107] into the environment thanks to its metabolism, depending on the activity it is performing and the type of clothing it is wearing [108]. Although there are many studies concerning the modelling of occupancy, in this work we decided not to model people's behaviour. In order to make the model realistic, we decided to use average occupancy values, as reported in [109], in [110], and [107]. Merging the different works together, we decided to use a value of 40 W m^{-2} as internal gain value per area: this value also includes other internal loads, such as household appliances, since we desire to use a single value to simplify the treatment. Consequently, once we calculate the value for each room, we design the internal load as explained in the Section 3.3.

3.4 Controllable Inputs

The last part that remains to be modelled are the controllable inputs, i.e. the inputs that are managed by the controller to heat the rooms. Because of the way the all-air heating system is constructed, we can model it as a collection of controllable heat power input that provides to each room a different instantaneous heating power. The data we can access to are the amount of opening of the vents, the air speed, and its temperature, calculated as the average between the supply and return temperatures of the technical water to the coil. Knowing the cross-section of the ducts and their disposition, we can determine the amount of air supplied into the room per instant of time and consequently the energy supplied per unit of time. Therefore, the system can be decoupled for each room and represented as a collection of independent power inputs, each with different power and connected to only the condenser representing the air mass of the room to which it relates. Since these inputs provide energy to the room, they can be modelled in the same way as internal loads. For this reason, these inputs can be represented with an ideal current generator, such as the one shown in Figure 3.8b.

3.5 Obtaining a State Space Model

In previous sections, a method for thermal modelling the elements that make up a building were presented. The elements interact with each other from a thermal point of view and, therefore, an useful model must describe their interactions. An electric circuit is a good way of presenting the interconnections between different elements. The connection of elements that exchange heat can be represented by connecting the two ends of the components to each other. By performing this operation for all components, an electrical network of resistors and capacitors is obtained, as in Figure 3.10. Although graphically impressive, this representation is difficult to manage mathematically. For this reason, it is preferred to transform the graphical representation into a more mathematically one. Since the relationships between the components are linear, it is possible to reduce the circuit to a state space model: indeed, it would be very quick to evaluate system properties and develop effective controllers. The method we take inspiration from is described in [111].

Without loss of generality, to describe the model we take care only of ideal current sources, with or without shunt resistors. Since voltage sources represent external or ground temperatures, they are always connected to a wall block: i.e., they are always represented as a voltage source connected in series to resistors. Therefore, it is possible to apply the Norton theorem and obtain an ideal current source in parallel with a shunt resistor. A graphic example is shown in Figure 3.11. We also assume that there are not null capacitances or resistances, and two or more resistors connected in series. These do not make us lose generality since it is always possible to reduce a series of resistors to a single one with resistance equal to the sum of each resistors in the series.

Let N_w be the number of external walls, N_r the number of rooms and N_f the number of windows. Since only rooms and walls are modelled by means of capacitors, let us define $N = N_w + N_r$.

Let $C \in \mathbb{R}^{N \times N}$ be the diagonal matrix containing all the model capacitances, i.e., $C_{ii} = C_i$, $i \in \{1, \dots, N\}$. Since they are the only dynamic parts of the model, we number them, order them, and we refer to them as node n_i. Obviously, since we use only positive capacitances, the matrix is positive definite. Similarly, let $R \in \mathbb{R}^{N_e \times N_e}$ be the diagonal matrix of resistors, i.e., $R_{jj} = R_j$, $j \in \{1, \dots, N_e\}$, where R_j indicates the j-th non-shunt resistance and N_e the total number of non-shunt resistors in the circuit. It is immediate to note that resistors can be seen as edges of a graph in which the nodes are the capacitors. It is useful to exploit this concept by introducing some specific graph matrices.

Let $\Gamma \in \mathbb{R}^{N \times N_e}$ be an oriented incidence matrix, i.e., the matrix that links nodes and

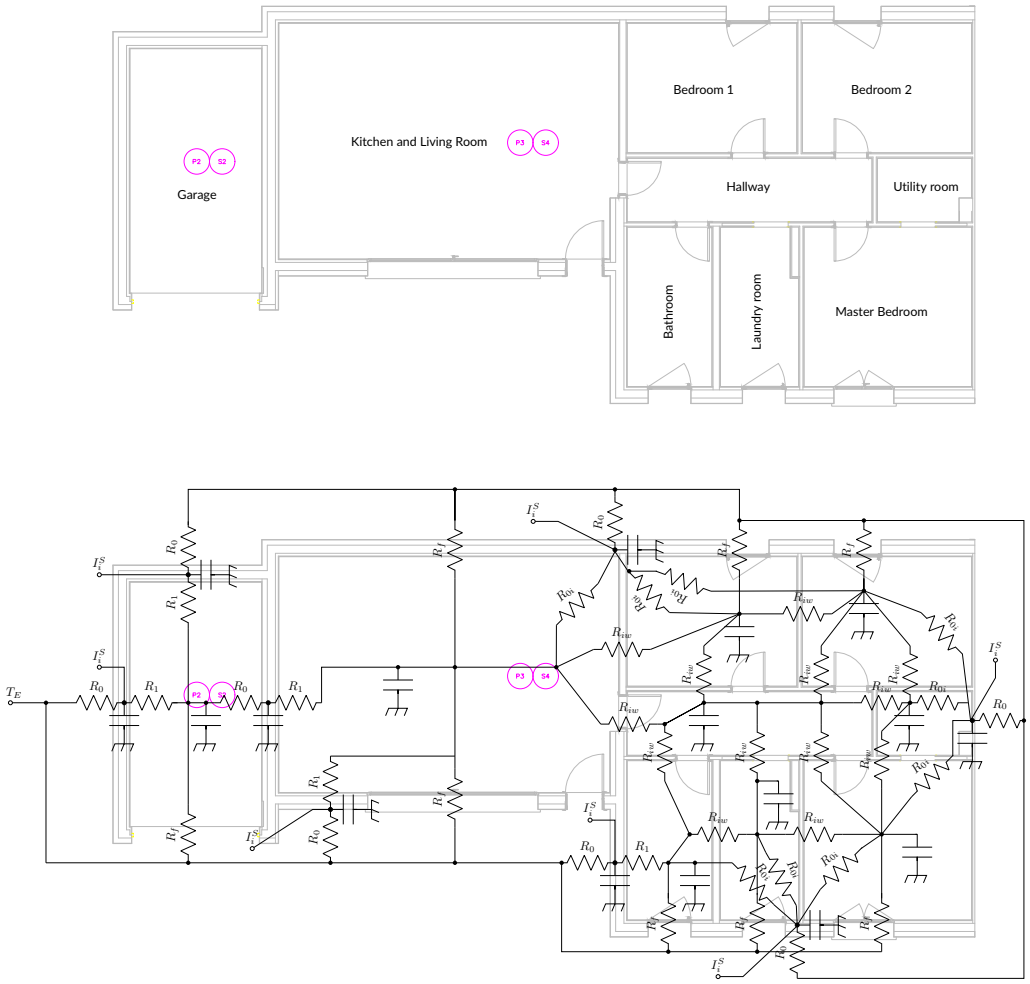

Figure 3.10: An example of modelling a house using an RC model.

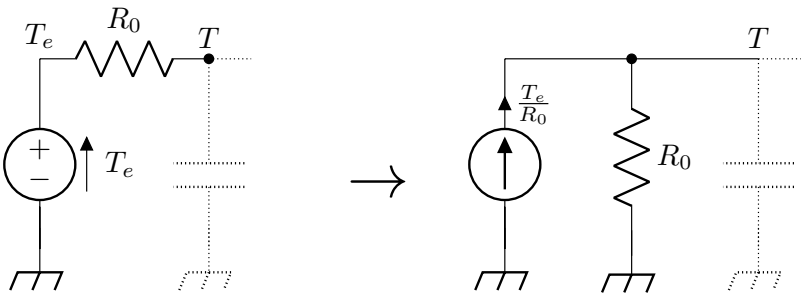

Figure 3.11: Equivalence between a voltage source and a current source.

edges. This matrix is defined as follows:

$$\Gamma_{ij} = \begin{cases} +1 & \text{edge } R_j \text{ starts from node } n_i \\ -1 & \text{edge } R_j \text{ ends into node } n_i \\ 0 & \text{otherwise} \end{cases}$$

This operation is very simple and can be automated, since the arcs indicate the resistors of the RC circuit and the nodes represent the capacitors. The orientation of the resistors is completely free, but, when it is defined, it shall be not changed in any phase of the process. To reduce possible errors, it is recommended to use the the passive sign convention (PSC) in the RC network. Furthermore, to simplify the treatment, we define $\mathcal{L} = \Gamma R \Gamma^\intercal$ as an irreducible Laplacian matrix.

Let $S \in \mathbb{R}^{N_s \times N_s}$ be the diagonal matrix of shunt conductance, i.e., the conductance parallel to the ideal current sources: their number, N_s, shall be the number of resistances in series to the voltage sources that represent the outside temperature and the ground temperature. Indeed, by the Norton procedure, each of them is transformed into a shunt conductance. The matrix is defined as $S_{kk} = 1/R_k^s$, $k \in \{1, \ldots, N_s\}$ where R_k^s is the k-th shunt conductance. Obviously, since the shunt resistances represent physical values, the matrix is positive definite.

Finally, let I^* be the column vector describing the current flows at the nodes due to the effect of external sources, i.e. the ideal current sources, where I_i^* is the current that flows into node i. I_i^* consists of several contributions, not all of which are always present: the external temperature, i.e., T_e/R_0^i, the ground temperature, i.e., T_g/R_0^i, the sun contribution I_i^s, internal loads I_i^l, and manipulating inputs I_i^c.

As reported in [111], by exploiting these matrices, it is possible to obtain the voltage circuit behaviour. Indeed, the network behaviour can be described by means of this equation:

$$\dot{V}(t) = \underbrace{-C^{-1}(\mathcal{L} + S)}_{F} V(t) + \underbrace{C^{-1} I^*}_{GU}$$

By identifying the voltage of the nodes as the state of a system, this equation can be rewritten as a state space model. Indeed, the transition matrix of states F and the contribution of external inputs GU, i.e., the effects of current sources, can be clearly identified. To improve the representation, the inputs can be rewritten as follows, highlighting the different causes

involved in the system:

$$G = [G_e|G_g|G^s|G^l|G^c]$$
$$U = [T_e, T_g, I_1^s, \ldots, I_N^s, I_1^l, \ldots, I_N^l, I_1^c, \ldots, I_N^c]$$

by identifying with subscript e the contributions from the outside temperature, with subscript g the contributions from the ground temperature and with superscripts s and l the contributions from the Sun radiation and internal loads for each room respectively. This representation takes also care of controllable inputs: they are identified by superscript c and, in our work, are equal to internal load values since we do not model the HVAC systems.

The overall 2R1C model of the building in a state-space representation can be represent as follows:

$$\begin{aligned} \dot{x}(t) &= Fx(t) + Gu(t) \\ y(t) &= Hx(t) \end{aligned} \tag{3.5}$$

by defining H as selection matrix: this matrix selects only the rooms that can be measured, i.e., the ones in which there are a sensor. It is now possible to deal with the design of the controller.

4

Problem Formulation

This work aims to define a methodology to improve comfort while reducing the energy consumption of a building. To pursue this objective, after defining a model, it is necessary to develop a controller to regulate its heating behaviour by controlling inputs. The controller must be able to access as much data as possible for optimum performance, both current data and forecasts.

Notice that a building's controllable inputs can be divided into two types: inputs that modify uncontrollable inputs, such as awnings, and inputs that add or extract heat from a zone, such as radiators or convection heater. In this chapter, we focus on the latter, leaving for later works the modelling of the formers: they represent the future of controls, especially in the residential sector.

In this work, we adopt a modified Linear-Quadratic-Gaussian controller, consisting of an augmented states LQR and a reduced order LQE, together with a custom feed-forwarding system that exploits historical data and frequency weighted signals. We develop the controller in continuous time and only discretise it at the end of design phase by means of Euler method. Furthermore, thanks to the separation principle, we design controller and observer in two different stages.

4.1 Control Target

The aim of this work is to provide an optimum level of comfort by reducing energy consumption for heating or cooling. In order to be compliant with national laws, we use temperature as an objective variable representing comfort. To achieve the goal, in case of heating situation, the objective function must simultaneously minimise both the tracking error to the desired minimum temperature T_d and the energy consumption. For the cooling case, the objective function reports the tracking error to the desired maximum temperature T_d^c. In formulae, the controller shall minimise:

$$\mathcal{J}_\infty(u, T_d) = \sum_{x \in \mathcal{R}} \int_0^\infty \mathbb{1}(T_d - x(t)) + \alpha\, u_i(t)\, dt \tag{4.1}$$

where $\mathcal{R} = \{x_1^R, \ldots, x_m^R\}$ are the temperature in each of rooms to be monitored, $u \in \mathbb{R}^m$ is the heating power applied to each room in W, and $\mathbb{1}$ is the Heaviside step function. α, on the other hand, aims to balance the two addends, allowing you to choose which of the two values is more important for the user. In this work, we analyse the two addends separately, in order to allow a more detailed analysis.

4.2 A Digital Controller

The controller described in this chapter is developed in discrete time. Although the physical model of a building is intrinsically in continuous-time and the simulation systems are very efficient at simulating continuous-time controllers, nowadays continuous time controllers are little used in reality. There are many reasons for this, but the most significant are the low cost of microcontrollers and their greater flexibility, in terms of spare parts, wear resistance, and noise resilience. For these reasons, after having developed the continuous-time model, we discretise it before using the information to develop the controller. To perform the discretisation, we used the Zero-Order-Hold (ZOH) method: it returns a discrete-time system equivalent to the continuous-time system sampled at regular intervals T_s, assuming that between samplings the continuous signal is constant. The approximation, which may be limiting in other areas, is entirely suitable for the building sector, where appreciable temperature changes take several minutes if not hours.

Given the continuous-time system (3.5), the discrete-time equivalent using a T_s sampling

time is derived as:

$$\begin{aligned} x(t+1) &= Ax(t) + Bu(t) \\ y(t) &= Cx(t) \end{aligned} \tag{4.2}$$

where

$$\begin{aligned} A &= e^{FT_s} \\ B = [B_e|B_g|B^s|B^l|B^c] &= \int_0^{T_s} e^{F\tau} d\tau \ [G_e|G_g|G^s|G^l|G^c] \\ C &= H \end{aligned}$$

as reported in [112, Chapter 9]. Since the continuous-time system is asymptotically stable, its discrete equivalent is also asymptotically stable. Furthermore, observability and reachability are not affected by the discretization, too.

4.3 Linear Quadratic Regulator

The purpose of our controller is to require the minimum energy on the inputs in such a way that a reference temperature is reached and maintained within a subset of rooms $\mathcal{R} = \{x_1^R, \ldots, x_m^R\}$, selected by matrix H_m. Let $r(t) \in \mathbb{R}^m$ be the reference temperature to be reached and maintained in each selected room. Therefore, the controller shall minimize

$$\|e(t)\| = \|y(t) - r(t)\| = \|H_m x(t) - r(t)\|$$

in a robust manner, i.e., we desire $y(t)$ to converge to $r(t)$ with no steady-state error for any constant or piecewise-constant input and disturbance. We assume that the temperature measurement is available for all rooms in $\mathcal{R}$: if it is not the case, it is sufficient to estimate them by means of a state observer, as it is reported in the Section 4.4.

To define the controller, i.e., find a constant feedback matrix from the state K, we adopt the Linear Quadratic Regulator (LQR) methodology. Let (4.2) be a discrete-time linear system in state space form in n states, m input and l outputs. For this discussion we use only the part of B that comprises the controllable part, i.e., B^c. Therefore, $A \in \mathcal{R}^{n \times n}$, $B^c \in \mathcal{R}^{n \times m}$, and $C \in \mathcal{R}^{l \times n}$. Furthermore, let (A, B^c) be a stabilizable pair, i.e., unstable mode of A must be controllable. The LQR methodology provides the optimal feedback

matrix K from the state that minimises the following index, given $x(0)$ as initial state:

$$J(u, x(0)) = \sum_{t=0}^{\infty} x(t)^\intercal Q x(t) + u(t)^\intercal R u(t) \tag{4.3}$$

where $Q = Q^\intercal \succeq 0$ is the state weigh matrix whereas $R = R^\intercal \succ 0$ the input weigh matrix. The section 4.5 shows the method we have adopted to define these matrices. The cost index defined above forces the controller to bring the system to the null state, seeking a trade-off between the speed of convergence and the cost of the input. Normally, to simplify the calculus and to obtain a constant matrix, an infinite horizon is used. Since (A, B) is stabilizable, the index is finite and the feedback matrix can be found. Obviously, we are interested in bringing the system to the state we want, which is not necessarily zero. Since the system is linear, moving it from state x to zero is equivalent to moving the system from state $x + r$ to r. Consequently, the discussion will focus on the techniques for set the state to zero: to apply them to the case of maintaining a temperature r, we need only use: $u(t) = -K(x(t) - r(t))$ instead of the standard $u(t) = -Kx(t)$ where K is the feedback matrix obtained using LQR procedure.

Let $M = M^\intercal \succ 0$ be a solution of an Algebraic Riccati Equation (ARE), i.e.:

$$Q + A^\intercal M A - A^\intercal M B^c (R + B^{c\intercal} M B^c)^{-1} B^{c\intercal} M A = M$$

where $Q \succ 0$ or (F, Q) is observable. Then, it can be proved [112] that M is unique, the minimization of (4.3) admits a solution for state feedback as $u = -Kx$ that stabilised the system, and the optimal cost is equal to

$$J(x(0), u) = x(0)^\intercal M x(0) = \min_{\tilde{u} \in \mathcal{U}} J(x(0), \tilde{u})$$

where $x(0)$ is the initial state and $u = \{u(t) \in \{0, 1, \ldots, \infty\}, u(t) = -Kx(t)\}$, since the solution is constant in time and defined as $K = (RB^\intercal M B)^{-1} B^\intercal M A$.

To improve controller performances, an augmented state can be used: the so-called *integral state*. Let $x_I \in \mathbb{R}^m$ be a vector of additional states defined as $x_I(t+1) = x_I(t) + e(t)$, $e(t) = y(t) - r(t)$. Therefore, the controller target can be also written as $x_I(t) \to 0$, since that implies $y(t) \to r(t)$. We can define the augmented model as follows:

$$\underbrace{\begin{bmatrix} x_I(t+1) \\ x(t+1) \end{bmatrix}}_{z(t+1)} = \underbrace{\begin{bmatrix} 1 & C_m \\ 0 & A \end{bmatrix}}_{A_z} \underbrace{\begin{bmatrix} x_I(t) \\ x(t) \end{bmatrix}}_{z(t)} + \underbrace{\begin{bmatrix} 0 & -1 \\ B^c & 0 \end{bmatrix}}_{B_z} \begin{bmatrix} u(t) \\ r(t) \end{bmatrix} \tag{4.4}$$

whilst quadratic cost function associated to this augmented model is:

$$J(u, z(0)) = \sum_{t=0}^{\infty} z^{\intercal}(t) Q_z z(t) + u^{\intercal}(t) R u(t) \tag{4.5}$$

$$= \sum_{t=0}^{\infty} x_I^{\intercal}(t) Q_I x_I(t) + x^{\intercal}(t) Q_x x(t) + u^{\intercal}(t) R u(t) \tag{4.6}$$

where $z(0)$ is the initial state. To obtain the optimal trajectory to a zero steady-state error, we shall develop a linear state-feedback law $u(t) = -Kz(t)$ that minimize (4.5). Since (A_z, B_z) are a stabilizable pair by construction, we can solve the associated continuous-time algebraic Riccati equation and obtain the optimal gain matrix $K = [K_I\, K_x]$: this matrix guarantees the closed loop is stable, as seen before.

However, to extract maximum performance for the controller, an observer has to be developed since the LQR method needs to know the full system state and this requirement can hardly be fulfilled in a building environment: for example, internal temperature of the walls or the roof are difficult to measure and are not available in our case study. For this reason, we have developed a reduced-order observer by exploiting the knowledge of the Kalman filter.

4.4 Reduced Order Estimator via Kalman

The LQR controller described in Section 4.3 needs a fully knowledge about the status of the system for an efficient state feedback. Since some nodes cannot be measured easily, like external wall nodes, we develop a reduced state observer: to reach the best performance, the feedback matrix is designed using the LQE methodology. Let (4.2) be a discrete-time linear system in state space form in n states, m input and l outputs. For this discussion we use only the part of B that comprises the controllable part, i.e., B^c. Therefore, $F \in \mathcal{R}^{n \times n}$, $G \in \mathcal{R}^{n \times m}$, and $H \in \mathcal{R}^{l \times n}$. Furthermore, let $w(t)$ be the process noise, i.e., the error due a non-perfect model, and $v(t)$ the measure noise, i.e., the errors due a noisy measure of sensors. Both of them shall be zero mean white noise and uncorrelated in time, i.e., $v(t) \perp w(t)$. Let $\tilde{Q} = E(ww^{\intercal})$ be the covariance matrix of process noise and $\tilde{R} = E(vv^{\intercal})$ be the covariance matrix of measure noise. We expect a much larger process error than the measurement error due to the many simplifications that have been made during modelling: for this reason, we have decided to develop a reduced-order observer, using the measurements from the plant as the basis for estimating the unobservable part of the state due to the model. The choice was made since using a full-order estimator is more computationally complex and the results could be even worse since high process noise is present.

Let $T \in \mathbb{R}^{N\times N}$ be the transformation matrix from state-space to the reduce-observer space, i. e., $\begin{bmatrix} x_e \\ x_y \end{bmatrix} = T^{-1}x$. First rows, $x_y \in \mathbb{R}^m$, represent the directly measurable nodes, i.e., rooms in $\mathcal{R}$, whereas the others, $x_e \in \mathbb{R}^{N-m}$, the nodes that shall be estimated. Therefore, is sufficient to develop an observer for x_e since $x_y(t) = y(t)$. Using T, we can partition the system and obtain

$$\begin{bmatrix} x_e(t+1) \\ x_e(t+1) \end{bmatrix} = \begin{bmatrix} A_{11} & A_{12} \\ A_{21} & A_{22} \end{bmatrix} \begin{bmatrix} x_y(t) \\ x_e(t) \end{bmatrix} + \begin{bmatrix} B_1^c \\ B_2^c \end{bmatrix} u(t).$$

To obtain the $x_e(t)$ estimation, it is sufficient to estimate the additional variable $v(t)$, defined as follows:

$$v(t) = x_e(t) + Ly(t),\ L \in \mathbb{R}^{(N-m)\times m}.$$

Indeed, the $v(t)$ dynamics is:

$$\begin{aligned} v(t+1) = &\underbrace{(A_{11} - LA_{21})}_{A_v} v(t) + \underbrace{(A_{12} + LA_{22} - LA_{21}L - A_{11}L)}_{B_y} y(t) \\ &+ \underbrace{(B_1^c + LB_2^c)}_{B_u} u(t) \end{aligned}$$

and the observer can be developed as

$$\begin{aligned} \hat{v}(t+1) &= A_v\hat{v}(t) + \begin{bmatrix} B_y & B_u \end{bmatrix} \begin{bmatrix} y(t) \\ u(t) \end{bmatrix} \\ \hat{x_e}(t+1) &= I_m\hat{v}(t) + \begin{bmatrix} L & 0 \end{bmatrix} \begin{bmatrix} y(t) \\ u(t) \end{bmatrix}. \end{aligned}$$

Matrix L can improve the estimation system behaviour: indeed, the system dynamics is governed by $A_v = A_{11} - LA_{21}$. Therefore, the estimate converges to the real value if and only if A_v is asymptotically stable: L allows A_v to be stabilised if the pair (A_{11}, A_{21}) is detectable, i.e., the pair (A, C) is detectable. By constriction, A is full rank and asymptotically stable. These considerations allow us to design L by means of Kalman procedure, the dual of LQR. An observer built using this procedure computes a state estimate $\hat{x_e}(t)$ that minimizes the steady-state error covariance P:

$$P = \lim_{t\to\infty} E((x_e(t) - \hat{x}_e(t))(x_e(t) - \hat{x}_e(t))^\intercal).$$

Similar to the LQR procedure, the optimal, stable, and constant feedback matrix for the reduce order estimator is:

$$L = A_{11} P A_{21}^{\intercal} (A_{21} P A_{21}^{\intercal} + R)^{-1}$$

where $P = P^{\intercal} \succ 0$ is the only solution of the Algebraic Riccati Equation:

$$P = A_{11} P + P A_{11}^{\intercal} + P A_{21}^{\intercal} R^{-1} A_{21} P + \tilde{Q}.$$

Now we shall define process noise covariance $\tilde{Q}$ and measurements noise covariance $\tilde{R}$, as reported in the following section.

4.5 LQG Weights Choice

LQR and LQE procedures described above provide control matrices that minimizes the cost index or the error covariance. Therefore, it is important to describe them precisely to reflect the parameters to be met. Our target is to control precisely the temperature in each room of $\mathcal{R}$ subset, using the minimum amount of energy.

The Bryson's rule [113] provides to us a way to define LQR matrices linking these values to a physical meaning. Indeed, by defining those diagonal matrices as:

$$Q_{ii} = x_{i\_max}^{-2} \text{ and } R_{jj} = u_{j\_max}^{-2},$$

x_{i_max} represents the max acceptable error with regards to the reference on the i-th state whereas u_{j_max} the max acceptable value on the j-th input. The adopted values in this work are reported in Table 4.1. These values are obtained after a session of try and error: the main issue encountered is to maintain a good condition number of Q.

Table 4.1: Adopted values in LQR and LQE design

Controller	Type		Value
LQR	State	Controlled	$Q_{ii} = 10^{+1}$
		Non controlled	$Q_{ii} = 10^{-9}$
		Integrators	$Q_{ii} = 10^{-5}$
		Inputs	$R_{ii} = 10^{-3}$
KE		Process noise	$\tilde{Q}_{ii} = 10^{5}$
		Measure noise	$\tilde{R}_{jj} = 10^{0}$

The observer weights, instead, communicate to the controller the reliability of measures

and the model. The ratio between the measures noise weight and the process noise power shall be chosen very carefully since using a ratio higher than 1 suggests the observer to trust more the measures than the model outcomes, and vice-versa. Since a building model has a lot of uncertainties, we choose to a ratio equal to 10^5. The diagonal matrices chosen are $\tilde{Q}_{ii} = 10^5$ and $\tilde{R}_{jj} = 1$, as can be seen in Table 4.1 too.

4.6 Fourier-based Feed Forward

At the moment, the developed controller has no knowledge about the behaviour of the surrounding environment. Consequently, it only reacts to changes and is unable to predict future actions effectively. However, measurements and prediction of external temperature and solar radiation are readily available, even with low sampling times. For this reason, we exploit them by implementing a feed forward compensation system for external temperature, solar radiation, and the temperature references. Some disturbances, such as ground temperature, can be approximated effectively with constants. Others, such as outdoor temperature and solar radiation, are variable signals: anyway, they can be described sufficiently accurately using monthly profiles from historical data, corrected day-by-day by means of weather forecasts. However, as far as target references are concerned, they can fall into either one or the other category since they are normally defined as piecewise constant function: users desire a constant temperature over a period of time but different temperatures depending on whether it is day or night. For this reason, we have decided to use two different approaches depending on the disturbances treated: the first is the nominal approach while the second is based on the frequency transformation of the signal.

4.6.1 Nominal Feed Forward

Let $d(t) = \bar{d} \; \forall \, t$ be a constant disturbance signal in time domain, for example, the ground temperature and let $r(t) = \bar{r} \; \forall \, t$ be a constant reference signal in time domain. Remembering Equation (4.2) for controlling a subset of nodes describes by selection matrix H_m, the system can be written as:

$$\begin{aligned} x(t+1) &= Ax(t) + [B_e|B_g|B^s|B^l]d(t) + B^c u(t) \\ y(t) &= C_m x(t) \end{aligned}$$

At steady-state, $x(t+1) = x(t)$; therefore, the situation in this state can be described as:

$$x_{DC} = (I - A)^{-1}([B_e|B_g|B^s|B^l]\bar{d} + B^c u_{ff}(t))$$
$$y_{DC} = C_m x_{DC}$$

To obtain a feed forward such that $y \to \bar{r}$, we shall impose:

$$\bar{r} = y_{DC} = H_m x_{DC}.$$

If only the constant disturbances $d(t)$ are present and the system is asymptotically stable, as in our case, then the reference value can be reached in steady-state by applying the constant control $u_{fff}(t)$ derived as follows:

$$-H_m(I - A)^{-1}([B_e|B_g|B^s|B^l]\bar{d} + B^c u_{ff}(t)) = \bar{r}$$
$$-H_m(I - A)^{-1}(B^c u_{ff}(t)) = \bar{r} + H_m(I - A)^{-1}([B_e|B_g|B^s|B^l]\bar{d})$$
$$u_{ff}(t) = -(H_m(I - A)^{-1}B^c)^{+}(\bar{r} + H_m(I - A)^{-1}([B_e|B_g|B^s|B^l]\bar{d}))$$

In this work, we apply this technique to reject the disturbance caused by ground temperature since it is the only disturbance that we can approximate in a good manner with a constant value. Although not supported by a strong theoretical framework, it is possible to adapt the previous result to accommodate time-varying signals. Two different approaches can be followed: the first is to model the time-varying disturbance with an average value and follow the procedure above. This methodology works well with low variance signals, where the work delegated to the LQR controller would then be very small. In our case, the temperature and insolation signals has got a high variance in the day period: therefore, this approach is useless, if not harmful. Indeed, in the case of insolation, the feed forward suggests to the controller to redirect the disturbance even at night, when there is no sunshine, overloading the LQR controller.

The second approach is to feed the control using the disturbance data read directly from the controller. In this case, the disturbance would no longer be constant, but would be updated at each sampling time of the sensor. This approach works only if the variability of the disturbance signal is slower than the system dynamics. In this way, the system would have enough time to reach the steady-state before a new disturbance change. However, in our case, the disturbances vary faster than the system dynamics: for this reason, this approach cannot be adopted either. The problem with these two approaches is that our disturbances are periodic, since the temperature and insolation curves are almost perfectly overlapping from one day to the next. Since each harmonic repeats itself almost identically from day to

day, it is possible to implement a nominal control in frequency domain: assuming constant amplitude, we can perform a nominal frequency-by-frequency control, as reported in the next section.

4.6.2 Discrete Fourier Transform Disturbances Rejection

The situation analysed involves an important presence of quasi-periodic disturbances: the behaviour of outdoor temperature and solar gain are very similar day after day, as sunrise and sunset are postponed or advanced by only one minute each day. For this reason, we can assume to model these disturbances as periodic signals and apply some kind of nominal control for each single frequency in order to reject the overall disturbance without triggering the LQR control part. The idea is to apply the reasoning done for a constant signal to a periodic signal exploiting the properties of the frequency domain.

Let us define the system on which apply the feed forward for controlling a subset of nodes describes by selection matrix H_m in the following form:

$$\begin{aligned}\dot{x} &= Fx + [B_e|B_g|B^s|B^l]d(t) + G^c u(t)\\ y &= H_m x.\end{aligned}$$

Unlike the other components, this procedure is based on the original continuous-time system and not on the discretised one. Indeed, the procedure produces a series of Fourier coefficients to be back-converted and, therefore, it is possible to produce the feed forward signal obtained either analogically or digitally: nowadays microcontrollers integrate by default functions to reproduce sinusoidal signals.

Let $d(t)$ be a continuous disturbance signal for our system with a time period T and $d(t) \in L^1([T])$: for example, the solar radiation intensity which varies over a period of approximately 24 hours. By means of the Discrete Fourier Transform, this signal can be expressed as a sum of exponential function, i.e.,

$$d(t) = \lim_{M\to\infty} \sum_{k=-M}^{M} D_k e^{jk\omega_0 t}$$

where

$$D_k = \frac{1}{T}\int_0^T d(t)e^{-jk\omega_0 t}dt$$

and $\omega_0 = \dfrac{2\pi}{T}$ is the fundamental pulsation. Our aim is to find $u_{fff}(t)$ such that the periodic disturbance $d(t)$ has no effect on our system. The idea is the same as nominal control but

instead of investigating the steady-state, we concentrate on controlling among a period, knowing that if we cancel the contribution of the disturbance in that period, we bring the state of the system to the steady-state without perturbations. For LTI BIBO systems such as our one, the system response can be calculated using a convolution between the input signal $u(t)$ and the impulse response $h(t)$, i.e., $y(t) = h(t) * u(t)$. Therefore, our target can be reduced in formulas as follows:

$$u_{fff}(t) = \underset{\tilde{u}(t)\in L^1([T])}{\arg\min} \| \int_0^T h^c(t) * u(t) - h^d(t) * d(t) dt \|^2 \tag{4.7}$$

where $h^c(t)$ is the impulse response of the system under a controlled input whereas $h^d(t)$ is the one calculated when the system is prompted by a disturbance. This can be replicated in the frequency domain thanks to the convolution theorem: it states that the convolution of two time signals is equivalent to the product of their transforms, i.e., $Y_k = \mathcal{H}(jk\omega_0)U_k$, by defining U_k as the Discrete Fourier Transform of $u(t)$, the $\mathcal{H}(j\omega)$ as system transfer function and $h(t)$ its inverse Fourier transformation, i.e., the impulse response. For state-space models, $H(j\omega)$ can be obtained as:

$$\mathcal{H}(j\omega) = H(j\omega I - F)^{-1}G \tag{4.8}$$

Furthermore, in the exponential input case, the system response of a exponential signal can be expressed as follows:

$$u(t) = e^{j\omega t} \implies y(t) = h(t) * u(t) = \mathcal{H}(j\omega)e^{j\omega t}$$

since multiplying a signal by an exponential means shifting the signal in frequency, i.e.,

$$\begin{aligned} y(t) = h(t) * e^{j\omega t} &= \frac{1}{T}\int_0^T h(t-\tau)u(\tau)d\tau \\ &= \frac{1}{T}\int_0^T h(t)e^{-j\omega\tau}d\tau\, e^{j\omega t} = \mathcal{H}(j\omega)e^{j\omega t} \end{aligned}$$

The Discrete Fourier Transform is a linear operator and it is also possible to perform the same operation using a sum of exponentials:

$$y(t) = h(t) * \sum_{k=-\infty}^{\infty} A_k e^{j\omega_k t} = \sum_{k=-\infty}^{\infty} A_k \mathcal{H}(j\omega_k)e^{j\omega_k t} \tag{4.9}$$

This is very useful since all periodic $L^1(T)$ signal can be described by a limited series of Fourier coefficients: this concept will be exploited to determine in advance for each signal

its contribution to the output and impose countermeasures in advance.

Notice that our target is to find the input $u_{fff}(t)$ to apply to the matrix G_c that allows the system to completely reject the disturbance $d(t)$. Let $\mathcal{H}_{\rfloor}(j\omega_k)$ be the transfer function of the system's controllable part, i.e., the Fourier transform of $h^c(t)$, whereas $\mathcal{H}^{\lceil}(j\omega_k)$ the one of the disturbance part, i.e., the Fourier transform of $h^d(t)$. Thanks to the Fourier transform, the easiest way to solve (4.7) is to look up the coefficients and frequencies of the harmonics to apply to the system in order to output the equal and opposite disturbance. In this way, the two effects would cancel each other out. Since $d(t)$ is also a finite energy signal in the period, i.e., $d(t) \in L^2([T])$, to reject the disturbance $d(t)$, we shall find the finite series of coefficients $\{A_k\}$ and frequencies $\{\omega_k\}$ such that, $\forall\, t \in [0, T)$:

$$\underset{\{A_k\}\in\mathbb{R},\,\{\omega_k\}\in\mathbb{R}^+}{\arg\min} \|h^d(t) * d(t) - \sum_k A_k \mathcal{H}^c(j\omega_k) e^{j\omega_k t}\|^2$$

A possible solution can be found in this manner using $d(t)$ Fourier series of coefficients, i.e., $\{D_k\}, k \in \{-M, -M+1, \ldots, M\}$:

$$\sum_{k=-M}^{M} H^d(jk\omega_0) D_k e^{jk\omega_0 t} - \sum_k A_k \mathcal{H}^c(j\omega_k) e^{j\omega_k t} = 0$$
$$H^d(jk\omega_0) D_k e^{jk\omega_0 t} = A_k \mathcal{H}^c(j\omega_k) e^{j\omega_k t}$$

then, the $2M$ series coefficients are:

$$A_k = \frac{H^d(jk\omega_0) D_k}{\mathcal{H}^c(jk\omega_0)} \quad \text{and} \quad \omega_k = k\omega_0 \,\forall\, k \tag{4.10}$$

To find the input signal, it is sufficient to back-transform:

$$u_{fff}(t) = \sum_{k=-M}^{M} -\frac{H^d(jk\omega_0) D_k}{\mathcal{H}^c(jk\omega_0)} e^{jk\omega_0 t}$$

If $d(t) \in \mathbb{R}$, the previous formulae can be written as:

$$u_{fff}(t) = -\frac{H^d(0) D_k}{\mathcal{H}^c(0)} - 2\sum_{k=1}^{M} \frac{H^d(jk\omega_0) D_k}{\mathcal{H}^c(jk\omega_0)} \cos(k\omega_0 t + \phi_k) \tag{4.11}$$

where $\phi_k = \arctan \dfrac{H(jk\omega_0) D_k}{\mathcal{H}^c(jk\omega_0)}$. This is valid because the spectre is symmetric.

The same reasoning can be adopted with regard to the reference signal. In this case, let $r(t)$ be a periodic signal of period T and $\{R_k\}, k \in \{-M, -M+1, \ldots, M\}$ its Fourier

series of coefficients. Then, we desire to find, $\forall\, t \in [0, T)$:

$$\underset{A_k \in \mathbb{R},\, \omega_k \in \mathbb{R}^+}{\arg\min} \|r(t) - \sum_k A_k \mathcal{H}^c(j\omega_k) e^{j\omega_k t}\|^2$$

A possible solution can be found in this manner:

$$\sum_{k=-M}^{M} R_k e^{jk\omega_0 t} - \sum_k A_k \mathcal{H}^c(j\omega_k) e^{j\omega_k t} = 0$$
$$R_k e^{jk\omega_0 t} = A_k \mathcal{H}^c(j\omega_k) e^{j\omega_k t}$$

then, the $2M$ series coefficients are:

$$A_k = \frac{R_k}{\mathcal{H}^c(jk\omega_0)} \quad \text{and} \quad \omega_k = k\omega_0 \,\forall\, k$$

Similar to the disturbance case, if $r(t) \in \mathbb{R}$, the previous formulae can be written as:

$$u_{fff}(t) = -\frac{R_k}{\mathcal{H}^c(0)} - 2\sum_{k=1}^{M} \frac{D_k}{\mathcal{H}^c(jk\omega_0)} \cos(k\omega_0 t + \phi_k)$$

where $\phi_k = \arctan \dfrac{R_k}{\mathcal{H}^c(jk\omega_0)}$.

The process of creating the feed-forward input from historical data and weather forecast is summarised graphically in Figure 4.1.

All this treatment can also be adapted for periodic signals with a non-finite series of coefficients: in this case, it is necessary to eliminate frequencies above a threshold in order to obtain a finite summation of signals, so that it can be implemented. This problem is closer than imagined: indeed, the temperature references for rooms are square waves, whose Fourier series is not finite. The same solution is also used to improve computation performance for periodic signals: in this case, the Discrete Fourier Transform is truncated when frequencies contribution is negligible. To improve performance, we suggest adopting advanced algorithms like Cooley–Tukey algorithm for Fast Fourier transform.

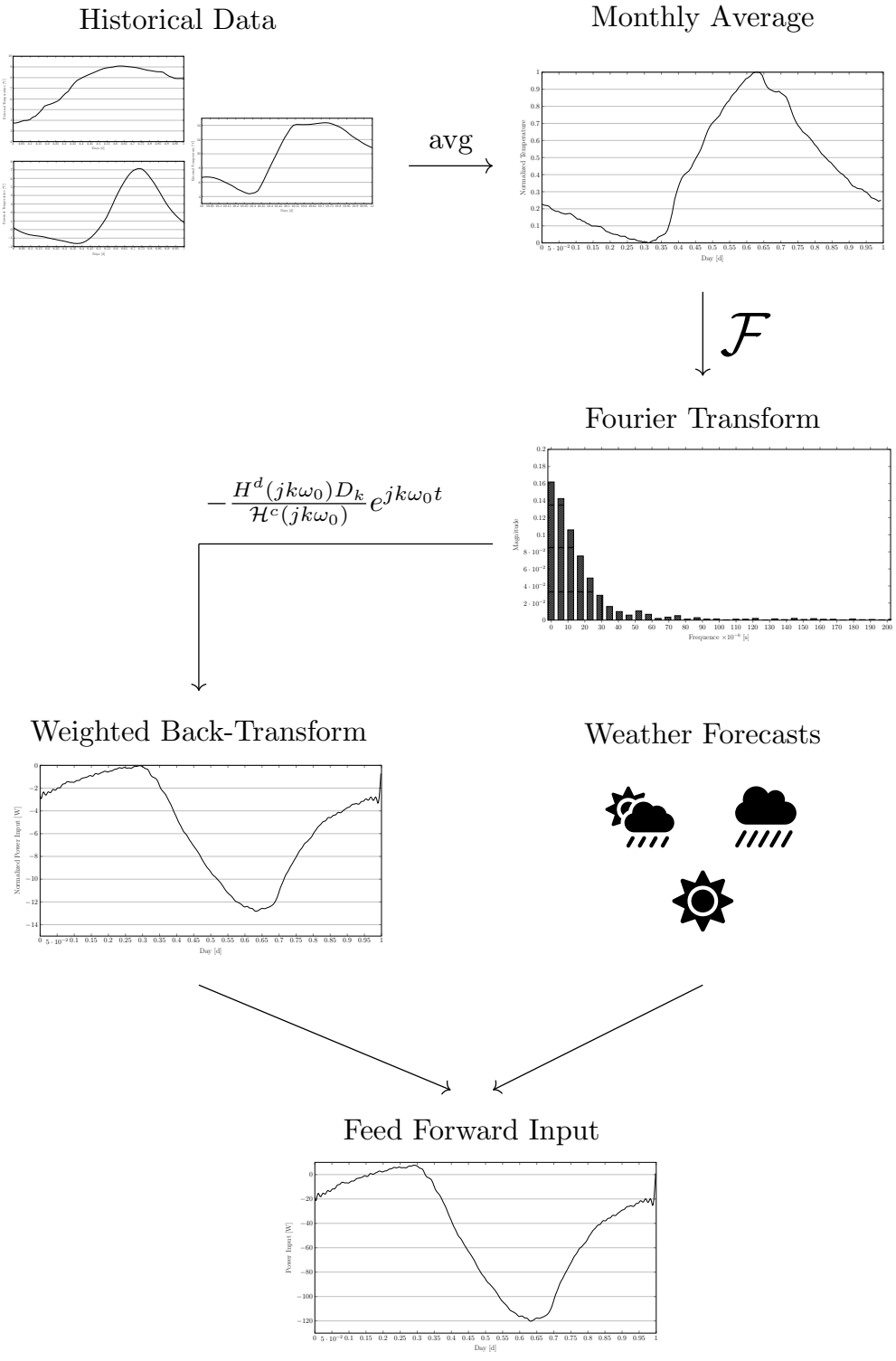

Figure 4.1: The process pipeline.

4.6.3 Create a Disturbance Profile

The theoretical treatment illustrated above requires signals to be perfectly periodic day-by-day. Although this assumption is easy to obtain in the case of the reference signal, since the demands do not change during the year for heating and cooling respectively, as far as disturbance rejection is concerned, this request is impossible to fulfil. Indeed, the movement of apparent path of the Sun during the days and the fact that the days get longer or shorter is negligible for small periods, but after a month it becomes appreciable, changing the shape of the disturbance signal and introducing appreciable differences between the modelled profile and reality. Our idea to mitigate this phenomenon consists of two steps: the first is to create a normalised profile for each month. This period is chosen since it is a sufficiently long time to maintain the slower modes of the system dynamics but, at the same time, to remain close to the reality. The second step consists of improving, every day, the next day period disturbance signal by means of a disturbance prediction, by varying only the value of the signal coefficients. This allows us to improve predictive capability and take almost all the reactive control work off the LQR controller, improving handling and comfort.

To create a monthly profile $\Pi(t)$, we proceeded as follows. Let $d(t)$ the disturbance to be modelled sampled every T_s seconds and $\mathcal{P} = \{p_1, \ldots, p_P\} \subset \mathcal{R}$ the days in the period. Let $\Pi(t)$ be the average normalised historical profile for a day ($t \in [0, \frac{T}{T_s}]$, $T = 86400$ the number of seconds in a day) of disturbance $d(t)$ in the period defined as follows:

$$\Pi(t) = \frac{1}{|\mathcal{P}|} \sum_{p \in \mathcal{P}} \bar{d}(t, p)$$

by using:

$$\begin{aligned} \bar{d}(t,p) &= \frac{d(pT+t) - D_m(p)}{D_M(p) - D_m(p)}, \quad t \in [0, T-1] \\ D_m(p) &= \min_{t \in [0, T-1]} d(pT+t), \qquad p \in \mathcal{P} \\ D_M(p) &= \max_{t \in [0, T-1]} d(pT+t), \qquad p \in \mathcal{P}. \end{aligned}$$

This normalized profile can be adapted using the day-by-day forecasts: in our case, the maximum f_M and the minimum f_m expected values. Indeed, the expected disturbance for the next day can be expressed as:

$$\Pi_{\text{day}}(t) = \Pi(t)(f_M - f_m) + f_m. \tag{4.12}$$

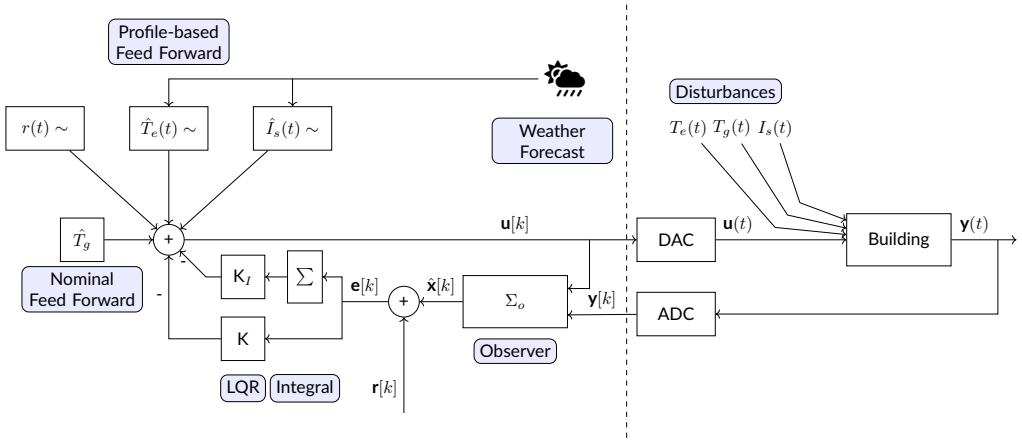

Figure 4.2: Closed-loop control scheme with improved feedback.

For calculating (4.11), we exploit the Fourier coefficients of the signal $\Pi(t)$. To improve performance, instead of recalculating $u_{fff}(t)$ every day to apply forecasts f_m and f_M, it is faster to calculate the control signal using the normalised profile and then modify it day by day directly in time domain. Since the Fourier transform is a linear operator, to create $u^p_{fff}(t)$, i.e., the feed forward signal for day p, it is possible to use:

$$u^p_{fff}(t) = (f_M - f_m)u_{fff}(t) + A_0 f_m$$

where A_0 is the zero coefficient of the control solution as defined in equation (4.11). This makes implementation very easy as most of the signal is calculated offline and only a couple of sums and multiplications are needed online, when the forecasts are ready.

4.7 The Overall System

Before testing the controller, it is useful to make a short recap. Our controller described in this chapter consists of several components: a reactive control part based on the LQR procedure, a reduced-order state estimator for nodes that cannot be measured directly, and an innovative feed forward based on historical temperature and insolation profiles. These subsystems are interconnected and interact in an advanced way, as shown in Figure 4.2. In fact, the contribution of the nominal feed forward for the ground temperature $\hat{T}_g$ is integrated with the contributions of the profile-based feed forward. In this work, this methodology has been used for outdoor temperature $\hat{T}_e$, solar irradiance $\hat{I}_s$, and reference $r(t)$. The profiles are updated thanks to the weather forecast. The overall feed forward contribution is then provided as input to the system, along with the reactive control part composed by the

observer and the extended LQR system. The aim is to eliminate uncontrollable disturbances in the system and provide adequate comfort to the tenants.

A controller such as the one presented in this work can be industrialised quite easily with the support of a BMS manufacturer. The manufacturer should provide a software interface to the BMS that receives at regular intervals a configuration file containing the set-points to be applied. After a feasibility check, the BMS updates its set points with those provided by the configuration file and communicate them to all the connected devices. The control system would then be responsible for providing configuration files with the set points at regular intervals: this allows compliance with the main standards and security laws since control of the plant remains within the BMS. The problem that remains to be solved is interoperability between different BMS: there is no standard yet, so it is difficult to implement such a control without a strong industrial partner in the sector.

5 A Case Study

Curiously, building control has always been little considered within automation: in fact, the major sectors in which automation has grown are aerospace, petrochemicals, electronics or automotive. One reason can be found in the fact that the thermal control sector is fairly resistant to errors, i.e. poor control is not noticed unlike in other sectors. Indeed, unlike other sectors like aerospace where sub-optimal control creates tangible production problems and economic impacts, the failure to achieve a comfort temperature in a building can be mitigated by people adding or removing clothing, with no direct or easily identifiable economic impact.

The aim of this chapter is to provide an overview of the performance of our controller, comparing it with the most common techniques used in real buildings in two different scenarios. In order to best evaluate the goodness of our work, it is first necessary to precisely define the characteristics that govern the test environment.

5.1 Test Environment

Several characteristics contribute to defining a test environment. We implement a virtual environment in MATLAB/Simulink to develop and test our controllers following the guidelines reported in Chapter 3. Several decisions were taken during the development especially with regard to defining the data available during the controller design phases. These issues about

availability of data can be divided into two groups: data to use to build the simulation model, and information for developing the controllers and data available in real time to them.

The simulation model is built following the procedure described in Chapter 3. EDILVI provided us with the blueprint, the used components and their characteristics, of a newly built "Casa Smart Plus" house of energy class *A4*. The house, built by means of CLIMABLOCK in 2020, has a gross volume of 571.77 m^3 and a useful surface area of 107.35 m^2. The house consists of an open plan kitchen and living, three bedrooms, a bathroom, a laundry room, and a utility room, as well as a garage. The room volumes are reported in Table 5.1 along with the heat power available per room. The blueprint of our case study is reported in Figure 5.1. All these rooms are modelled and included in the model: all except the garage are measurable and controllable via the all-air system. Since we do not model the all-air system, to control these rooms we assume to provide an internal load equal to the heat power that the all-air system would have fed in. As the tests are only carried out only in winter since it is the most important period for household energy consumption, the controllers are only able to impose to the system to provide energy into the rooms and not extract it. This is a limitation that is also present in reality since thermal systems can only operate in one mode, summer or winter, and it cannot be changed during the designated period.

The model consists of twenty-three states and eight controllable inputs: there are an air emission terminal for each room. There are three non-controllable inputs: outdoor temperature, ground temperature, and solar irradiance. The first two are represented in scalar form while the third input is a vector to take into account the different apparent position of the sun during the single day and the passing of the days.

Table 5.1: Air volume in rooms of case study.

Room	Volume (m^3)	Heat Power (W)
Kitchen/Living	119.07	800
Bedroom 1	32.94	500
Bedroom 2	32.94	500
Utility room	8.64	100
Master Bedroom	39.96	600
Laundry room	18.09	100
Bathroom	20.25	200
Hallway	23.22	200
Garage	48.33	0

The data of the surrounding environment, i.e., the disturbance inputs, are collected from the ARPA Lombardia website [114]: we use data coming from the municipality of Costa Volpino (BG), Italy, as a reference. This municipality has very similar climatic data to the

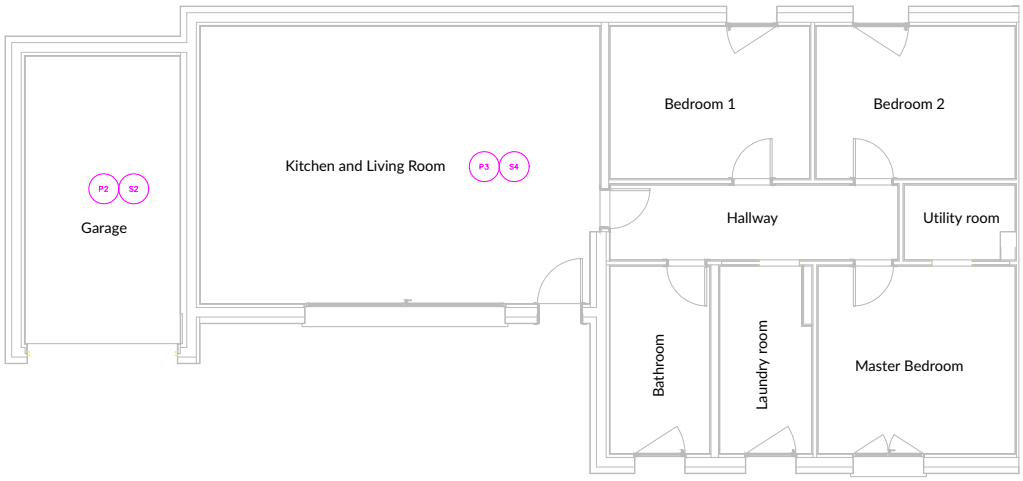

Figure 5.1: Case Study Blueprint

place where the real house was built: it is in climate zone E with 2403 degree days per year. From this website, we collect and process solar radiation and outdoor temperature data for the years 2019 and 2020: the first year is used to create the profiles whereas the second is used as environmental input for the model during simulations. The ground temperature is set constant at $T_g = 12$ °C, the average temperature of soil at two metre depth: we calculate it taking inspire from [115]. The test period adopted is February 2020, from 1 to 28. The initial conditions of the simulated building are equal to 10 °C for all nodes composing the building.

Since that an exact state space model has been built for simulation relying on the nominal construction data, a second model in state space shall be assembled to develop the controllers. In realty, this data is not perfectly known and sometimes, during the construction phase, some modification can be carried on. Therefore, to make the control design more realistic, we perturbate the nominal model parameters up to 20% to derive the model up on which the controller is design: in this way, we reproduce a real situation where design data to make the controller are available but the characteristics of the real counterpart are unknown. Consequently, the S model created with the design data was used for the simulations, while the model with the noise-stained data $\tilde{S}$ was used to develop the controller. As regards historical data, only weather data logged in 2019 is available to develop the controllers. Instead, the data available in real time for the controllers is the 2020 environmental ARPA data mentioned above, with a sampling time of fifteen minutes. The forecast data, on the other hand, is only available as the maximum and minimum

expected temperature of the next day. It is provided by calculating the actual minimum and maximum environmental temperature or isolation in the next day, with the addition of Gaussian noise with a standard deviation of 2 °C or 100 W m^{-2}.

5.2 Test Suite

To test the performance of a controller, like the one defined in Chapter 4, it is essential to define a test suite: first of all, it is necessary to indicate other control technologies and methodologies that are tested together to compare the results. Then, the environment in which tests take place shall be defined before to settle the indicators that are adopted to objectively measure the performance.

The first controller we use to compare our controller with is a continuous-time Proportional-Integral-Derivative (PID) controller with anti-windup control: although it is a fairly old technology, it has been included because it is the state of the art at industrial level for buildings. Its success mainly derives from its excellent performance with a low material cost: very often, it is implemented with analogue components, especially in older machines. However, this controller is not able to collect information about the environment and it controls each room independently of the others, thus failing to optimise the whole. To define the operating parameters of the PID, we use MATLAB automatic tuning procedure based on the system $\tilde{S}$. We set a rise time of 30 minutes and an overshoot of maximum 3%, i.e, about of half Celsius degree in our cases, in order to keep the closed loop stable but at the same time effective in control. In order to test the goodness and usefulness of the profile-based feed forward introduced in this work, we decided to define two cases by removing some parts of the complete controller. The first, which will be identified in the plots as *LQR + Int*, consists of our controller excluding the feed forward part. In the second, identified by the abbreviation *FF OL*, we test the developed feed forward by running the control system in open loop, i.e., by relying only on the feed forward part. Following this nomenclature, the complete controller is identified in the plots by the words *LQR + Int + FF*.

After defining the controls to be tested, it is necessary to identify the scenarios in which we test them. Taking inspiration from the most common situations within a house, we assume to test the controllers in tracking a reference temperature defined by a square wave with a daily period. In houses, in fact, it is usual to define a daily temperature and a night temperature, which is normally lower. In our case, the references are 21 °C from 8 am to 10 pm and 16 °C during the rest of the day. A plot of the reference is reported in Figure 5.2. We prepare two different scenarios: in the first, the aim is to chase the temperature reference only in the kitchen whist in the other the reference temperature shall be followed in five

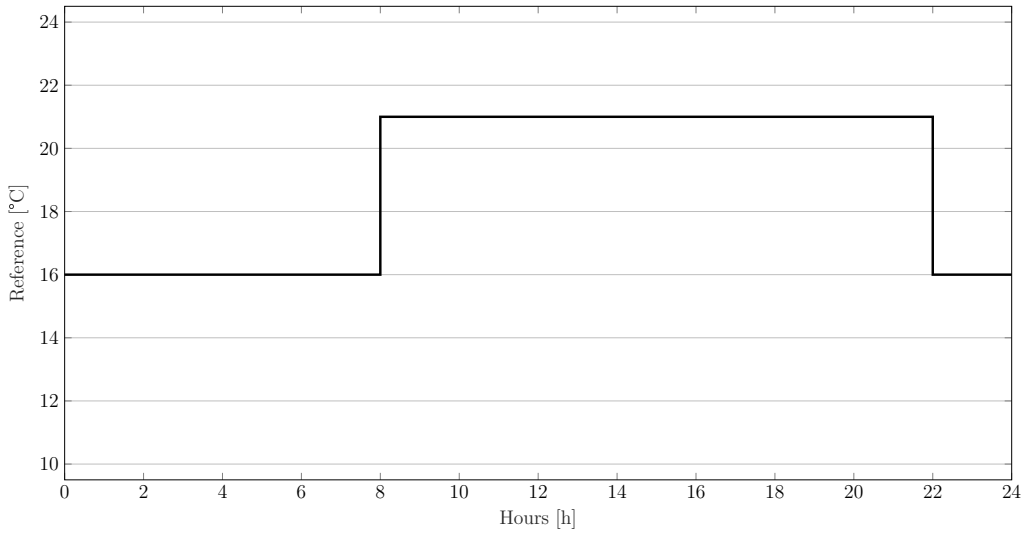

Figure 5.2: The reference signal used in tests.

controllable rooms.

The key performance indicators we choose to compare the different controllers are two: the tracking error and the total energy consumption of the controller. Both of them are *lower is better* indicators, i.e., controllers shall try to minimise them. These two indexes are very useful as they define the most important qualities of a controller, but they must be seen in a common perspective: having very good performance in one but very poor performance in the other identifies an inefficient controller. For example, keeping the system switched off allows zero consumption, i.e. the optimum achievable for the energy usage test, but not for this reason it is a useful control. To calculate the tracking error, we use a custom Root-Mean-Square Error (RMSE): in the case of several rooms to be controlled, we report the average RMSE of each individual room. Indeed, since the contribution of the Sun is appreciable in the rooms and it is not possible to extract heat from the rooms by construction, we calculate the RMSE only when the reference is not reached, not penalising the part exceeding the reference. Indeed, if the reference is exceeded, a penalty is already calculated in the other indicator since it penalises energy wastes. To determine the energy used, we set up in the simulator environment an integrator at the input of the plant which adds up all the control contributions. Obviously, only the positive contributions are summed up, as the negative ones are ignored by the plant. To allow for more advanced analysis, in some types of controllers we set up counters at the end of each component to determine which of the reactive, feed forward, and saturation parts makes the greatest contribution in terms of energy used.

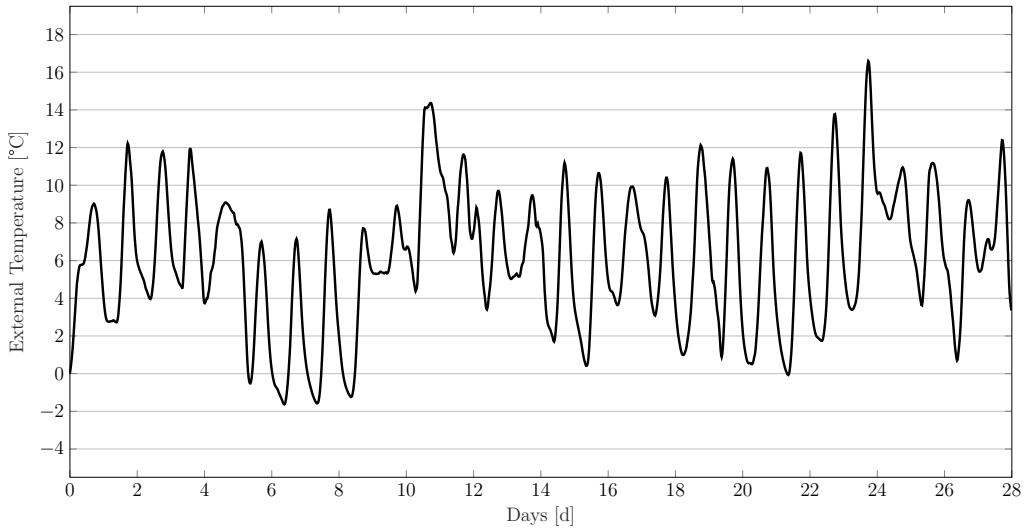

Figure 5.3: Trend of outdoor temperature in the test environment.

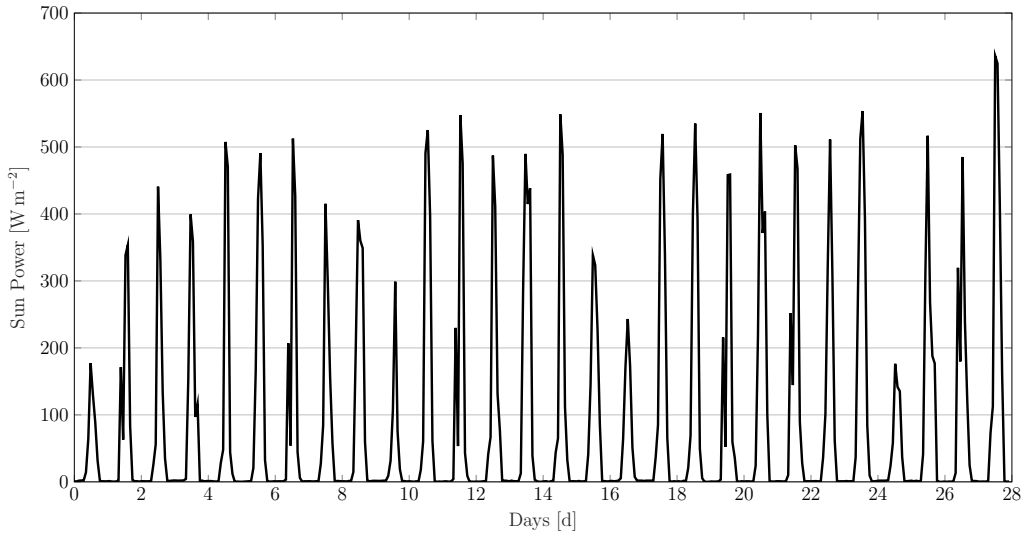

Figure 5.4: Trend of Sun irradiance in the test environment.

5.3 Results

This section presents the results of the tests carried out in the two scenarios defined above. In order to standardise the treatment, in both cases we first show the synthetic results by means of KPIs and then investigate the causes of these results by showing graphs of tracking error or input provided by controllers.

Before illustrating the results, in Figure 5.3 and Figure 5.4 are reported the external temperature and the solar irradiation that we use in the tests to describe the environment

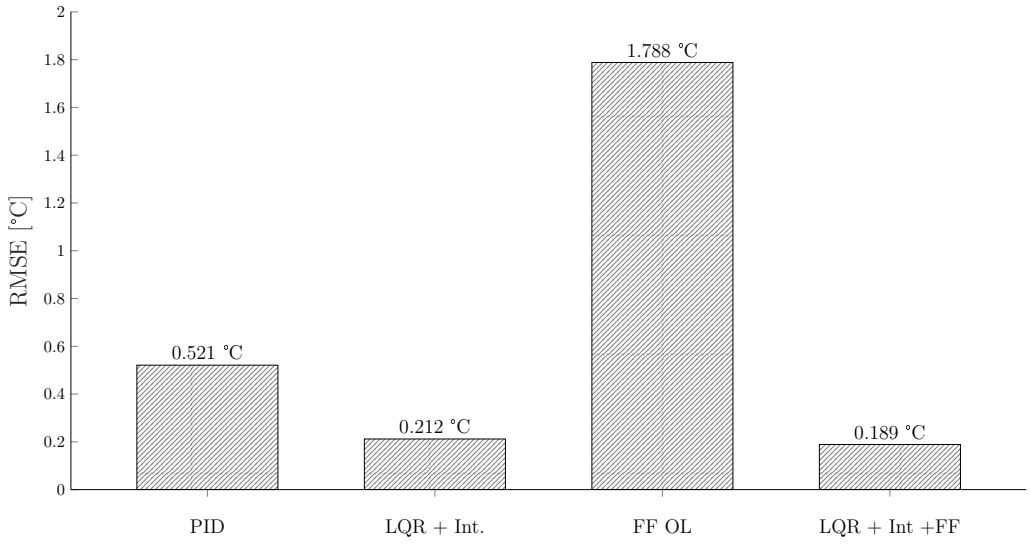

Figure 5.5: RMSE of tracking error for heating the kitchen using different types of controls.

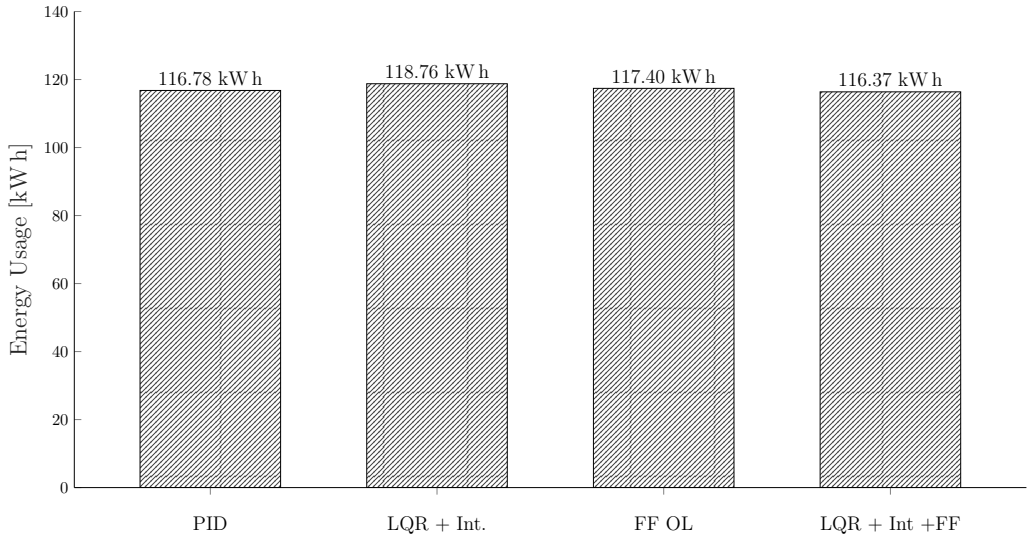

Figure 5.6: Energy consumption for heating the kitchen using different types of controls.

around the building. We recall that this data was collected in 2020 in the municipality of Costa Volpino (BG), Italy by ARPA Lombardia.

5.3.1 First Scenario

The target of the first test scenario is to control the temperature of the kitchen by following the reference, being able to act only on the kitchen heating controls. Figure 5.5 shows the

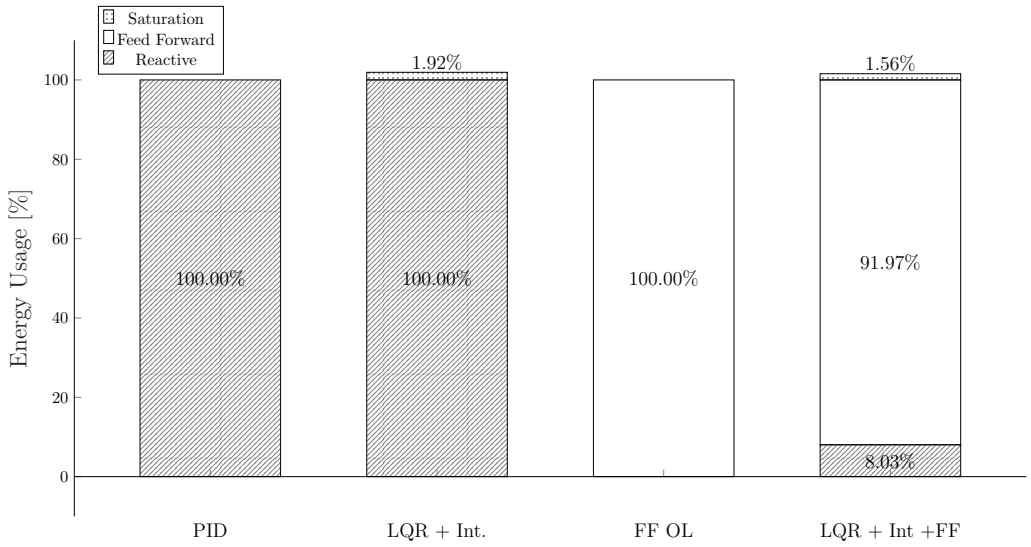

Figure 5.7: Energy consumption of the different parts of the control for heating the kitchen using different types of controls. Percentage values over real comsuption. Negative inputs at plant are ignored.

RMSE whereas in Figure 5.6 is reported the overall energy consumption. From these plots, it can be seen that the controller presented in this work improves room comfort appreciably, especially compared to the PID controller, without increasing energy consumption. Indeed, using the same energy, our control tracking capabilities are 275% better than the PID controller ones. The feed forward part alone is not able to follow the reference, but its contribution is appreciable when assisted by the LQR controller. In fact, it allows to reduce the consumption by 2% and the tracking error by 12% than not using the feed forward part.

In Figure 5.7 it is reported the energy consumption plot, broken down by the type of control responsible. It can be seen that the several parts that make up a controller make different contributions. In the case of the PID controller, 100% of the control is reactive, i.e. it responds to changes in the environment as they occur. Thanks to the anti-windup technology, no saturation occurs. The same situation happens using the LQR-based controller with the addition of integral states. Instead, in the case of the open loop controller that relies entirely on feed forward, only the feed forward part is active. The full controller tries to mix the two approaches, even if it relies for about 92% on the information provided by the feed forward. Indeed, the LQR part acts for the remainder as a mitigator, correcting what the feed forward cannot predict by relying on the historical profiles and weather forecast. In our case, the feed forward is too generous in feeding power, probably due to some particularly unfortunate parameter obtained in the model for the controller design. However, this shows how a small amount of reactive adjustment can turn a very

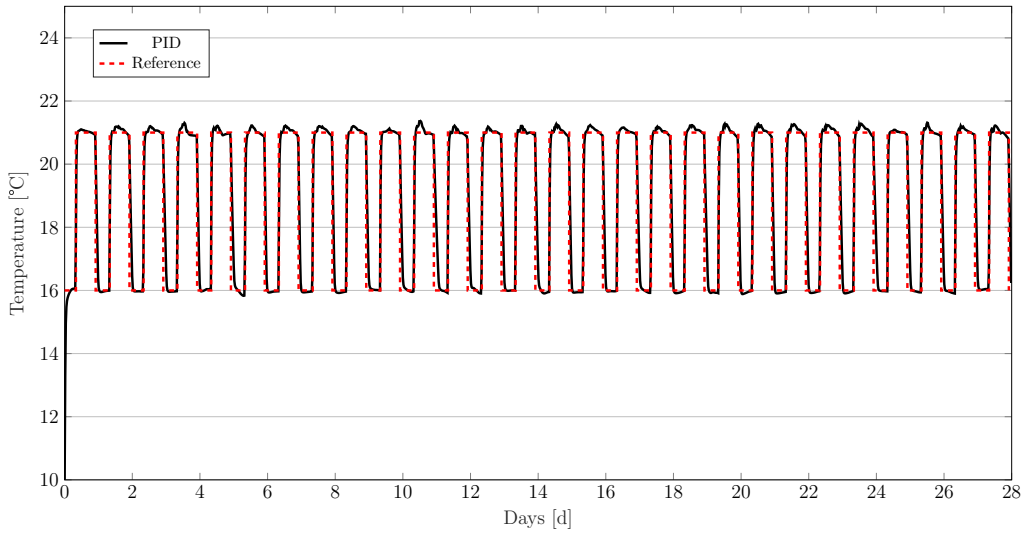

Figure 5.8: Kitchen Temperature by using PID controller versus Reference.

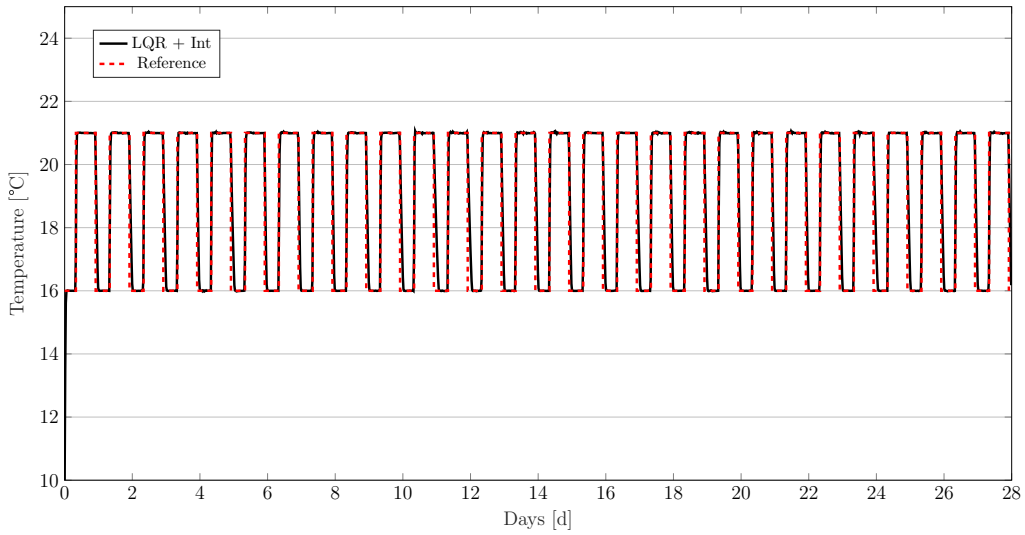

Figure 5.9: Kitchen Temperature by using our controller without feed forward versus Reference.

problematic control into an added value.

In order to better assess the reasons determining the performance achieved, in Figure 5.8, Figure 5.9, Figure 5.10, and Figure 5.11 are reported the output trend throughout the simulation obtained using the four controllers defined above. As it can be seen, the controller that relies only on feed forward is not ready to be implemented in real scenario as it is yet. The other controls performance, instead, is acceptable and can be used in a real scenario. Analysing the graphs in detail, it can be seen that the PID controller suffers from

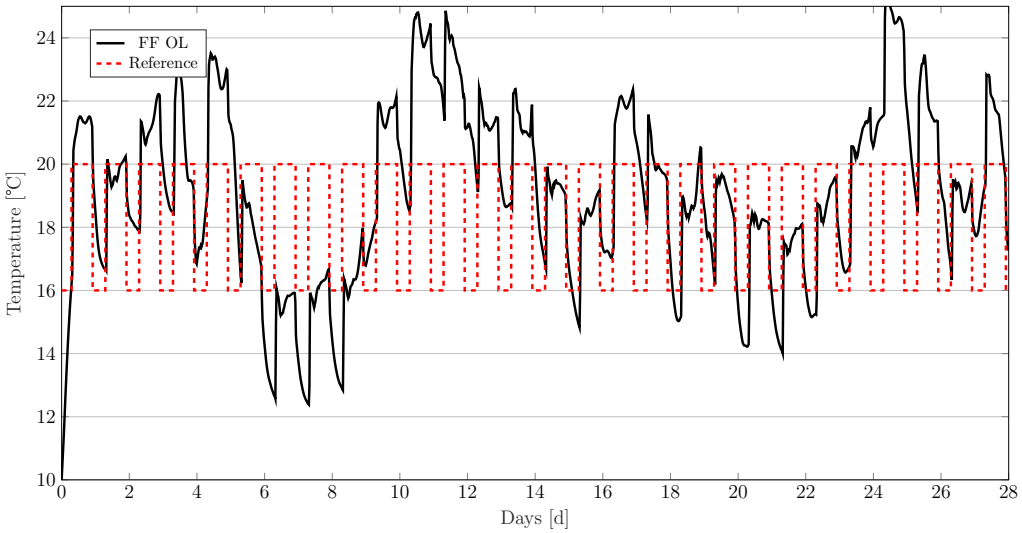

Figure 5.10: Kitchen Temperature by using only feed forward part versus Reference.

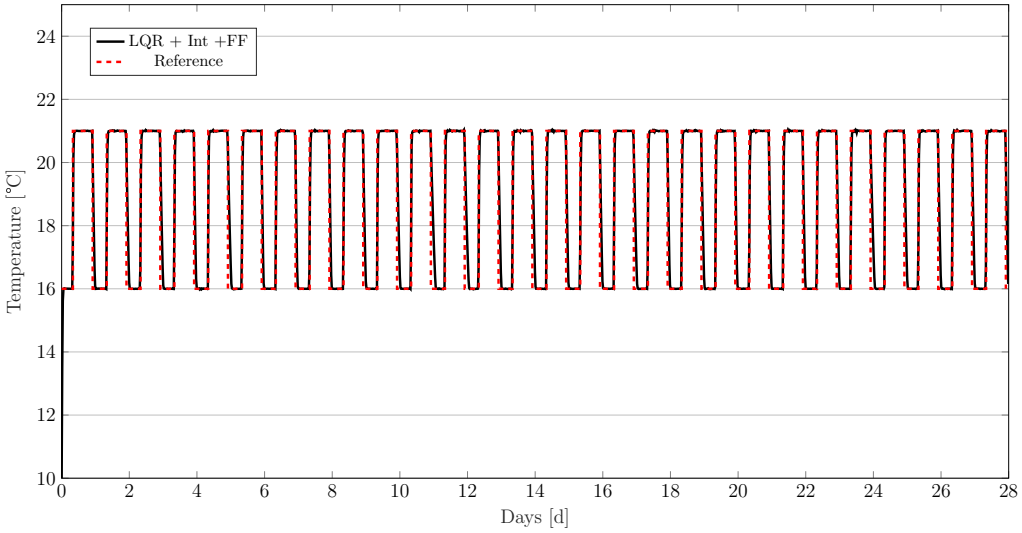

Figure 5.11: Kitchen Temperature by using the full controller versus Reference.

changes in environmental conditions, exceeding the reference and wasting energy that could have been saved. Probably, the integral part that helps in the ascent phase penalises the controller in responding effectively to changes in external conditions. This is not the case for LQR-based controls, which can rely on a more advanced knowledge of the model and the interconnections between the different nodes.

To verify this behaviour in detail, in Figure 5.12 it is presented the temperature trend during a single day in the controlled room using the PID controller and the full controller,

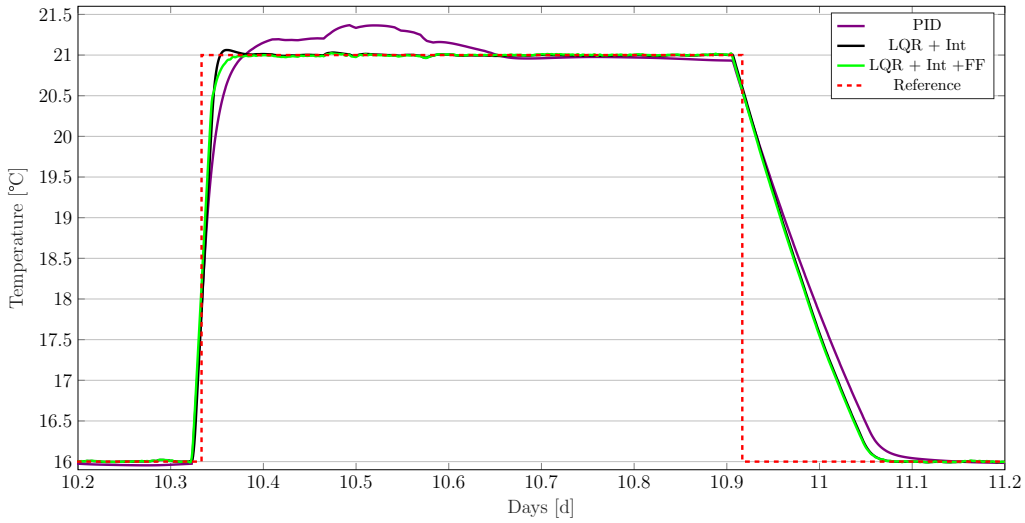

Figure 5.12: Kitchen Temperature using three different controller versus Reference during the tenth day of simulation.

with and without the feed forward component. As it can be seen, the PID controller produces an over-response that increases consumption, since it is unable to know the behaviour of the adjacent rooms and does not expect the arrival of solar heat. The LQR control without feed forward is more responsive but still suffers from overshoot, underlining how the contribution of the feed forward is mainly to make the system response much smoother.

5.3.2 Second Scenario

The second scenario aims to evaluate the behaviour of the controller in the case of several rooms to be controlled. We evaluate the controllers behaviour when simultaneously controlling the temperature of the kitchen, the bathroom, the hallway, the master and the first bedrooms. The challenge is very demanding because the different rooms have different volumes and heating capacities, as reported in Table 5.1.

In Figure 5.13 are reported the RMSE errors calculated in each room: for ease of reading, a horizontal line has been inserted to indicate the average RMSE over the rooms controlled by that controller. It can be seen that the trends seen in the previous section are repeated: the PID controller has the worst performance whereas the controller presented here reduces tracking errors by a third on average (about -200 %) compared to it. The contribution of the feed forward is notable since it allows a reduction of up to 10% in the tracking errors, greatly improving the results obtained in the previous test.

The energy consumption of each controller is presented in Figure 5.14. From this plot, it can be seen that to improve comfort it is not necessary to increase consumption: our

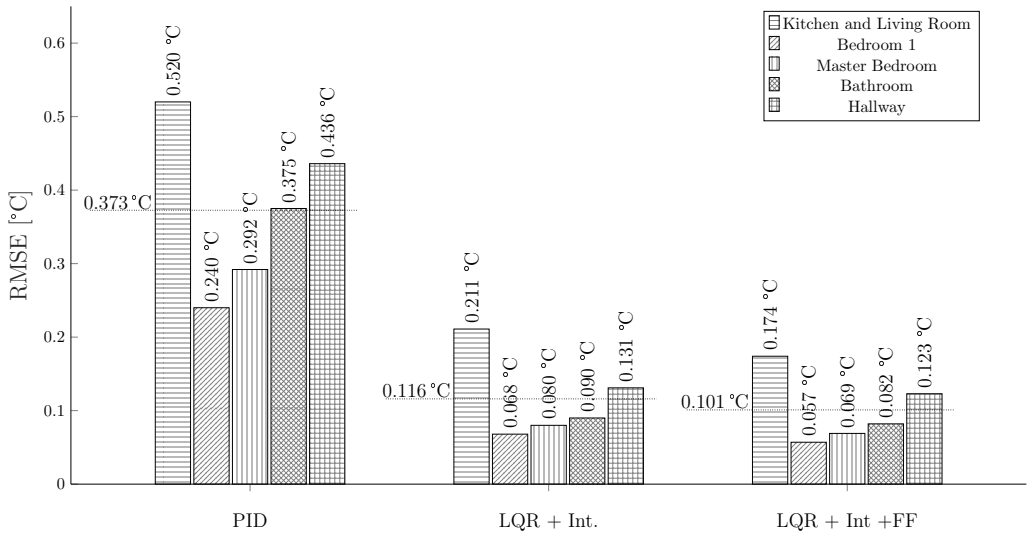

Figure 5.13: RMSE of tracking error for heating the five rooms using different types of controls. Over the horizontal lines are reported the average value among all rooms.

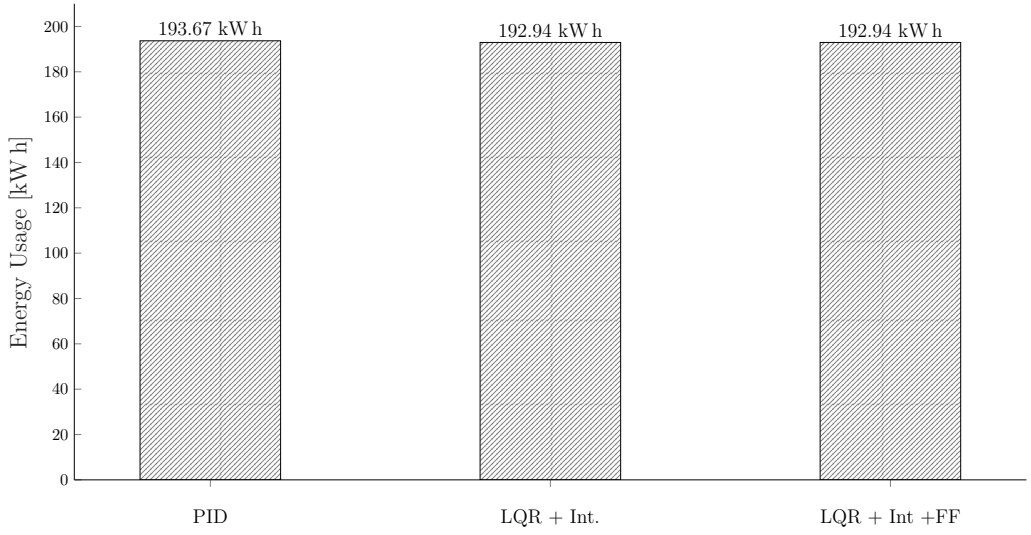

Figure 5.14: Energy consumption for heating the five rooms using different types of controls.

controller provides better performances than the others using the same amount of energy. To analyse more in detail the energy usage, Figure 5.15 shows the breakdown for each room. It is very interesting to note that, in this scenario, the energy consumption required to maintain the temperature reference in the kitchen has decreased compared to scenario one, shown in Figure 5.6. This stems from the fact that in scenario one, the adjacent rooms absorbed heat from the kitchen, as they were not heated. In this scenario, however, they are almost all at the same temperature, thus interrupting the heat exchange between one

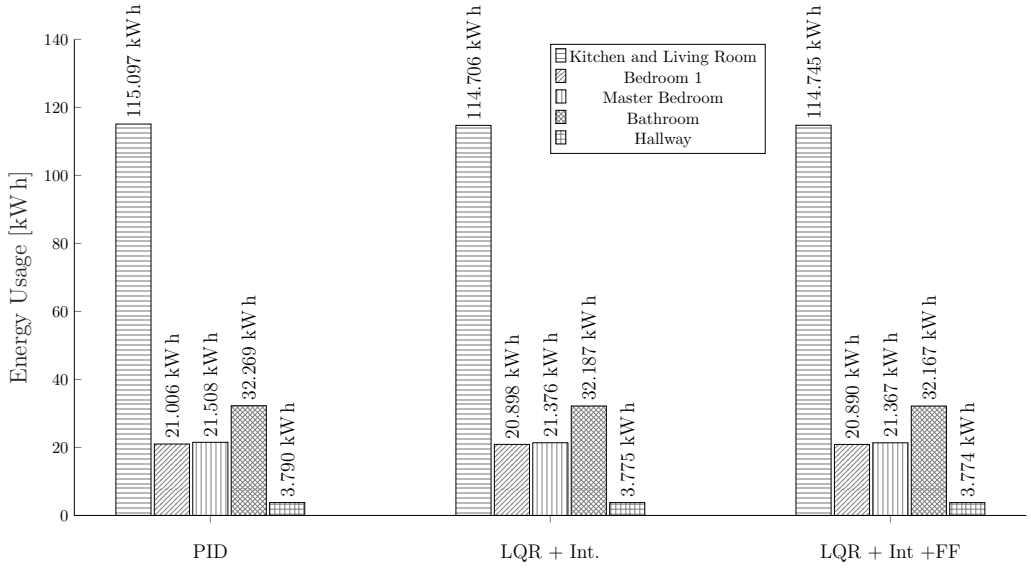

Figure 5.15: Energy consumption for heating the five rooms using different types of controls. Breakdown per room.

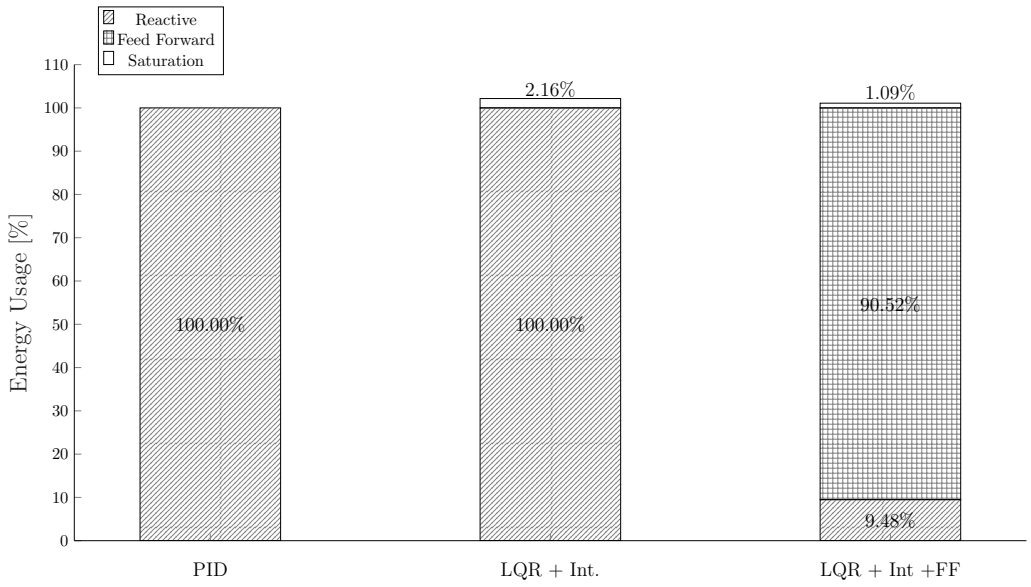

Figure 5.16: Energy consumption for heating the five rooms using different types of controls. Breakdown per type of control.

room and another. This is clearly visible in the case of the hallway: since it has no surface in contact with the outside environment, the energy required to heat it is very low, much less than the required amount to heat a room with similar volumetric dimensions, like the bathroom.

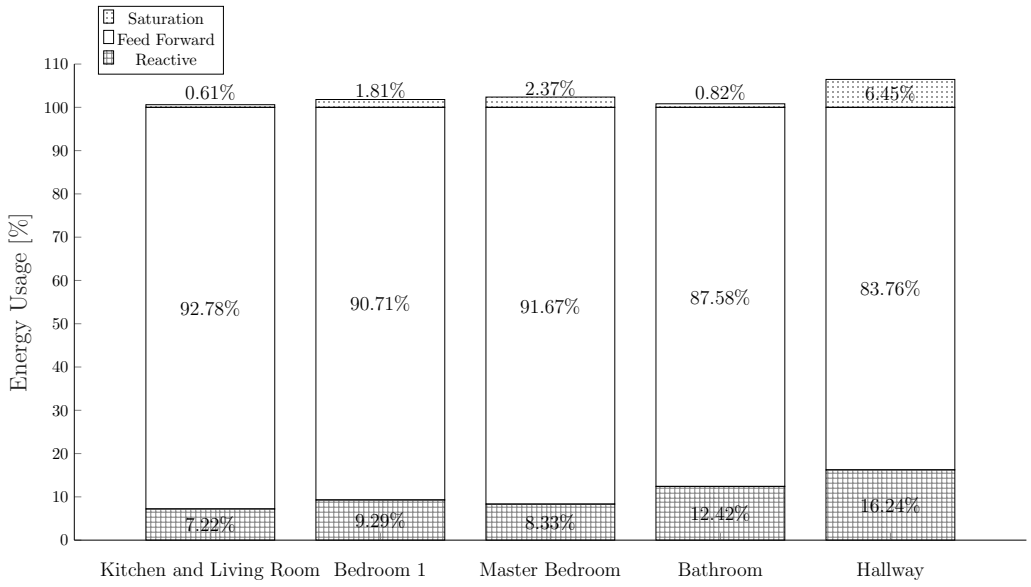

Figure 5.17: Energy consumption for heating the five rooms using different our controller. Breakdown per type of control and room.

In Figure 5.16 it is reported the overall energy usage, breakdown for each controller part. Similar to the previous scenario, our controller relies more than 90% on feed forward data and the reactive part of the controller is only necessary to regulate unplanned disturbances or forecasting errors. In Figure 5.17 the different contributions of the various parts of our controller, divided by room, are presented. As it can be seen, the hallway is the room that makes the least use of the feed forward contribution. This was expected since it has no direct contact with the outside world and, therefore, only the feed forward is present to mitigate changes in the reference. Indeed, the control is conditioned by the heat exchanged with adjacent rooms which was not assumed during the definition of the feed forward. Note, also, the significant saturation present in this room, probably the result of the undersized heating unit due to the low demand.

5.4 Discussion

The results of the tests carried on in the two scenarios show how the use of this new feed forward technique makes it possible to significantly improve comfort by reducing the load on the reactive part of the controller. This has several implications for systems and energy optimisation. The first is the possibility of setting up two different machines for the different types of load to be driven: knowing that the most part of the input is given by the feed forward, a manufacturer or an installer could optimise the main machine on that profile and

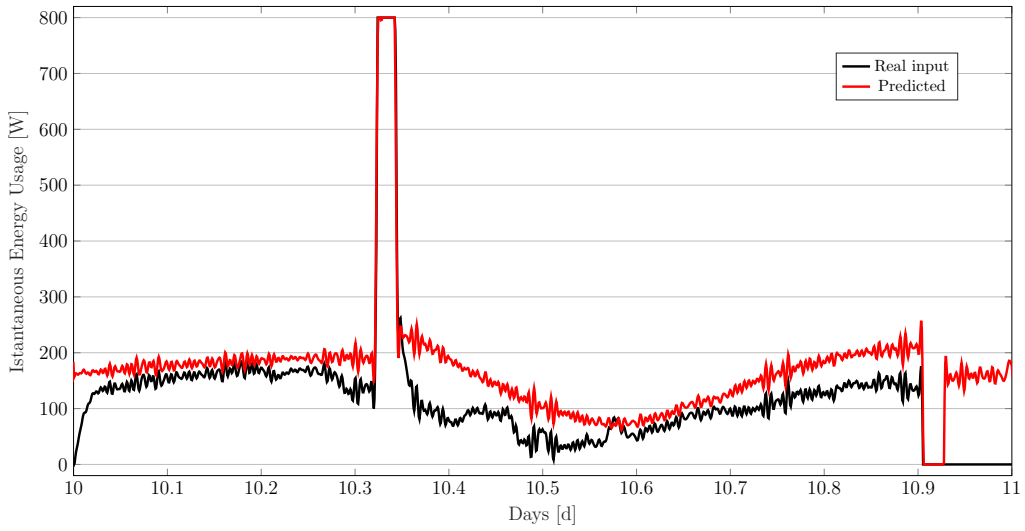

Figure 5.18: Actual and predicted consumption for our controller during the tenth day of testing for first scenario.

add a smaller machine for the reactive part only. There are two advantages for adopting this technique: the first is the larger machine can always work at its optimum operating point, improving performance and reducing energy usage. The second advantage is that it is possible, since the reactive control is only used for a short period of time, to operate it on an event-driven basis, activating the smaller machine only when the reference error exceeds a certain threshold.

The fact that a large part of the applied control depends on the predictive feed forward allows to know in advance the energy consumption for the next day. With this information, it is possible to participate to energy markets for the next day, since the expected hourly consumption is estimated with good quality. Although it is not advantageous in household scenarios, applying this method to several commercial or industrial plants would allow ESCos to make margins also in energy purchasing and not only in reducing the amount used. The Figure 5.18 shows the difference between actual and predicted consumption of our controller for the 10th of February in the first scenario. The predicted consumption was calculated using the weather forecast published the ninth day for the tenth day. From the plot, it can be seen that the feed forward slightly overestimates the consumption, especially at night. However, with appropriate adjustments, it is possible to adapt this forecasting system to trade energy: usually, the energy can be bought per quarter-hour or hourly packages. We report the cumulative consumption error prediction per quarter of hour in Figure 5.19. From this plot, we can assess that our solution is sufficiently precise during the quarter of hour since errors of less than a tenth of a kilowatt hour are present in the

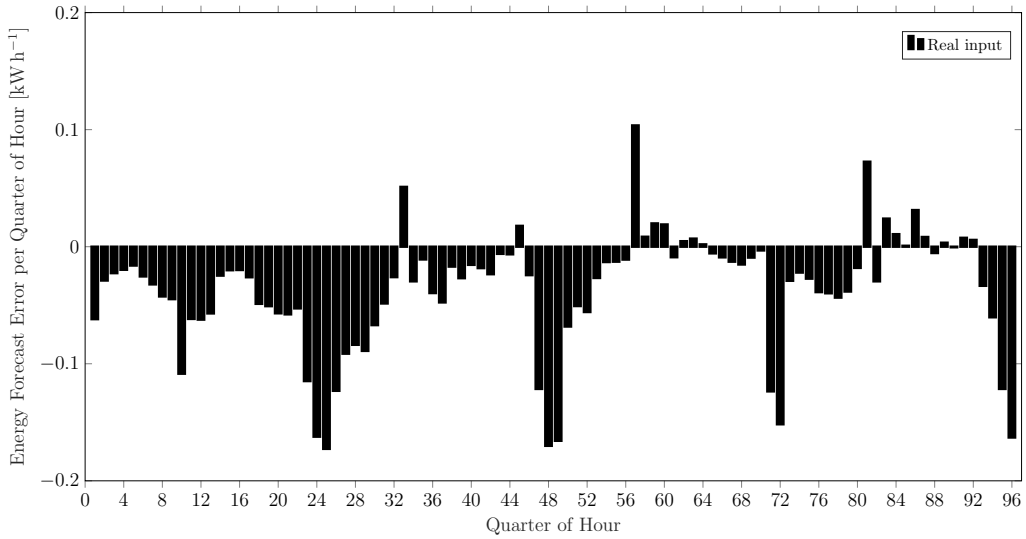

Figure 5.19: Energy forecast error in first scenario: grouping by a quarter of an hour during the tenth day of simulation.

predictions. However, feed forward in itself is not suitable for open-chain control of the system: the initial conditions and slow modes that characterise buildings do not match the appreciable changes in climate between one day and the next. Anyway, it has proved to be a valuable aid in improving both comfort and the expected consumption forecast.

6

Conclusions & Future Works

6.1 Conclusions

The aim of this work was to present a modelling and control methodology for residential and commercial buildings for improving comfort and reducing energy consumption compared to the techniques most commonly used in the market.

After introducing the motivations and challenges for this research in Chapter 1, Chapter 2 presented the real state of the most common buildings from electronic point of view. Furthermore, in this Chapter it is reported an analysis about what data an energy manager has at his disposal to carry out his work of optimising and monitoring thermal plants. It was also an opportunity to present the work commissioned by EDILVI for the creation of the EPCA platform. This platform, based on widely used open source technologies, aims to collect data from plants in an easy and secure way and store it safely within the company's servers. In addition, the platform provides several tools to calculate the most important KPIs for an energy manager from the collected and stored data. This platform was exploited also for this work, greatly simplifying the work of collecting and storing the weather data that would later be used for simulations.

In Chapter 3, a methodology to develop building models using the 2R1C technique was described, after demonstrating the physical derivation of this methodology. Then, our focus shifted from modelling the components of a building to the impact that external

disturbances have on it. Modelling the disturbances, we then noted the periodicity of some of them, such as outdoor temperature and solar radiation.

In Chapter 4, we presented our idea of an ideal building controller that would fulfil the aims given to us at the beginning: a controller that relies only on what is already present in a building and does not need specific hardware or specific solvers to optimise the performance. For this reason, we adopted LQR technology to develop the reactive part of the controller and relied on a Kalman filter to estimate states that are not measurable.

The innovative idea, however, was to use an advanced technique of feed forward based on historical profiles. Since the main disturbances are periodic and the system is linear, then the outputs will also be periodic and composed of the same harmonics as the disturbances. It is, therefore, possible to take action at the level of a single harmonic with a customized feed forward. After obtaining the historical temperature and insolation profiles from internet databases, we processed them in such a way as to obtain a monthly average temperature and radiation profiles normalised to the peak. Then, we transformed them into frequency domain using the Discrete Fourier Transform for calculating what theoretical input is needed to cancel the disturbance. The normalised feed forward signal can then be obtained by back-transform into time domain: it is ready to be multiplied by the predicted excursion day by day. From a computational point of view, this technique can be easily implemented in real time. Indeed, the profile is calculated offline using the historical design data and once defined, it only needs to be adjusted day by day using the data coming from a local weather forecast service. This operation can be done very fast by multiplying the pre-calculated signal at the considered instant using a gain.

Chapter 5 presents the performance of the controller obtained. After defining two typical usage scenarios, one in which only the kitchen is managed and the second in which the main rooms of the house are controlled, we selected two controllers to test our controller with. The first one is a PID controller with anti-windup, the most advanced standard for commercial heat pumps. The second is a controller based on LQR technology, the expected standard of the near future but not yet widespread. The results reward our solution, which is able to provide much better comfort than the other controllers using the same amount of energy. The feed forward control, which is supported by the reactive part in LQR technology, allows the temperature reference to be followed perfectly throughout the duration of the test month. Being able to rely on the feed forward part for a large time of the control allows energy managers to know in advance the energy consumption for the following days and, then, to be able to participate in the energy markets for the next day. It also makes it possible to split loads among several machines and optimise each one according to the type of load assigned.

6.2 Future Works

Due to the pandemic caused by the spread of the SARS-Cov-2 virus and the related countermeasures taken in the last two years, it was not possible to trial in a real environment the modelling and control methodology presented in this thesis. Indeed, the testing and validation part is very important for works based on developing virtual environments and, therefore, should be a priority in follow-up works.

The testing work in the real environment shall focus on two different tracks: the first is the validation of the 2R1C model, i.e. verifying that the simulated model provides the same outputs as the real system given the same inputs and conditions measured. In this way, we are sure to have defined a methodology to develop reliable virtual environments from design data. This work is quite simple to complete although physical access to buildings is necessary: simply install additional sensors and logging machines in the test building to monitor the temperature inside each room and verify that the measurements match those obtained from the simulated virtual environment. This needs to be monitored for at least a whole year to verify that the model responds correctly in all the different weather conditions characterising a year.

The second future work path is the implementation and testing of the algorithms that make up the controller in a real system. The solution presented here is ready to use and can be easily implemented in an inexpensive microcomputer such as the *Raspberry Pi Zero W*. During the preparation of the system that would implement our controller, we came up against the reluctance of system manufacturers and installers to allow us to control set points automatically and independently. For the system to work effectively, the manufacturer of the machine to be controlled must provide a communication interface with our system, which reads the inputs we provide and returns the status of the machine. The most advantageous idea is to define a communication protocol based on a data interchange format, such as JSON or XML, in which indicate the set points to be provided to the machine: in response, the machine should provide the system status and whether the communicated requests can be satisfied. Obviously, security constraints must be well assessed, such as what countermeasures to take if the machine does not receive input from the controller for more than a predefined time. The support of the machine manufacturer or the plant supervisor is therefore essential to collaborate in defining the protocol and the data exchange. For this reason, we suggest extending the collaboration implemented in this work to a supervisory systems manufacturer, in order to have direct support for the implementation and testing of this project.

A follow-up to this work, which goes beyond the subject of pure control, is the feasibility analysis and possible implementation of an automatic system to participate in energy

trading using the forecasts provided by the feed forward system. As shown above, with appropriate actions, it is possible to satisfactorily forecast energy usage on the next day, divided by time slot. By analysing the behaviour of the market, it would be possible to know the most profitable times to buy and use energy. Then, by modifying the feed forward profiles accordingly, it would be possible to store energy in the building when its cost is lowest. Similarly, if the building is equipped with solar panels, the profile can be adjusted to maximise self-consumption. This is a very attractive branch of research, especially for ESCos, that are always interested in new ways to get margins from installations.

Bibliography

[1] U.S. Energy Information. *How much energy is consumed in U.S. buildings?* URL: https://www.eia.gov/tools/faqs/faq.php?id=86&t=1.

[2] C. Wang, K. Pattawi, and H. Lee. "Energy saving impact of occupancy-driven thermostat for residential buildings". In: *Energy and Buildings* 211 (Mar. 2020), p. 109791. DOI: 10.1016/j.enbuild.2020.109791.

[3] U. Desideri, L. Arcioni, D. Leonardi, L. Cesaretti, P. Perugini, E. Agabitini, and N. Evangelisti. "Design of a multipurpose "zero energy consumption" building according to European Directive 2010/31/EU: Architectural and technical plants solutions". In: *Energy* 58 (Sept. 2013), pp. 157–167. DOI: 10.1016/j.energy.2013.02.063.

[4] U. Desideri, L. Arcioni, D. Leonardi, L. Cesaretti, P. Perugini, E. Agabitini, and N. Evangelisti. "Design of a multipurpose "zero energy consumption" building according to European Directive 2010/31/EU: Life cycle assessment". In: *Energy and Buildings* 80 (Sept. 2014), pp. 585–597. DOI: 10.1016/j.enbuild.2014.05.027.

[5] K. Qu, X. Chen, A. Ekambaram, Y. Cui, G. Gan, A. Okland, and S. Riffat. "A novel holistic EPC related retrofit approach for residential apartment building renovation in Norway". In: *Sustainable Cities and Society* 54 (Mar. 2020), p. 101975. DOI: 10.1016/j.scs.2019.101975.

[6] M. Kummert, P. Andre, and J. Nicolas. "Optimised thermal zone controller for integration within a Building Energy Management System". In: *Proceedings of CLIMA 2000 conference. Brussels, Belgium1997*. 1997.

[7] D. Zolotozubov and O. Karmanova. "Analysis of the impact of changes in insolation of apartments energy saving". In: *PNRPU Construction and Architecture Bulletin* 7.1 (2016), pp. 82–92. DOI: 10.15593/2224-9826/2016.1.11.

[8] *EDILVI S.p.A. website*. URL: https://www.edilvi.it/.

[9] M. Corina. "The energy performance contract-key towards energy efficiency in Europe?" In: *Proceedings of the International Conference on Business Excellence*. Vol. 11. 1. Sciendo. 2017, pp. 103–110. DOI: 10.1515/picbe-2017-0011.

[10] K. Arendt, M. Jradi, H. R. Shaker, and C. Veje. "Comparative analysis of white-, gray-and black-box models for thermal simulation of indoor environment: Teaching building case study". In: *Proceedings of the 2018 Building Performance Modeling Conference and SimBuild co-organized by ASHRAE and IBPSA-USA, Chicago, IL, USA*. 2018, pp. 26–28.

[11] F. Amara, K. Agbossou, A. Cardenas, Y. Dubé, and S. Kelouwani. "Comparison and Simulation of Building Thermal Models for Effective Energy Management". In: *Smart Grid and Renewable Energy* 06.04 (2015), pp. 95–112. DOI: 10.4236/sgre.2015.64009.

[12] X. Li and J. Wen. "Review of building energy modeling for control and operation". In: *Renewable and Sustainable Energy Reviews* 37 (Sept. 2014), pp. 517–537. DOI: 10.1016/j.rser.2014.05.056.

[13] J. R. Vázquez-Canteli and Z. Nagy. "Reinforcement learning for demand response: A review of algorithms and modeling techniques". In: *Applied Energy* 235 (Feb. 2019), pp. 1072–1089. DOI: 10.1016/j.apenergy.2018.11.002.

[14] T. Hong, Z. Wang, X. Luo, and W. Zhang. "State-of-the-art on research and applications of machine learning in the building life cycle". In: *Energy and Buildings* 212 (Apr. 2020), p. 109831. DOI: 10.1016/j.enbuild.2020.109831.

[15] Y. Wei, X. Zhang, Y. Shi, L. Xia, S. Pan, J. Wu, M. Han, and X. Zhao. "A review of data-driven approaches for prediction and classification of building energy consumption". In: *Renewable and Sustainable Energy Reviews* 82 (Feb. 2018), pp. 1027–1047. DOI: 10.1016/j.rser.2017.09.108.

[16] M. D. Zeiler and R. Fergus. "Visualizing and Understanding Convolutional Networks". In: (Nov. 2013). arXiv: 1311.2901 [cs.CV].

[17] O. Kilinc and I. Uysal. "Learning Latent Representations in Neural Networks for Clustering through Pseudo Supervision and Graph-based Activity Regularization". In: (Feb. 2018). arXiv: 1802.03063 [cs.LG].

[18] X. Luo. "A novel clustering-enhanced adaptive artificial neural network model for predicting day-ahead building cooling demand". In: *Journal of Building Engineering* 32 (Nov. 2020), p. 101504. DOI: 10.1016/j.jobe.2020.101504.

[19] A. H. Neto and F. A. S. Fiorelli. "Comparison between detailed model simulation and artificial neural network for forecasting building energy consumption". In: *Energy and Buildings* 40.12 (Jan. 2008), pp. 2169–2176. DOI: 10.1016/j.enbuild.2008.06.013.

[20] S. Prívara, J. Cigler, Z. Váňa, F. Oldewurtel, C. Sagerschnig, and E. Žáčeková. "Building modeling as a crucial part for building predictive control". In: *Energy and Buildings* 56 (Jan. 2013), pp. 8–22. DOI: 10.1016/j.enbuild.2012.10.024.

[21] P. Van Overschee and B. De Moor. *Subspace identification for linear systems: Theory - Implementation - Applications*. Springer Science & Business Media, 2012.

[22] J. C.-M. Yiu and S. Wang. "Multiple ARMAX modeling scheme for forecasting air conditioning system performance". In: *Energy Conversion and Management* 48.8 (Aug. 2007), pp. 2276–2285. DOI: 10.1016/j.enconman.2007.03.018.

[23] University of Wisconsin–Madison. Solar Energy Laboratory. *TRNSYS, a transient simulation program*. Loose-leaf for updating.;March 31, 1975.;"This manual, and the TRNSYS program it describes, were developed under grants from the RANN program of the National Science Foundation (Grant GI 34029), and from the Energy Research and Development Administration (Contract E(11-1)-2588). Madison, Wis. : The Laboratory, 1975., 1975. URL: https://search.library.wisc.edu/catalog/999800551102121.

[24] D. B. Crawley, C. O. Pedersen, L. K. Lawrie, and F. C. Winkelmann. "EnergyPlus: Energy Simulation Program". In: *ASHRAE Journal* 42 (2000), pp. 49–56.

[25] P. Fritzson and P. Bunus. "Modelica - a general object-oriented language for continuous and discrete-event system modeling and simulation". In: *Proceedings 35th Annual Simulation Symposium. SS 2002*. IEEE Comput. Soc, 2002. DOI: 10.1109/simsym.2002.1000174.

[26] N. Björsell, A. Bring, L. Eriksson, P. Grozman, M. Lindgren, P. Sahlin, A. Shapovalov, and M. Vuolle. "IDA indoor climate and energy". In: *Proc. of the 6-th IBPSA Conference*. 1999, pp. 1035–1042.

[27] T. J. Hughes. *The finite element method: linear static and dynamic finite element analysis*. Courier Corporation, 2012.

[28] A. C. Polycarpou. "Introduction to the Finite Element Method in Electromagnetics". In: *Synthesis Lectures on Computational Electromagnetics* 1.1 (Jan. 2006), pp. 1–126. DOI: 10.2200/s00019ed1v01y200604cem004.

[29] G. Tan and L. R. Glicksman. “Application of integrating multi-zone model with CFD simulation to natural ventilation prediction”. In: *Energy and Buildings* 37.10 (Oct. 2005), pp. 1049–1057. DOI: 10.1016/j.enbuild.2004.12.009.

[30] B. Hudobivnik, L. Pajek, R. Kunič, and M. Košir. “FEM thermal performance analysis of multi-layer external walls during typical summer conditions considering high intensity passive cooling”. In: *Applied Energy* 178 (2016), pp. 363–375. DOI: https://doi.org/10.1016/j.apenergy.2016.06.036.

[31] C. Koo, S. Park, T. Hong, and H. S. Park. “An estimation model for the heating and cooling demand of a residential building with a different envelope design using the finite element method”. In: *Applied Energy* 115 (Feb. 2014), pp. 205–215. DOI: 10.1016/j.apenergy.2013.11.014.

[32] A. Foucquier, S. Robert, F. Suard, L. Stéphan, and A. Jay. “State of the art in building modelling and energy performances prediction: A review”. In: *Renewable and Sustainable Energy Reviews* 23 (July 2013), pp. 272–288. DOI: 10.1016/j.rser.2013.03.004.

[33] P. Rumianowski, J. Brau, and J. Roux. “An adapted model for simulation of the interaction between a wall and the building heating system”. In: *Proceedings of the Thermal Performance of the Exterior Envelopes of Buildings IV Conference*. 1989, pp. 224–233.

[34] C. Be´nard, B. Guerrier, and M.-M. Rosset-Loue¨rat. “Optimal Building Energy Management: Part I—Modeling”. In: *Journal of Solar Energy Engineering* 114.1 (Feb. 1992), pp. 2–12. DOI: 10.1115/1.2929978.

[35] A. P. Ramallo-González, M. E. Eames, and D. A. Coley. “Lumped parameter models for building thermal modelling: An analytic approach to simplifying complex multi-layered constructions”. In: *Energy and Buildings* 60 (May 2013), pp. 174–184. DOI: 10.1016/j.enbuild.2013.01.014.

[36] M. Długosz. “The Minimum Energy Building Temperature Control”. In: *System Modeling and Optimization*. Ed. by D. Hömberg and F. Tröltzsch. Berlin, Heidelberg: Springer Berlin Heidelberg, 2013, pp. 471–480. DOI: 10.1007/978-3-642-36062-6_47.

[37] M. Gouda, S. Danaher, and C. Underwood. “Low-order model for the simulation of a building and its heating system”. In: *Building Services Engineering Research and Technology* 21.3 (Aug. 2000), pp. 199–208. DOI: 10.1177/014362440002100308.

[38] B. Bueno, L. Norford, G. Pigeon, and R. Britter. "A resistance-capacitance network model for the analysis of the interactions between the energy performance of buildings and the urban climate". In: *Building and Environment* 54 (Aug. 2012), pp. 116–125. DOI: 10.1016/j.buildenv.2012.01.023.

[39] J. Vivian, A. Zarrella, G. Emmi, and M. D. Carli. "An evaluation of the suitability of lumped-capacitance models in calculating energy needs and thermal behaviour of buildings". In: *Energy and Buildings* 150 (Sept. 2017), pp. 447–465. DOI: 10.1016/j.enbuild.2017.06.021.

[40] L. Danza, L. Belussi, I. Meroni, F. Salamone, F. Floreani, A. Piccinini, and A. Dabusti. "A Simplified Thermal Model to Control the Energy Fluxes and to Improve the Performance of Buildings". In: *Energy Procedia* 101 (Nov. 2016), pp. 97–104. DOI: 10.1016/j.egypro.2016.11.013.

[41] K. Deng, P. Barooah, P. G. Mehta, and S. P. Meyn. "Building thermal model reduction via aggregation of states". In: *Proceedings of the 2010 American Control Conference*. IEEE, June 2010. DOI: 10.1109/acc.2010.5530470.

[42] S. Goyal and P. Barooah. "A method for model-reduction of non-linear thermal dynamics of multi-zone buildings". In: *Energy and Buildings* 47 (Apr. 2012), pp. 332–340. DOI: 10.1016/j.enbuild.2011.12.005.

[43] J. Penman. "Second order system identification in the thermal response of a working school". In: *Building and Environment* 25.2 (Jan. 1990), pp. 105–110. DOI: 10.1016/0360-1323(90)90021-i.

[44] Y. Oussar and G. Dreyfus. "How to Be a Gray Box: The Art of Dynamic Semi-Physical Modeling". In: *Neural Networks* 14.1 (Nov. 2001), pp. 1161–1172. URL: https://hal.archives-ouvertes.fr/hal-00922197.

[45] H. Harb, N. Boyanov, L. Hernandez, R. Streblow, and D. Müller. "Development and validation of grey-box models for forecasting the thermal response of occupied buildings". In: *Energy and Buildings* 117 (Apr. 2016), pp. 199–207. DOI: 10.1016/j.enbuild.2016.02.021.

[46] T. Berthou, P. Stabat, R. Salvazet, and D. Marchio. "Development and validation of a gray box model to predict thermal behavior of occupied office buildings". In: *Energy and Buildings* 74 (May 2014), pp. 91–100. DOI: 10.1016/j.enbuild.2014.01.038.

[47] P. Bacher and H. Madsen. "Identifying suitable models for the heat dynamics of buildings". In: *Energy and Buildings* 43.7 (July 2011), pp. 1511–1522. DOI: 10.1016/j.enbuild.2011.02.005.

[48] E. T. Maddalena, Y. Lian, and C. N. Jones. "Data-driven methods for building control — A review and promising future directions". In: *Control Engineering Practice* 95 (Feb. 2020), p. 104211. DOI: 10.1016/j.conengprac.2019.104211.

[49] A. Dounis and D. Manolakis. "Design of a fuzzy system for living space thermal-comfort regulation". In: *Applied Energy* 69.2 (June 2001), pp. 119–144. DOI: 10.1016/s0306-2619(00)00065-9.

[50] G. Ulpiani, M. Borgognoni, A. Romagnoli, and C. D. Perna. "Comparing the performance of on/off, PID and fuzzy controllers applied to the heating system of an energy-efficient building". In: *Energy and Buildings* 116 (Mar. 2016), pp. 1–17. DOI: 10.1016/j.enbuild.2015.12.027.

[51] M. Shahrokhi and A. Zomorrodi. "Comparison of PID controller tuning methods". In: *Department of Chemical & Petroleum Engineering Sharif University of Technology* (2013), pp. 1–2. URL: http://yunus.hacettepe.edu.tr/~ounver/documents/OMU412/Lectures/Zomorrodi_Shahrokhi_PID_Tunning_Comparison.pdf.

[52] A. J. Shaiju and I. R. Petersen. "Formulas for Discrete Time LQR, LQG, LEQG and Minimax LQG Optimal Control Problems". In: *IFAC Proceedings Volumes* 41.2 (2008), pp. 8773–8778. DOI: 10.3182/20080706-5-kr-1001.01483.

[53] R. E. Kalman. "A New Approach to Linear Filtering and Prediction Problems". In: *Journal of Basic Engineering* 82.1 (Mar. 1960), pp. 35–45. DOI: 10.1115/1.3662552.

[54] A. Yahiaoui, J. Hensen, L. Soethout, and D. van Paassen. "Design of model based LQG control for integrated building systems". In: *Proceedings of the 8th IASTED International Conference on Control and Applications, International Association of Science and Technology for Development*. 2006.

[55] P. C. YOUNG and J. C. WILLEMS. "An approach to the linear multivariable servomechanism problem†". In: *International Journal of Control* 15.5 (May 1972), pp. 961–979. DOI: 10.1080/00207177208932211.

[56] J. Drgoňa, J. Arroyo, I. C. Figueroa, D. Blum, K. Arendt, D. Kim, E. P. Ollé, J. Oravec, M. Wetter, D. L. Vrabie, and L. Helsen. "All you need to know about model predictive control for buildings". In: *Annual Reviews in Control* 50 (2020), pp. 190–232. DOI: 10.1016/j.arcontrol.2020.09.001.

[57] P. O. Fanger et al. "Thermal comfort. Analysis and applications in environmental engineering." In: *Thermal comfort. Analysis and applications in environmental engineering.* (1970).

[58] J. Široký, F. Oldewurtel, J. Cigler, and S. Prívara. "Experimental analysis of model predictive control for an energy efficient building heating system". In: *Applied Energy* 88.9 (Sept. 2011), pp. 3079–3087. DOI: 10.1016/j.apenergy.2011.03.009.

[59] R. Bălan, J. Cooper, K.-M. Chao, S. Stan, and R. Donca. "Parameter identification and model based predictive control of temperature inside a house". In: *Energy and Buildings* 43.2-3 (Feb. 2011), pp. 748–758. DOI: 10.1016/j.enbuild.2010.10.023.

[60] C. Verhelst, F. Logist, J. V. Impe, and L. Helsen. "Study of the optimal control problem formulation for modulating air-to-water heat pumps connected to a residential floor heating system". In: *Energy and Buildings* 45 (Feb. 2012), pp. 43–53. DOI: 10.1016/j.enbuild.2011.10.015.

[61] Y. Ma, A. Kelman, A. Daly, and F. Borrelli. "Predictive Control for Energy Efficient Buildings with Thermal Storage: Modeling, Stimulation, and Experiments". In: *IEEE Control Systems* 32.1 (Feb. 2012), pp. 44–64. DOI: 10.1109/mcs.2011.2172532.

[62] D. Sturzenegger, D. Gyalistras, M. Morari, and R. S. Smith. "Model Predictive Climate Control of a Swiss Office Building: Implementation, Results, and Cost–Benefit Analysis". In: *IEEE Transactions on Control Systems Technology* 24.1 (Jan. 2016), pp. 1–12. DOI: 10.1109/tcst.2015.2415411.

[63] D. Sturzenegger, D. Gyalistras, V. Semeraro, M. Morari, and R. S. Smith. "BRCM Matlab Toolbox: Model generation for model predictive building control". In: *2014 American Control Conference*. IEEE, June 2014. DOI: 10.1109/acc.2014.6858967.

[64] G. P. Henze. "Model predictive control for buildings: a quantum leap?" In: *Journal of Building Performance Simulation* 6.3 (Apr. 2013), pp. 157–158. DOI: 10.1080/19401493.2013.778519.

[65] A. I. Dounis and C. Caraiscos. "Advanced control systems engineering for energy and comfort management in a building environment—A review". In: *Renewable and Sustainable Energy Reviews* 13.6-7 (Aug. 2009), pp. 1246–1261. DOI: 10.1016/j.rser.2008.09.015.

[66] R. Eini and S. Abdelwahed. "A Neural Network-based Model Predictive Control Approach for Buildings Comfort Management". In: *2020 IEEE International Smart Cities Conference (ISC2)*. IEEE, Sept. 2020. DOI: 10.1109/isc251055.2020.9239051.

[67] Z. Zou, X. Yu, and S. Ergan. "Towards optimal control of air handling units using deep reinforcement learning and recurrent neural network". In: *Building and Environment* 168 (Jan. 2020), p. 106535. DOI: 10.1016/j.buildenv.2019.106535.

[68] G. Gao, J. Li, and Y. Wen. "DeepComfort: Energy-Efficient Thermal Comfort Control in Buildings Via Reinforcement Learning". In: *IEEE Internet of Things Journal* 7.9 (Sept. 2020), pp. 8472–8484. DOI: 10.1109/jiot.2020.2992117.

[69] J. King and C. Perry. *Smart buildings: Using smart technology to save energy in existing buildings*. Amercian Council for an Energy-Efficient Economy, 2017.

[70] S. Naylor, M. Gillott, and T. Lau. "A review of occupant-centric building control strategies to reduce building energy use". In: *Renewable and Sustainable Energy Reviews* 96 (Nov. 2018), pp. 1–10. DOI: 10.1016/j.rser.2018.07.019.

[71] B. N. Silva, M. Khan, and K. Han. "Futuristic Sustainable Energy Management in Smart Environments: A Review of Peak Load Shaving and Demand Response Strategies, Challenges, and Opportunities". In: *Sustainability* 12.14 (July 2020), p. 5561. DOI: 10.3390/su12145561.

[72] W. V. Johnston and G. W. Lindberg. "Stability and Calibration of Miniature Platinum Resistance Thermometers". In: *Review of Scientific Instruments* 39.12 (Dec. 1968), pp. 1925–1928. DOI: 10.1063/1.1683273.

[73] J. S. Steinhart and S. R. Hart. "Calibration curves for thermistors". In: *Deep Sea Research and Oceanographic Abstracts* 15.4 (Aug. 1968), pp. 497–503. DOI: 10.1016/0011-7471(68)90057-0.

[74] J. Toftum and P. O. Fanger. "Air humidity requirements for human comfort". In: *ASHRAE transactions* 105 (1999), p. 641.

[75] S. Sikarwar and B. Yadav. "Opto-electronic humidity sensor: A review". In: *Sensors and Actuators A: Physical* 233 (Sept. 2015), pp. 54–70. DOI: 10.1016/j.sna.2015.05.007.

[76] B. Okcan and T. Akin. "A thermal conductivity based humidity sensor in a standard CMOS process". In: *17th IEEE International Conference on Micro Electro Mechanical Systems. Maastricht MEMS 2004 Technical Digest*. IEEE, 2004. DOI: 10.1109/mems.2004.1290644.

[77] W. J. Fisk and A. T. D. Almeida. "Sensor-based demand-controlled ventilation: a review". In: *Energy and Buildings* 29.1 (Dec. 1998), pp. 35–45. DOI: 10.1016/s0378-7788(98)00029-2.

[78] S. J. Patil, A. V. Patil, C. G. Dighavkar, K. S. Thakare, R. Y. Borase, S. J. Nandre, N. G. Deshpande, and R. R. Ahire. "Semiconductor metal oxide compounds based gas sensors: A literature review". In: *Frontiers of Materials Science* 9.1 (Feb. 2015), pp. 14–37. DOI: 10.1007/s11706-015-0279-7.

[79] T. Yasuda, S. Yonemura, and A. Tani. "Comparison of the Characteristics of Small Commercial NDIR CO2 Sensor Models and Development of a Portable CO2 Measurement Device". In: *Sensors* 12.3 (Mar. 2012), pp. 3641–3655. DOI: 10.3390/s120303641.

[80] J.-C. Kim, T.-V. Dinh, I.-Y. Choi, and K.-Y. Song. "Physical and chemical factors influencing the continuous monitoring of carbon monoxide using NDIR sensor". In: *2015 9th International Conference on Sensing Technology (ICST)*. IEEE, Dec. 2015. DOI: 10.1109/icsenst.2015.7438414.

[81] I. Khajenasiri, A. Estebsari, M. Verhelst, and G. Gielen. "A Review on Internet of Things Solutions for Intelligent Energy Control in Buildings for Smart City Applications". In: *Energy Procedia* 111 (Mar. 2017), pp. 770–779. DOI: 10.1016/j.egypro.2017.03.239.

[82] L. Pocero, D. Amaxilatis, G. Mylonas, and I. Chatzigiannakis. "Open source IoT meter devices for smart and energy-efficient school buildings". In: *HardwareX* 1 (Apr. 2017), pp. 54–67. DOI: 10.1016/j.ohx.2017.02.002.

[83] E. Karapistoli, F.-N. Pavlidou, I. Gragopoulos, and I. Tsetsinas. "An overview of the IEEE 802.15.4a Standard". In: *IEEE Communications Magazine* 48.1 (Jan. 2010), pp. 47–53. DOI: 10.1109/mcom.2010.5394030.

[84] G. Mulligan. "The 6LoWPAN architecture". In: *Proceedings of the 4th workshop on Embedded networked sensors - EmNets '07*. ACM Press, 2007. DOI: 10.1145/1278972.1278992.

[85] A. P. Plageras, K. E. Psannis, C. Stergiou, H. Wang, and B. Gupta. "Efficient IoT-based sensor BIG Data collection–processing and analysis in smart buildings". In: *Future Generation Computer Systems* 82 (May 2018), pp. 349–357. DOI: 10.1016/j.future.2017.09.082.

[86] ISO. "7730: Ergonomics of the thermal environment Analytical determination and interpretation of thermal comfort using calculation of the PMV and PPD indices and local thermal comfort criteria". In: *Management* 3.605 (2005), e615.

[87] G. Baldinelli, F. Bianchi, A. Rotili, and A. Presciutti. "Transient Heat Transfer in Radiant Floors: A Comparative Analysis between the Lumped Capacitance Method and Infrared Thermography Measurements". In: *Journal of Imaging* 2.3 (July 2016), p. 22. DOI: 10.3390/jimaging2030022.

[88] A. Acquaviva, D. Apiletti, A. Attanasio, E. Baralis, L. Bottaccioli, F. B. Castagnetti, T. Cerquitelli, S. Chiusano, E. Macii, D. Martellacci, and E. Patti. "Energy Signature Analysis: Knowledge at Your Fingertips". In: *2015 IEEE International Congress on Big Data*. IEEE, June 2015. DOI: 10.1109/bigdatacongress.2015.85.

[89] P. Brunello. *Lezioni di fisica tecnica*. Napoli: EdiSES, 2017. ISBN: 9788879599436.

[90] W. Li, P. Xu, H. Wang, and X. Lu. "A new method for calculating the thermal effects of irregular internal mass in buildings under demand response". In: *Energy and Buildings* 130 (Oct. 2016), pp. 761–772. DOI: 10.1016/j.enbuild.2016.08.057.

[91] N. Laaroussi, A. Cherki, M. Garoum, A. Khabbazi, and A. Feiz. "Thermal Properties of a Sample Prepared Using Mixtures of Clay Bricks". In: *Energy Procedia* 42 (2013), pp. 337–346. DOI: 10.1016/j.egypro.2013.11.034.

[92] P. Kosky, R. Balmer, W. Keat, and G. Wise. *Exploring Engineering*. Elsevier, 2021. DOI: 10.1016/c2017-0-01871-2.

[93] A.-J. N. Khalifa. "Natural convective heat transfer coefficient – a review". In: *Energy Conversion and Management* 42.4 (Mar. 2001), pp. 505–517. DOI: 10.1016/s0196-8904(00)00043-1.

[94] F. Leccese, G. Salvadori, F. Asdrubali, and P. Gori. "Passive thermal behaviour of buildings: Performance of external multi-layered walls and influence of internal walls". In: *Applied Energy* 225 (Sept. 2018), pp. 1078–1089. DOI: 10.1016/j.apenergy.2018.05.090.

[95] G. Fraisse, C. Viardot, O. Lafabrie, and G. Achard. "Development of a simplified and accurate building model based on electrical analogy". In: *Energy and Buildings* 34.10 (Nov. 2002), pp. 1017–1031. DOI: 10.1016/s0378-7788(02)00019-1.

[96] R. Wrobel and P. H. Mellor. "A General Cuboidal Element for Three-Dimensional Thermal Modelling". In: *IEEE Transactions on Magnetics* 46.8 (Aug. 2010), pp. 3197–3200. DOI: 10.1109/tmag.2010.2043928.

[97] S. M. Rahman. "Simplified 3R2C building thermal network model: A case study". In: *International Journal of Structural and Construction Engineering* 13.6 (2019), pp. 288–294.

[98] K. Ismail. "Modeling and simulation of a simple glass window". In: *Solar Energy Materials and Solar Cells* 80.3 (Nov. 2003), pp. 355–374. DOI: 10.1016/j.solmat.2003.08.010.

[99] P. R. Lyons, D. Arasteh, and C. Huizenga. "Window performance for human thermal comfort". In: *Transactions-American Society of Heating Refrigerating and Air Conditioning Engineers* 106.1 (2000), pp. 594–604.

[100] K. Antonopoulos and E. Koronaki. "On the dynamic thermal behaviour of indoor spaces". In: *Applied Thermal Engineering* 21.9 (June 2001), pp. 929–940. DOI: 10.1016/s1359-4311(00)00091-0.

[101] H. Johra and P. Heiselberg. "Influence of internal thermal mass on the indoor thermal dynamics and integration of phase change materials in furniture for building energy storage: A review". In: *Renewable and Sustainable Energy Reviews* 69 (Mar. 2017), pp. 19–32. DOI: 10.1016/j.rser.2016.11.145.

[102] H. Johra, P. Heiselberg, and J. Le Dréau. "Numerical analysis of the impact of thermal inertia from the furniture/indoor content and phase change materials on the building energy flexibility". In: *Proceedings of 15th IBPSA Conference, International Building Performance Simulation Association, San Francisco, CA, USA*. 2017. DOI: https://doi.org/10.26868/25222708.2017.012.

[103] I. Hazyuk, C. Ghiaus, and D. Penhouet. "Optimal temperature control of intermittently heated buildings using Model Predictive Control: Part I – Building modeling". In: *Building and Environment* 51 (May 2012), pp. 379–387. DOI: 10.1016/j.buildenv.2011.11.009.

[104] J. An, D. Yan, S. Guo, Y. Gao, J. Peng, and T. Hong. "An improved method for direct incident solar radiation calculation from hourly solar insolation data in building energy simulation". In: *Energy and Buildings* 227 (Nov. 2020), p. 110425. DOI: 10.1016/j.enbuild.2020.110425.

[105] A. Jenkins. "The Sun's position in the sky". In: *European Journal of Physics* 34.3 (Mar. 2013), pp. 633–652. DOI: 10.1088/0143-0807/34/3/633.

[106] O. Mansouri, R. Belarbi, and F. Bourbia. "Albedo effect of external surfaces on the energy loads and thermal comfort in buildings". In: *Energy Procedia* 139 (Dec. 2017), pp. 571–577. DOI: 10.1016/j.egypro.2017.11.255.

[107] S. Attia. "NZEB Case Studies and Learned Lessons". In: *Net Zero Energy Buildings (NZEB)*. Elsevier, 2018, pp. 303–341. DOI: 10.1016/b978-0-12-812461-1.00011-3.

[108] P. Bröde, K. Kuklane, V. Candas, E. A. D. Hartog, B. Griefahn, I. Holmér, H. Meinander, W. Nocker, M. Richards, and G. Havenith. "Heat Gain From Thermal Radiation Through Protective Clothing With Different Insulation, Reflectivity and Vapour

Permeability". In: *International Journal of Occupational Safety and Ergonomics* 16.2 (Jan. 2010), pp. 231–244. DOI: 10.1080/10803548.2010.11076842.

[109] H. Kim, K.-s. Park, H.-y. Kim, and Y.-h. Song. "Study on Variation of Internal Heat Gain in Office Buildings by Chronology". In: *Energies* 11.4 (Apr. 2018), p. 1013. DOI: 10.3390/en11041013.

[110] R. Elsland, I. Peksen, and M. Wietschel. "Are Internal Heat Gains Underestimated in Thermal Performance Evaluation of Buildings?" In: *Energy Procedia* 62 (2014), pp. 32–41. DOI: 10.1016/j.egypro.2014.12.364.

[111] F. Dörfler, J. W. Simpson-Porco, and F. Bullo. "Electrical networks and algebraic graph theory: Models, properties, and applications". In: *Proceedings of the IEEE* 106.5 (2018), pp. 977–1005.

[112] E. Fornasini and G. Marchesini. *Appunti di teoria dei sistemi*. Libreria progetto, 2011.

[113] A. Bryson. *Applied optimal control : optimization, estimation, and control*. Washington New York: Hemisphere Pub. Corp. Distributed by Halsted Press, 1975. ISBN: 9780891162285.

[114] *ARPA Lombardia - Richiesta Dati Misurati*. URL: https://www.arpalombardia.it/Pages/Meteorologia/Richiesta-dati-misurati.aspx.

[115] G. R. Ruiz, V. G. González, E. L. Segarra, G. C. Gordillo, and C. F. Bandera. "Characterization Of Building Foundation In Building Energy Models". In: *Proceedings of Building Simulation 2019: 16th Conference of IBPSA*. IBPSA, 2019. DOI: 10.26868/25222708.2019.210925.